Republic of Iraq
Ministry of Higher Education
and Scientific Research
University of Babylon

Heat Transfer Analysis of Air Flow through Geometrically Irregular Ducts

A Thesis

Submitted to the College of Engineering, University of Babylon in

Partial Fulfillment of the Requirements for the Award of Degree of

Master of Science in

Mechanical Engineering (Power)

By

Dhurgham Haider Talib Al-Hussainy

B.Sc. (Mech. Eng.)

2017

Supervised by

Prof. Dr. Adil Abbas Alwan AL-Moosawy

Assist. prof. Dr. Rafel Hekmat Hameed

2 021A.M *14 43A.H*

بسم الله الرحمن الرحيم

﴿ يَرْفَعِ اللَّهُ الَّذِينَ آمَنُوا مِنْكُمْ وَالَّذِينَ أُوتُوا الْعِلْمَ دَرَجَاتٍ وَاللَّهُ بِمَا تَعْمَلُونَ خَبِيرٌ ﴾

صدق الله العلي العظيم

سورة المجادلة آية ﴿11﴾

DEDICATION

To those who Gave Me Support, Inspiration, Courage, and Strength Especially My Father , My Mother, and My Family.

Dhurgham 2021

Certification

We certify that this thesis entitled "Heat Transfer Analysis of Air Flow Through Geometrically Irregular Ducts " was prepared by **Dhurgham Haider Talib** under our supervisions at the University of Babylon as a partial fulfillment of the requirements for the degree of Master of Science in Mechanical Engineering (Power Engineering).

We recommend that this thesis be forwarded for examination in accordance with the regulation of the University of Babylon.

Signature

Assist. prof. Dr. Rafel. H. Hameed

(Supervisor)

Date: / / 202

Signature

Prof. Dr. Adil Abbas Alwan

(Supervisor)

Date: / / 202

Examining Committee Certification

We certify that we have read this thesis entitled " **Heat Transfer Analysis of Air Flow Through Geometrically Irregular Ducts**" and, as an examining committee, examined the student " **Dhurgham Haider Talib**" in its content and in what is concerned with it, and that in our opinion it meets the standard of a thesis for the degree of Master of Science in Mechanical Engineering (Power Mechanics).

Signature:

Name: ***Prof. Dr. Adil A. Alwan***

Date: / /202

(Supervisor)

Signature:

Name: ***Assist. Prof.Dr.. Rafel. H. Hameed***

Date: / /202

(Supervisor)

Signature: Hayder K. Rashid

Name: ***Assist. Prof.Dr. Hayder K. Rashid***

Date: / /202

(Member)

Signature: Hameed K. Hamzah

Name: ***Assist. Prof.Dr. Hameed K. Hamzah***

Date: / /202

(Member)

Signature:

Name: ***Prof. Dr. Ihsan Y. Hussain***

Date: 12 /1 / 202 2

(Chairman)

Approval of Mechanical Engineering Department

Signature:

Name: ***Assist. Prof. Dr. Samer M. Abdul Haleem***

Date: / /202

Head of the Mechanical Engineering Department

Approval of the College of Engineering

Signature:

Name: ***Prof. Dr. Hatem Hadi Obeid***

Date: / /202

Dean of the Engineering College

ACKNOWLEDGMENT

I would like to express my deepest thanks and gratitude to my supervisorS, Prof. Dr. Adil Abbas Alwan, and Assist. Prof. Dr. Rafel .H.Hameed for their guidance invaluable discussions, and constructive comments, which greatly improved the structure, and presentation of this thesis.

My thanks also go for all staff of Mechanical engineering depertment and especially, My deep thanks to. Mr. Hussain H. Rashid.

Dhurgham 2021

Abstract

In the present work the experimental investigation has been carried out to study the effect of irregular geometry duct on the heat transfer and fluid flow characteristics. During this study, it was measured the temperature distribution, and air velocity through duct with different cases study of boundary conditions. In the first case, heat flux was used as a boundary condition. In the second case, fan coil was used to supply hot air. At third case, using air cooler to supply cool air. In all cases, the air flow supplied to the duct by a blower from left side and right side of rig duct. The temperature distribution was measured for three cases with y-axis at different values of z-axis inside the irregular duct (test section).

It was noted during experimental study for all cases the temperature measurements increases through the y-axis with different values of air velocity supply (1.4, 2.8, and 4.2). It was pointed increasing in temperature a little with increasing the values of air velocity. It was measured highest temperature in case one is 72.2 ^{o}C at inlet velocity 4.2 m/s when the air is heated by heat flux at the top and side wall of irregular duct (test duct).

At the same boundary conditions of three cases, the laminar air flow velocity is measured inside irregular duct (test duct). These values are measured with supplying three values of inlets velocities from the left and right side of rig duct. Also, at the same time, it measured the inlet and outlet velocity for rig duct.

For three cases, the Reynolds number is inversely proportional with the values of friction factor, and pressure drop inside the irregular duct in the experimental work .

Numerical simulation is performed in a two dimensional and predicted model deals with the temperature distribution inside test irregular duct by solving numerically the finite difference that represents energy equation. These are estimated by mathematical model which is simulated by a computer program in Matlab software. The air flow velocity was simulated by ANSYS - Fluent 19.2 inside irregular duct.

Table of Contents

Nomenclature

Latin Symbols		
Symbol	**Description**	**Units**
A	Cross-sectional area	m^2
C_P	Specific Heat Capacity	J/kg. ^oC
D_h	Hydraulic diameter	m
fr	friction factor	-
h	height	[m]
h_x	Coefficient of Heat Transfer	$W/m^2.^oC$
j,k	Indices Indication the Point Along y,z Direction	-
k	Thermal conductivity	W/m .^oC
L	axial length of test section	m
m^*	mass flow rate	kg/s
Nu	Nusselt number	-
Pr	Prandtl number	
p	Power	watt
q′	Heat flux	w/m^2
Re	Reynolds number	-
T_f	the average temperature of air flow	^oC
T_s	the temperature of curve top surface of irregular duct	^oC
V	velocity	m/s
V_{in}	Inlet velocity	m/s
V_{out}	Outlet velocity	m/s
u, v, w	velocity components in x-, y- and z-directions	m/s
x, y, z	Cartesian coordinates	m

ΔT	Temperature difference	^{o}C
Δp	Pressure drop	N/m^2

Greek Symbols		
Symbol	**Description**	**Units**
α	thermal diffusely	m^2/s
μ	Dynamic viscosity	kg/m. s
ρ	Mass density	kg/m^3
Δy	Increment Distance Through y-axis	m
Δz	Increment Distance Through z-axis	m
λ	Convergence Parameter	-
$X_{average}$	the average readings of temperature	-
X_i	the values for measurements data of temperature	-

Chapter One

Introduction

Introduction

1.1. General

Determining the heat transfer of fluid flow in different geometries of ducts is critical in mechanical and chemical engineering. Such calculations are directly used for a broad range of industrial purposes, such as synthesizing, designing, and optimization of the performance of different procedures and systems. As a result, several studies have used theoretical, computational and experimental methods to determine the impact on the heat transfer of various cross-sectional forms, flow zones, fluid types and thermal boundary conditions as shown by **Zhang et al [1]**. Heat transfer and fluid flow in a geometric duct are frequently encountered in many industrial applications such as the cooling of electronic components, cooling channels in gas turbine blades, ventilation and air conditioning systems, turbomachinery, nuclear reactors, and various compact heat exchangers. In the context of heating and cooling systems, laminar flow describes the smooth, unhindered passage of air through ductwork. When air flows through the system smoothly, energy is conserved, whereas when the air flows turbulently, friction increases, momentum is lost and energy is wasted.

fully developed flow and heat transfer of viscoelastic materials in curved ducts under constant heat flux have been investigated. Here, staggered mesh is used as computational grids and flow and heat transfer parameters have been allocated in this mesh with marker and cell method. Numerical solution of governing equations has being performed finite difference method. Developing and fully developed flow one of the characteristics of the study

was considered a fully developed flow, and it was defined as the region in the duct where two specific conditions are investigated by **Norouzi[2]**. The velocity profile is fully developed and remains unchanged.

1.2. Duct Classification

Ducts are classified in terms of velocity and pressure as noted by **Grondzik [3]** as shown in figure(1-1).

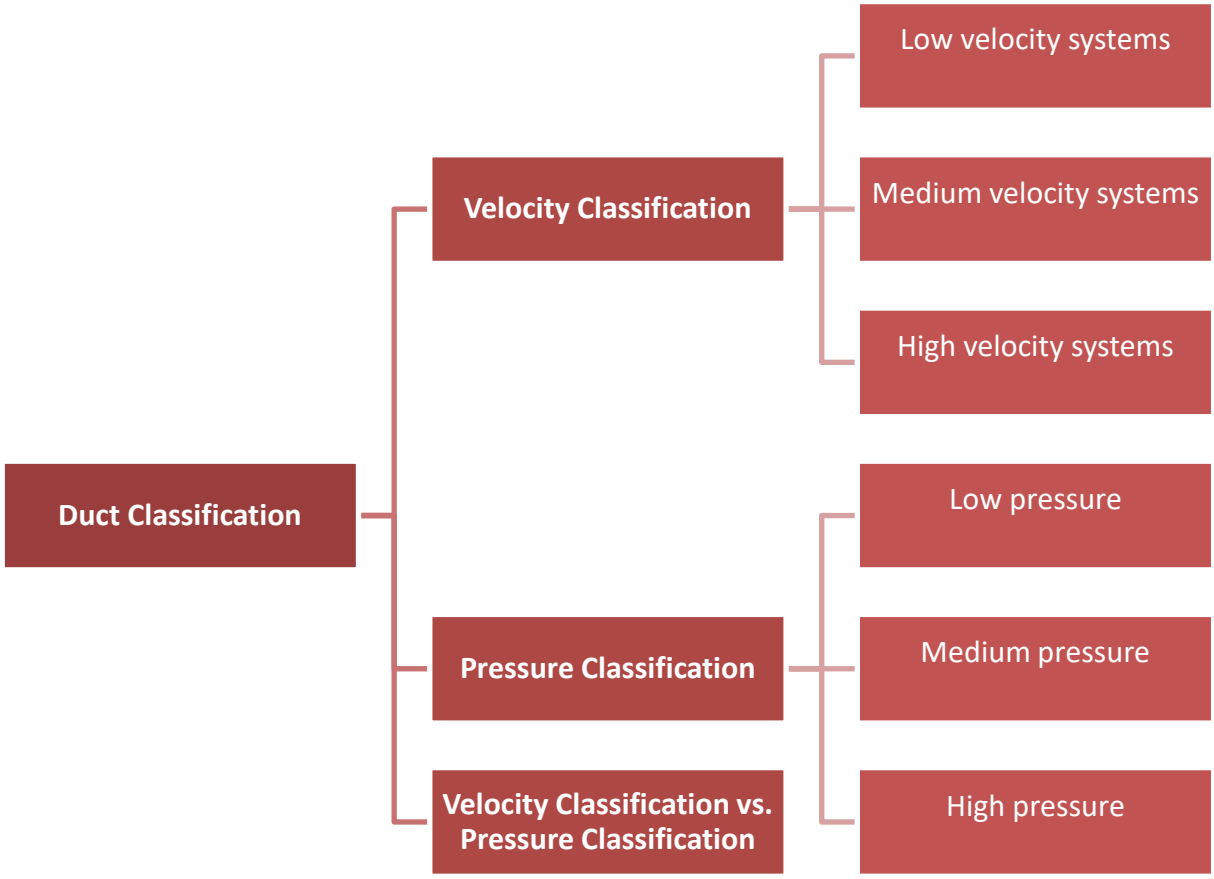

Figure(1-1) duct classification

1.3. Air Duct Shapes

Ducts commonly used for carrying air are of a round, square, or rectangular shape. The most efficient duct is a round duct, based on the volume of air handled per perimeter distance. The most common shapes are round, rectangular, and oval ducts as noted by **Grondzik [3]**. There are some advantages and disadvantages of each duct shape as shown in figure(1-2).

1- Round ducts are the most efficient in transporting air. They use less material than rectangular ducts to handle the same amount of air.

2- Square or rectangular ducts are designed to fit building construction. While they fit into walls and above ceilings, these ducts use more metal than round ducts to produce the same airflow rate.

3- Oval ducts are flat and have smaller height requirements than round ducts. These ducts tend to become more round when under pressure.

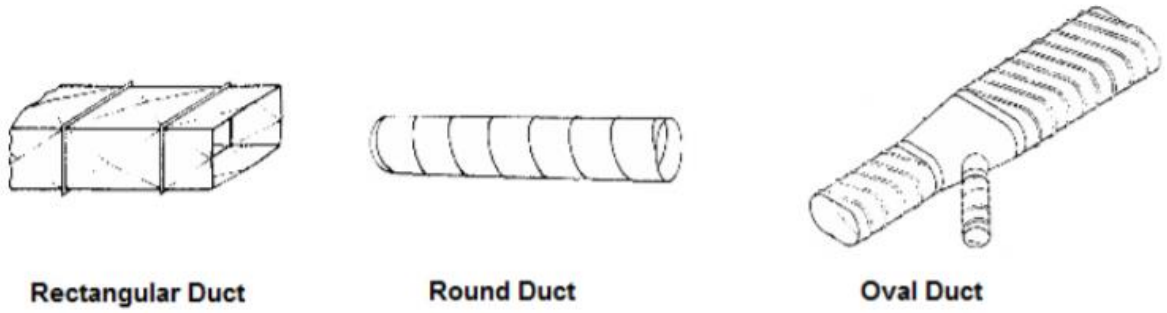

Figure(1-2) air duct shapes

1.4. Duct Materials

Ducting is generally formed by folding sheet metal into the desired shape. Traditionally, air conditioning ductwork is made of galvanized steel, next in popularity is aluminum. Other metals used under special circumstances are copper and stainless steel. **Grondzik [3]** showed metals that are used extensively depend on the application of the duct and are listed below.:

1. Galvanized Steel: It is a standard, most common material used in fabricating ductwork for most comfort air conditioning systems.

2. Aluminium: It is widely used in cleanroom applications. These are also preferred systems for moisture-laden air, special exhaust systems, and ornamental duct systems.

3. Stainless Steel: It is used in duct systems for kitchen exhaust, moisture-laden air, and fume exhaust.

4. Copper: It is mainly used for certain chemical exhaust and ornamental ductwork.

1.5. Pressure losses in the air distribution system

The system resistance in ductwork has three components as shown in figure (1-3) :

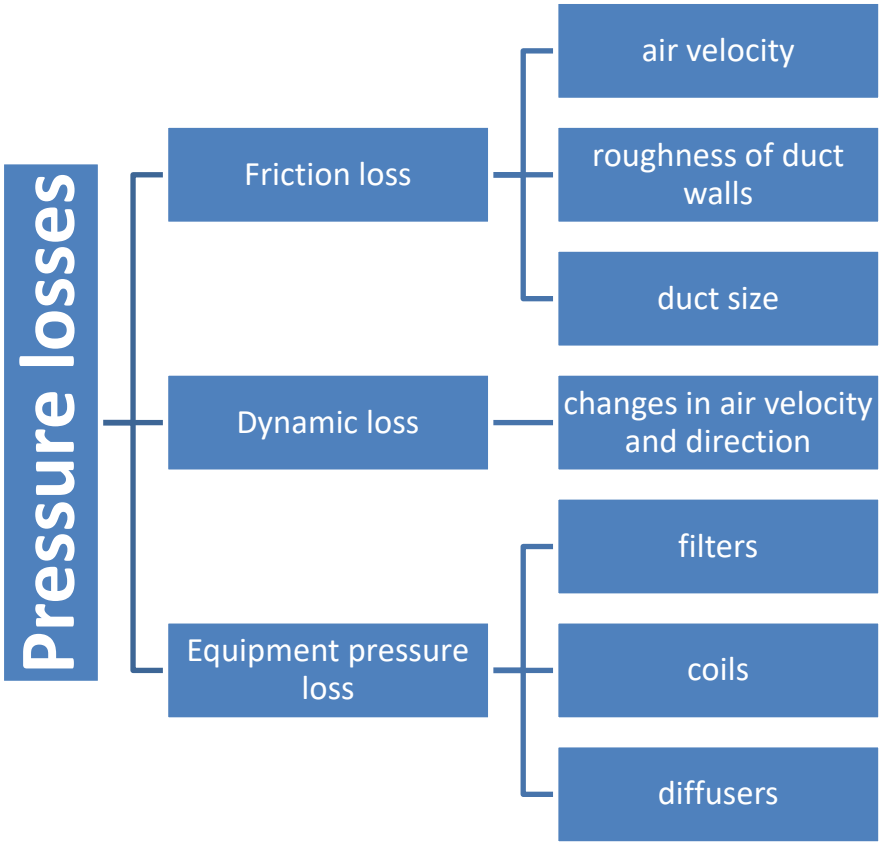

Figure(1-3) pressure losses in the air distribution system

1.6. Objective of The Present Work

1- Design of curve in a duct consists of three parts, the purpose of this work is to control air speed.

2- To predict the temperature and velocity distributions, depending upon the friction coefficient, pressure drop, and the Nusselt number.

3- To perform a mathematical model in a two dimensions deals with the temperature distributions along irregular test duct by using a finite difference method which was solving the energy equation. Matlab software is used to simulate the temperature distributions by a computer program. While, it is studied the flow characteristics and air flow velocity through all the rig duct by using Ansys-fluent 19.2.

1.7. Outline of the Thesis

1. Chapter One deals with an introduction and outlines the aims and strategies of this thesis.

2. Chapter Two is concerned reviews, the previous related literature, which presents the contributions and work

3. Chapter Three accounts of details of experimental apparatus, setup, and procedure

4. Chapter Four displays theoretical explains the mathematical model to analyze the temperature and velocity through irregular duct.

5. Chapter Five introduces the results and discusses the experimental and theoretical work.

6. Chapter Six sums up the conclusions arrived at the end of the suggestions for future works.

Chapter Two

Literature Review

Literature Review

Investigation of flow and heat transfer in irregular duct is an interesting subject for researchers in the present and the past. The most of these researches related to regular duct while, a few number of researches have been done about irregular duct .The literature review suggests that heat transfer and flow resistance characteristics of fluid flow inside duct of irregular cross section was studied by few researchers but results are discrete.

Farhanieh and Sunden [4] visualized numerically the simultaneously developing laminar flow and heat transfer in the entrance region of a straight trapezoidal duct under constant wall temperature boundary condition using the finite-volume method. The governing equations are solved numerically by using common-site variables and Cartesian velocity components to form a finite volume in complex three-dimensional geometries. The numerical method is defined in detail. The method's accuracy was also calculated by comparing the computed results to empirical and numerical results reported in the public domain. The range of Reynolds number is 150-1700. For the boundary state of uniform wall temperature.as shown in figure(2-1).

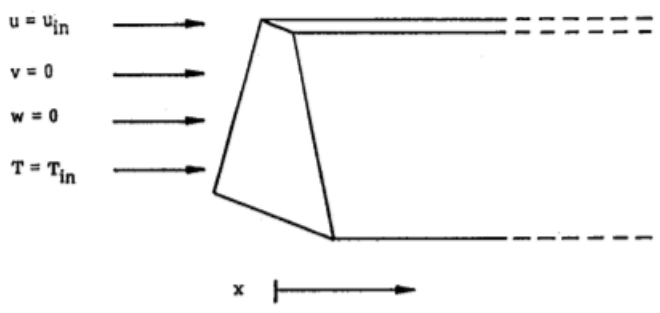

Figure (2-1) Trapezoidal duct

Manglik and Ding[5] considered fully developed, constant property, laminar flows of viscous power-law fluids in irregular ducts. The double-sine cross section represents a limiting inter-plate channel geometry in plate heat exchangers with sinusoidally corrugated plates. The range of Reynolds number is 300-1000. Both fluid flow and convective heat transfer problems under (T) and (H1) thermal boundary conditions are analyzed. The effects of fluid rheology (pseudoplasticity or dilatancy), duct geometry, and thermal boundary conditions on the velocity and temperature field, are delineated. Also, isothermal friction factor and Nusselt number results for various conditions are presented, and strategies for predicting Re and Nu are evaluated.

Campo et al [6] presented a fast and dependable numerical procedure for the solution of the fully established velocity and temperature of low-Reynolds number flows inside straight ducts with irregular, singly connected cross sections. The range of Reynolds number is 1000-3000. Relying on finite volume discretization of the momentum and energy equations in a boundary-fitted coordinate system, the procedure has been applied with great success to a wide variety of ducts whose cross sections present different levels of difficulty. Numerical predictions for the pressure drop (friction factor) and the heat transfer rate (Nusselt number) for a sample of simple ducts are compared with benchmark results published by other researchers. Other numerical predictions for complex shapes where results are absent in the literature are compared among themselves using various degrees of refinement for the grids.

Sadasivam et al [7] modeled single and hexagonal channels completely formed laminar flow. The range of Reynolds number is 300-3000.

A coordinate transformation is used to map the irregular cross section on a rectangular arithmetic field. Thermic boundary conditions are taken into account since they are the most common defining conditions in most applications. For a broad range of airway aspect ratios and four distinct trapezoidal angles, solutions to changes in velocity and temperature are obtained. The results for the coefficient of friction and the Nusselt number show a strong dependence on the duct geometry (aspect ratio g and trapezoid angle y).

Zhang and Chen [8] studied the fluid flow and heat transfer in a cross-corrugated triangular duct were modeled and experimentally tested under a uniform heat flux boundary condition. The range of Reynolds number is 300-3400..In membrane-based air-to-air heat mass exchangers, cross-corrugated triangular ducts have high heat mass transfer capabilities. On membrane surfaces, the mixing effect will increase the convective heat mass transfer coefficients. The model is validated using heat transfer experiments and a high-speed hot wire strength measurement technique. Pressure drop and average Nusselt numbers are determined using correlations under uniform boundary conditions for heat flow. As shown in figure(2-2).

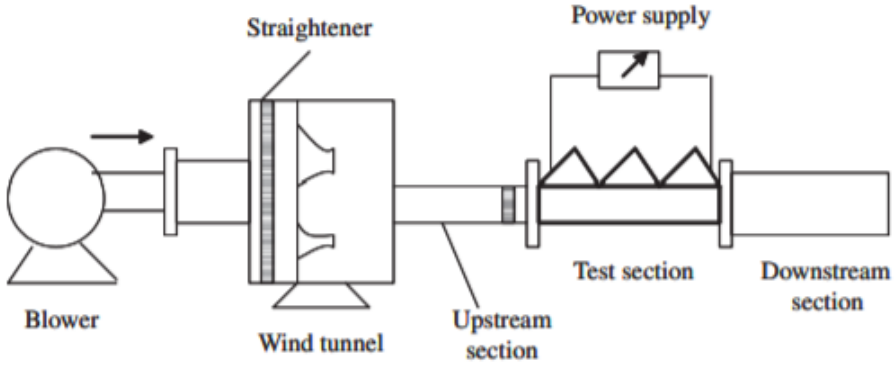

Figure(2-2) Schematic of the experimental setup.

Muzychka and Yovanovich [9] considered the development of a new model for numeral prediction in the combined entrance area of non-circular channels and channels, as well as laminar heat transfer in the combined inlet zone of non-circular channels. This model predicts local and mean Nusselt numbers for both isothermal and flow-limited conditions. Flat plate convection, thermally evolving fluxes in non-circular channels, and completely formed flux in non-circular channels were used to design the model. The effect of the duct form on the Nusselt number is reduced by using a new characteristic length scale, the square root of the cross-sectional area. Several existing models of circular tube and parallel plate channels, as well as numerical data from several non-circular channels, are compared. For most types of air ducts, agreement between the proposed model and digital data is 615 percent or better.

Renksizbulut and Niazmand [10] investigated numerical methods in the Reynolds number range of 10 to 1000, establish three-dimensional laminar flow and heat transfer in the entrance region of trapezoidal channels. Both related heat and momentum exchange parameters, as well as the primary and secondary velocity fields, have been investigated. The current findings for the fully formed flow area of the channels are consistent with previous research. The axial velocity profiles grow overshoots near the walls and especially at the channel corners in the entrance area. For Reynolds numbers over 50 and after a few hydraulic diameters from the channel inlet, boundary-layer style approximations, which lead to Reynolds number-independent Poiseuille and Nusselt numbers, can be used. Hydrodynamic entrance lengths measured using methods based on fully developed flow data have often

shown to be grossly inaccurate. For the entrance length, as well as the friction and heat transfer coefficients, new correlations are suggested.

Yan and chiu [11] studied radiation's impact on the properties of thermal mixed fluid flow and heat transfer in oblique channels The vortices - velocity method was used to solve the three-dimensional Navier-Stokes equations as well as the energy equation. The discrete coordinate approach was used to solve the equation for integrated differential radiative conversion. The effects of thermal buoyancy and radiative transport on the distributions of mass fluid temperature, friction factor, and Nesselt number are discussed in great detail. The findings show that radiation has a substantial impact on heat transfer and tends to mitigate the effects of thermal buoyancy.

Philip et al.[12] determined experimentally the surface of a circular to rectangular transmission channel used to calculate local heat transfer using a transient liquid crystal heat transfer technique. The length-to-diameter ratio of the transmission channel is 1.5, and the aspect ratio of the exit stage is 3. The equation of the super-ellipse determines the cross-section geometry. The cross-sectional area was the same at the entrance and exit, but fluctuated by up to 15% during the transition. For Reynolds numbers based on inlet diameters ranging from 0.4×10^6 to 2.4×10^6 and two free current turbulence strength produced by the grid of about 1%, test results are recorded, which is typical for wind tunnels, and up to 16 percent, which may be more typical For real engine conditions.

Ray and Misra [13] employed for two types of boundary conditions, namely, constant axial heat input and uniform peripheral wall temperature, and uniform axial and peripheral heat input, the least squares point matching

technique was completely developed by triangular and square channels with round corners. They concluded that the friction factor and electiveness of the round portion for both of the considered duct geometries increased rapidly with increasing the radius of the round corners.

Liu and Wang [14] reported in a tightly curved rectangular duct, the latest work on bifurcation and stability is completely developed. The physical mechanism and driving forces for the different flow mechanisms in obstetrics are still being debated. The flow stability on the various branches is calculated using a simple transient calculation based on the complex responses of multiple solutions. Finite random disturbances cause flows from one steady state to another steady state, cyclic oscillation, periodic oscillation, other cyclic oscillation, and chaotic oscillation as the dean number increases. For all physically achievable fluxes, the average friction factor and the average Nusselt number are determined.

Wong and Leung [15] conducted experimentally, with Reynolds numbers based on hydraulic diameter ranging from 4300 to 15000, in a fully established hydrodynamic turbulence condition. In an air-cooled equilateral horizontal triangular tube, arterially rough inner surfaces are used to improve the steady state of forced load (peak angle of 60). Four types of internal surfaces are required for triangular test ducts with the same axial length of 2.4 m and hydraulic diameter of 0.44 m. The inner surfaces of the triangular channels were coarse articulated allies either by milling / shaping methods, in addition to the smooth surface with an average surface roughness of less than 1 m.

Kurnia et al. [16] performed heat transfer output of spiral ducts with different cross-section areas within an aircraft. In total, six channel cross-sections - rectangle, rectangular 2 1, rectangular 4 1, trapezoid, semicircular, and triangular cross-sections - were examined and their form and merit were compared to the straight channel. The findings show that the coil ducts within the plane have a higher heat transfer rate on average. It should be noted, however, that the heat transfer rate of a coil within a plane with a rectangular, triangle, or half circular cross-section is lower than that of a straight duct under constant heat flow conditions. In contrast to the straight channel, it also has a much higher pressure drop penalty. As a result, choosing the intra-plane winding channel geometry for the heat transfer application necessitates a detailed review of the operating conditions. The heat transfer output of the in-plane coil duct for electronic refrigeration applications will be studied in an expansion analysis.

Mohammad Mohsen et al. [17] obtained for the first time, a precise analytical solution for heat transfer in straight ducts with rectangular cross sections has been discovered. This solution was true for boundary conditions involving fully defined heat transfer in the duct walls with continuous heat flow. The closed form of the temperature distribution is found using the method of separating variables and various other mathematical techniques. The aspect ratio functions are often used to obtain the local and average NSLT numbers. In non-dimensional analysis of boundary conditions, a new physical restriction was introduced to solve the Newman problem. This is one of the current study's major inventions. When calculating local and mean NSTL numbers, analytical results reveal a uniqueness with a critical width-to-height ratio of 2.4912.

Khatri and Agarwal [18] used the finite element approach to solve partial differential equations of fluid flow, computational simulation of laminar flow in a parallel plate channel for different entry velocity. A partial differential equation (Poisson's equation) is used to describe fluid flow. The energy equation is used to analyze heat transfer. The partial temperature flow differential equations are then solved using the flow field of this liquid. The effects of heat flux from outside the system on the temperature flux field was also investigated. Analyzes are carried out by looking at the flow field, as well as the temperature and pressure fields, for various entry velocity values. The change in entry velocity had a major effect on fluid flow, temperature flow, and strain, according to the findings.

Chen et al.[19] investigated heat transfer through irregular channels with cross corrugation and the use of uniform boundary conditions for heat flow was achieved. The results of the coefficient of friction and a Nusselt number obtained from experiments and simulations exhibit that the flow in the duct with a = 90° has the greatest. The included angle affects the flow and heat transfer in the intersecting wavy triangular channels in different ways. For example, under the same Re, friction D at angle = 120° is lower than friction at angle = 60° and 45°, while, Nusselt D at angle = 120° is higher than Nusselt D at angle = 60° and 45°.

Ebaid et al [20] showed in irregular ducts, completely formed laminar flow. In all possible combinations, the analysis focuses on the irregular area between the triangular and circular equilateral canals. The governing equations are solved using the high-order finite element method for this reason. In any case regarding particular engineering, higher values of area ratio lead to a monotonic increase in the value of Renolde number at the

values for hydraulic diameter for the uniform loop. Most notably, the non-uniform rings outperformed the usual rings, so they could be used in double-channel heat exchangers instead of the traditional normal rings. As a result, the pumping power needed in such industrial applications will be substantially reduced.

Braz. [21] showed valid analysis of low values of Rayleigh rotational number. It was discovered for the elliptic channels in the fully formed flow area. Rayleigh rotation number, adjusted Reynolds number, Rem number, Prandtl and Pr are functions of axial velocity and temperature profiles, as well as Nusselt number and coefficient of friction. These effects are marginal at such a small diameter. Rayleigh rotational number, Rat, and Prandtl number, Pr, vary around the main diameter, but the axial velocity profiles are unaffected. The adjusted Reynolds number increases the maximum value of the temperature and axial velocity profiles by a large amount.

Sivakumar et al. [22] explained the heat transfer and pressure drop of smooth and three different sized square ribbed divergent rectangular ducts were compared in a systematic experimental study. The rib tabulators (e) were 3, 6, and 9 mm tall. With a fixed rib pitch (p) to test section inlet width (w) ratio of 0.6 and an equal mass flow rate, this yields a rib height (e) to mean hydraulic diameter of the duct (Dim) ratio of 0.035, 0.0697, and 0.1046 respectively. The results of the ribbed ducts were compared to those of a smooth (no ribs) divergent rectangular duct with the same parameter. As shown in figure(2-3).

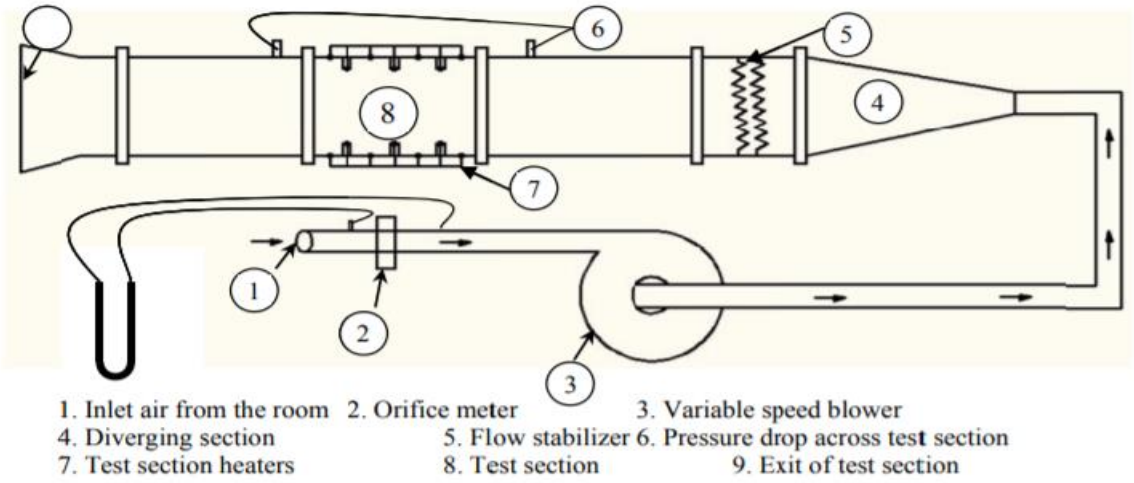

Figure(2-3) Experimental setup schematic of the divergent duct

Schrittwieser et al.[23] analyzed of computational fluid dynamics was used to study fluid flow in the stator ducts of a hydro accumulator. The main aim is to find out how much of the model can be streamlined in order to speed up the simulation. As a result, the relationship between the rotor and the stator is critical and must be considered. The Frozen Rotor and the Stage model are two steady-state simulation reference models that can be connected using the ANSYS CFX software kit. Their variations are visible in two parameters that are used to compare these two entirely different reference models. The comparison of fluid flow and heat transfer along one of the stator channels is another important aspect stated in this paper.

Onur and Arslan [24] investigated experimentally of a horizontal smooth trapezoidal duct with different corner angles in the Reynolds number range of 102 to 103, steady-state laminar forced flow and heat transfer are studied. Under a uniform surface temperature state, the flow is hydrodynamically completely formed and thermally evolving. New engineering correlations for heat transfer and friction coefficients for each

corner angle were presented based on current experimental data of laminar flow in the thermal entrance area. The findings show that as the Reynolds number rises, the heat transfer coefficient rises while the Darcy friction factor falls. Also, as the duct's corner angle increases, the average Nusselt number increases while the average Darcy friction factor decreases.

Hartnett and Minkowycz [25] illustrated the numerical process, completely formed hydrodynamic fluid flow within irregular cross-section ducts. To convert the partial differential equations of a random and irregular spatial plan from a physical field to a square arithmetic field, the elliptical grid generation method is used. The problem is then solved for uniform wall temperature as well as uniform wall heat flow boundary conditions. For the triangular, rhombic, sinusoidal, and irregular cross sections commonly used in heat exchangers, numerical results of the Nusselt number and friction factor are shown.

Bhadouriya et al [26] presented the heat transfer and friction factor for air flow within a square duct were measured experimentally and through 3D numerical simulations under uniform wall temperature limits, twist ratios of 11.5 and 16.5, and Reynolds numbers of 600–70,000. Using commercially available tools, a three-dimensional study of fully defined static laminar flow within the square cross-section flow region of the Reynolds number range of 100 to 100,000 is performed. For a twist ratio of 2.5 and a Reynolds number of 3000, the product of friction factor and Reynolds number reaches its maximum value. For the same values of Prandtl number 20, the maximum Nusselt number is observed. The vortex modulus of the laminar flow system was used to establish correlations for the friction factor and Nusselt number. The local distribution of the friction factor to Nusselt number across the cross

section has been demonstrated. To compare twisted and straight channels, the reinforcement factor is calculated using parameters of constant pumping capacity. The enhancement factor is used to rank the twisted square duct options. The convoluted duct was discovered to function well in laminar flow. For the entire range of Prandtl numbers examined, the twisted square channel is suggested in a laminar flow system.

Ghobadi and Muzychka [27] reviewed in the curved tube, the heat transfer and pressure drop correlation of a fully formed laminated Newtonian fluid flow. Curved engineering is one of the passive heat transfer methods that can be used in a variety of applications, including power generation, chemical and food processing, electronics, and environmental engineering. The main goal of this review paper is to give researchers a detailed list of similarities and concepts that they may need during their study. The paper starts with an overview of the governing equations and key dimensionless figures for curved tube flow. The flow production in curved and coiled circular tubes has also been shown to have correlations. The study's key contribution is an analysis of the numerical and experimental correlations for calculating the coefficient of friction and the Nusselt number in circular curved tubes. Thermodynamic boundary conditions and procedure are used to classify Nusselt number correlations.

Wang et al [28] developed the heat transfer and flow characteristics of irregular channels with various centric lengths (P = 120 mm, 140 mm, and 160 mm) and comparisons to rectangular and trapezoidal channels The governing equations, including the mass conservation equation, momentum equation, and energy conservation equation, were developed in the curved channels. The parabolic channel, trapezoidal channel, and rectangular channel

had the highest average heat transfer efficiency of the three channels, from best to worst. The parabolic channel, which is 5.1 percent and 25.4 percent larger than the trapezoidal and rectangular channels, has the best overall improved heat transfer efficiency.

Tokgoz and Sahin [29] determined the flux characteristics and thermal efficiency of different duct engineering numerically and experimentally. Complete studies of Reynolds numbers were conducted in the range of 3103 Re 6103. In order to increase the aspect ratio, S / H, the thermal efficiency of these geometries was numerically examined. The turbulence intensity rate on the corrugated channel axis increases as the ripple height is increased, as predicted. Using the particle image velocity (PIV) technique, experimental studies were performed to describe the hydrodynamic structures and verify the numerical solution results. In order to reveal the hydrodynamic properties and thermal efficiency of the corrugated channel flow, velocity distributions, rheological patterns, and corresponding turbulent statistics were calculated experimentally and numerically.

Maithani et al [30] calculated three-dimensional computational fluid dynamics (CFD) a coarse solar air heating duct was investigated for heat transfer and friction properties. The roughness of the delta wavy ailerons' form has never been confirmed before. For different Reynolds numbers between 3000 and 18000, the Nusselt number and friction factor properties are calculated. The k-perturbative model was used for the study after reviewing the literature. On the flat plate with a relative longitudinal pitch of 3 and five winglets at Reynolds count 5000 and a 10.3-fold increase in friction factor, the maximum Nusselt number enhancement was found to be

2.23 times. The configuration achieved a maximum thermal-hydraulic efficiency of 2.08.

Zunaid et al. [31] described a rectangular and semi-cylindrical fine-channel heat sink's heat transfer and pressure drop properties The copper heat dispersants were aligned in a series of 21 micro channels, each measuring 231 m wide and 713 m long. Water was being used as a coolant and moving through the channels. With a constant heat flux of 106 W / m2 defined with respect to the region of the heat sink platform, a 3D analysis was performed for Reynolds numbers ranging from 200 to 1000. An ANSYS-CFX kit was used to test the temperature rise and pressure drop of the liquid in the straight-line micro-channel heat sink, and experimental data was used to verify the results.

Nandan and Janoske [32] formulated numerical of the heat transfer properties of. Here are three-dimensional laminar flows in a rectangular duct with four separate ailerons. The standard Delta airfoils make up the four wing forms, while the three modern ailerons are the Arrow, Delta Slash, and X wing. The goal is to see how the shape of the wing affects the rate of heat transfer, pressure loss, and thermal boost factor. The heat transfer rate and thermal efficiency of the rectangular duct flux with the wing should increase, according to the numerical results. A higher Reynolds number means a faster rate of heat transfer, a higher heat-boosting factor, and more pressure loss. Increases in flux attack angle were found to be beneficial to the X winglet but detrimental to the delta and delta ailerons. The current study's increase in heat transfer rate and heat boost factor were found to be 1.382.18 and 1.331.94, respectively, over air duct flows without wing.

Zhang and Li[33] presented a trapezoidal heat transfer surface, which can overcome the defects of the rectangular heat transfer surface, and it has a uniform temperature distribution in the direction of air flow. A standard wind tunnel test bed was built, and the heat transfer coefficients of the trapezoidal and rectangular heat exchanger with the same total heat transfer area and flow conditions were compared. In the meanwhile, the feasibility of the numerical simulation method was also verified.. Besides, the trapezoidal duct has a uniform temperature field distribution in the direction of air flow. By introducing evaluation index TPF (Thermal performance factor), we concluded that: the trapezoidal duct has better comprehensive heat transfer performance than that of the rectangular.

Zhang and Wan [34] formulated numerically in rectangular trapezoidal channels, laminar flow and heat transfer are studied. The temperature difference distribution and pressure drop in trapezoidal channels are greater than those in rectangular channels under some conditions, resulting in an advantage of improved heat transfer. The maximum Colburn factor (j) in trapezoidal channels increases by 8% over rectangular channels in the same heat transfer area, while the minimum friction factor (f) decreases by 22.6 percent. The thermo-hydraulic properties of the trapezoidal channels increase first, then decrease as the slope angle (b) increases, according to the numerical results. In short, when B 40, trapezoidal channels have stronger thermo-hydraulic properties than rectangular channels. On the other hand, As a consequence, when b> 40, the output of the rectangular channel outperforms the trapezoidal channels. The taguchi approach was used to illustrate the applicability of the above conclusions.

Zhang [35] considered the laminar flow inside rectangular duct in the development of a heat exchanger with a low Reynolds number. Heat transfer from a rectangular cross section with different aspect ratios to thermally developed and dynamically evolving inside an air duct has been well researched and reported in various books, but little work has been done for lamellar fin ducts. The primary assumption in this research is that the conduit is held at a constant temperature and that the heat fluxes on two fins are distributed in a symmetric deflection pattern. The thermal conductivity of a liquid is studied as a conjugate problem at the same time. The Nusselt numbers, which can be used to estimate the heat transfer efficiency of finned heat exchangers with different thermal conductivity and thicknesses, are obtained in the developing field, the length of the heat input, and the fully defined values for these pathways.

Rang et al. [36] conducted experimental investigations to study the forced convective heat transfer and pressure drop characteristics of the hydrodynamic fully developed flow in heated uniformly horizontal triangular ducts for smooth and different surface roughness. Non-dimensional expressions for the determination of the heat transfer coefficient and friction factor of the triangular ducts were developed. The mixing effect would intensity the convective heat mass transfer coefficients on membrane surfaces. Heat transfer experiments and a high-speed hot wire intensity are used to measure the temperature.

Talib et al. [36] investigated experimental to study the effect of an irregular shape geometry duct on the heat transfer and fluid flow characteristics. During the study, it was measured the temperature distribution, and air velocity through a duct with the different cases study of

boundary conditions. The main part of the duct is designed with dimensions 3.65 m length,0.4 m width, 0.5 m height, and 1mmthickness. Three duct components: length 1.25 m, width 0.4 m and height 0.25 m for the entrance section, length .2 m for the test section and length 1.25 m, width 0.4 m and height 0.5 m for the exit section. In a two-dimensional laminar flow, numerical simulation is carried out and the projected model deals with the distribution of temperature along the irregular duct test by numerically solving the finite difference method describing the energy equation. ANSYS - 19.2 Fluent. The flow characteristics of airflow through the irregular duct was analyzed.

2.1. Summary

According to the literature review, some normal duct configurations have been extensively investigated, while irregular duct configurations have reviewed a little study. They are focused on the laminar steady flow of Newtonian fluid in the duct spacing between normal and irregular ducts in all possible configurations. The heat transfer, pressure drop, and defined velocity of air flow through duct are all described in this literature. Many researchers used finite differences and finite element analysis to study heat transfer, and flow characteristic.. Table(2-1) illustrated the researchers which are worked in this filed.

In the present work, numerical and experimental are investigated. The temperatures distribution for hot and cold air through irregular duct are studied. Also, it is studied the flow of air characteristic inside the irregular duct in order to solve the temperatures distribution by using finite difference scheme.

Authors	Type of Study	Re	The aim
Bijan Farhanieh ,and Bengt Sunden. (1991)	Numerical study	**150-1700**	The laminar convective flow and heat transfer in a duct with a trapezoidal cross-sectional area are studied numerically
Manica F. Naccache and Paulo R. Souza Mendes (1996)	Numerical study	**300-1000**	Heat transfer to non-newtonian fluids flowing laminarly through rectangular ducts is examined.
R.M.ManglikJ.Ding(1997)	Numerical study	**1000-3000**	considered fully developed, constant property, laminar flows of viscous power-law fluids in irregular ducts
A. Campo, J. C. Morales, A. E. Larreteguy(1997)	Numerical study	**350-1900**	presented a fast and dependable numerical procedure for the solution of the fully established velocity and temperature of low-Reynolds number flows inside straight ducts with irregular, singly connected cross sections.
Rajashankar Sadasivam, Raj M. Manglik, Milind A. Jog.(1999)	Numerical study	**100-350**	Laminar, fully developed ¯ow through single- and double-trapezoidal (or hexagonal) ducts is modeled using a ®nite-di€ erence method.
Li-zhi Zhang , Zuo-yi Chen. (2000)	Experimental study	**300-2400**	Cross-corrugated triangular ducts provide high heat mass transfer capabilities in membrane based air-toair heat mass exchangers.

Table (2-1) summery for the previous studies.

Authors	Type of Study	Re	The aim
A new model for predicting Nusselt numbers in the combined entrance	Numerical study	**50-180**	A new model for predicting Nusselt numbers in the combined entrance region of noncircular ducts and channels is developed.
Metin Renksizbulut,and Hamid Niazmand(2006)	Numerical study	**10-1000**	Simultaneously developing three-dimensional laminar flow and heat transfer in the entrance region of trapezoidal channels have been investigated using numerical methods
Wei-Mon Yan, Han-Chieh Chiu , (2007)	Numerical study	**$10-10^3$**	A numerical study was carried out to investigate the radiation effect on the characteristics of the mixed convection fluid flow and heat transfer in inclined ducts
Haydar KÜÇÜK, Mete AVCI, Orhan AYDIN and Habip ASAN. (2008)	Numerical study	**20-150**	A numerical study is conducted on the heat and fluid flow characteristics in an annulus between two concentric square ducts..
Philip Poinsatte, Douglas Thurman,andSteven Hippensteele (2008)	Experimental study	**10^3-10^6**	Local heat transfer measurements were experimentally mapped using a transient liquid-crystal heat transfer technique on the surface of a circular-to-rectangular transition duct
Ray and Misra (2008)	Numerical study	**150-4500**	employed for two types of boundary conditions, namely, constant axial heat input and uniform peripheral wall temperature, and uniform axial and peripheral heat input
Fang Liu , Liqiu Wang (2009)	Experimental study	**1000-2500**	The present work is on bifurcation and stability of fully-developed forced convection in a tightly curved rectangular duct

Authors	Type of Study	Re	The aim
Wong and Leung (2009)	Experimental study	**4300-15000**	conducted experimentally, with Reynolds numbers based on hydraulic diameter ranging from 4300 to 15000, in a fully established hydrodynamic turbulence condition
Kayhani, M. R. H. Nobari, and M. Karimi Demneh. (2009)	Numerical study	**50-200**	fully developed flow and heat transfer of viscoelastic materials in curved ducts with square cross section under constant heat flux have been investigated
K. R. Aharwal, B. K. Gandhi, J. S. Saini . (2010)	Experimental study	**2000-20000**	Artificial roughness in the form of repeated ribs is generally used for enhancement of heat transfer heated surface to the working fluid.
Jundika. KURNIA , Agus. SASMITO , and Arun. MUJUMDAR (2012)	Numerical study	**100-1000**	The objective of this study was to carry out a parametric study of laminar flow and heat transfer characteristics of coils made of tubes of several different cross- -sections e. g. square, rectangular, half-circle, triangular, and trapezoidal
Mahmood NOROUZI, Mohammad Hassan,AMIRI DELOUEI. (2012)	Numerical study	**150-2000**	An exact analytical solution is obtained for convective heat transfer in straight ducts with rectangular cross-sections for the first time
Rajesh Khatri, and Pankaj Agarwal. (2012)	Numerical study	**641-3605**	heat transfer and fluid flow characteristics in a channel has been theoretically investigated.
Zuoyi CHEN , Lizhi ZHANG, and Han SONG (2013)	Experimental study	**250-2500**	Included angles (a) have vital effect on the flow and heat transfer in cross-corrugated triangular ducts

Authors	Type of Study	Re	The aim
Munzer S.Y. Ebaid , Osamah M. Haddad,and Laith R. Batarseh (2013)	Numerical study	**100-2800**	The aim of this study is to reduce the required pumping energy by obtaining accurately the friction factor – Reynolds number product (fRe) of the steady fully developed laminar flow in annular ducts
P Braz, A Latos-Bielenska, M O'Mahony(2013)	Numerical study	**20-100**	showed valid analysis of low values of Rayleigh rotational number. It was discovered for the elliptic channels in the fully formed flow area.
K.Sivakumar, Dr.E.Natarajan, Dr. N.Kulasekharan. (2014)	Experimental study	**20000-60000**	- the work reported in this paper is a systematic experimental heat transfer and pressure drop comparison between smooth and three different sized square ribbed divergent rectangular ducts
Schrittwieser, Andreas Marn, Ernst Farnleitner, and Gebhard Kastner. (2014)	Numerical study	**100-17000**	describes the analysis of the fluid flow in the stator ducts of a hydrogenerator using computational fluid dynamics.
N. Onura & K. Arslanb. (2014)	Experimental study	**80-1000**	steady-state laminar forced flow and heat transfer in a horizontal smooth trapezoidal duct having different corner angles were experimentally investigated in the Reynolds number range from 10^2 to 10^3 .
JP Hartnett, WJ Minkowycz(2015)	Numerical study	**10-1000**	illustrated the numerical process, completely formed hydrodynamic fluid flow within irregular cross-section ducts
Rambir Bhadouriya, Amit Agrawal, S.V. Prabhu(2015)	Experimental study	**230-4000**	Heat transfer and friction factor characteristics of air flow inside twisted square duct are studied experimentally and through three-dimensional numerical simulations

Authors	Type of Study	Re	The aim
Mehdi Ghobadi & Yuri Stephan Muzychka. (2015)	Numerical study	**930-70000**	Heat transfer and pressure drop correlations for fully developed laminar Newtonian fluid flow in curved and coiled circular tubes are reviewed
Xilong Zhang, Yichun Wang , Runze Jia, Rui Wan(2016)	Experimental study	**10-1000**	The laminar convective flow and heat transfer in trapezoidal ducts with a rectangular cross-section are studied numerically
Rajesh Maithania*, Siloria , Jitesh Ranaa , Sunil Chamoli (2017)	Numerical study	**1800-17000**	In the present investigation, 3-dimensional Computational fluid dynamics investigation has been carried out to study the heat transfer and friction characteristics of a solar air heater duct roughened with wavy delta winglets
M. Zunaid1 , A. Jindal1 , D. Gakhar1 , A. Sinha1. (2017)	Numerical study	**250-1500**	The heat transfer and pressure drop characteristics of a straight rectangular and semi cylindrical projections microchannel heat sink were investigated.
Varchasvi Nandana∗ , Uwe Janoske(2018)	Numerical study	**160-2800**	Local heat transfer measurements were experimentally mapped using a transient liquid-crystal heat transfer technique on the surface of a circular-to-rectangular transition duct
Yongliang Zhang1 & Min Li1(2019)	Numerical study	**4000-18000**	presented a trapezoidal heat transfer surface, which can overcome the defects of the rectangular heat transfer surface, and it has a uniform temperature distribution in the direction of air flow
Xilong Zhang, Bilong Liu , Jiang Liu, Xingang Wang, Hongbo Zhang (2019)	Experimental study	**1000-6000**	the heat transfer and flow characteristics of parabolic ducts with different focal lengths are analyzed and compared with rectangular and trapezoidal ducts respectively

Chapter Three

Experimental Work

Experimental Work

3.1. Introduction

Experimental study gives more description and global analysis to measure the heat transfer of fluid flow through irregular geometric duct.

In the present work, the experimental investigations has been carried out to study the effect of irregular shape geometry duct on the heat transfer and fluid flow characteristics . During this study, it was measured the temperature distribution, and air velocity through duct with different case studies of boundary conditions.

3.2. Test Equipment

1-Duct

The main part of rig design in experimented work is a duct which is designed irregular dimensions duct, and 1mm thickness as shown in figure (3-1). It made of galvanized steel. This material is standard for using fabricating ductwork for most comfort air conditioning systems. This rig duct consists of three parts. The first part is entrance section with dimensions 1.25 m length, 0.4 m width and 0.25 m height. This part is designed as a rectangular shape with the value of length 1.25 m in order to achieve a fully developed zone. The second part is test section, which is designed irregular as curve shape with length 1.2 m as shown in figure (3-2). The third part is the exit duct section which is designed as a square shape with dimension 1.25 m length, and rectangular section (0.5 x 0.4) m to minimize the rate of the exit effects of the test section. All parts of duct were insulated in order to minimize the rate of thermal loss through metal of duct in experimental measurements.

2- Blower

The blower is centerfugial which is sucked air into geometrical duct. It has an electrical motor with specifications 800 watts , 220 volts ,and frequency 50 Hz . It has range velocity between (1m/s to 6m/s), as shown in figure (3-3) .

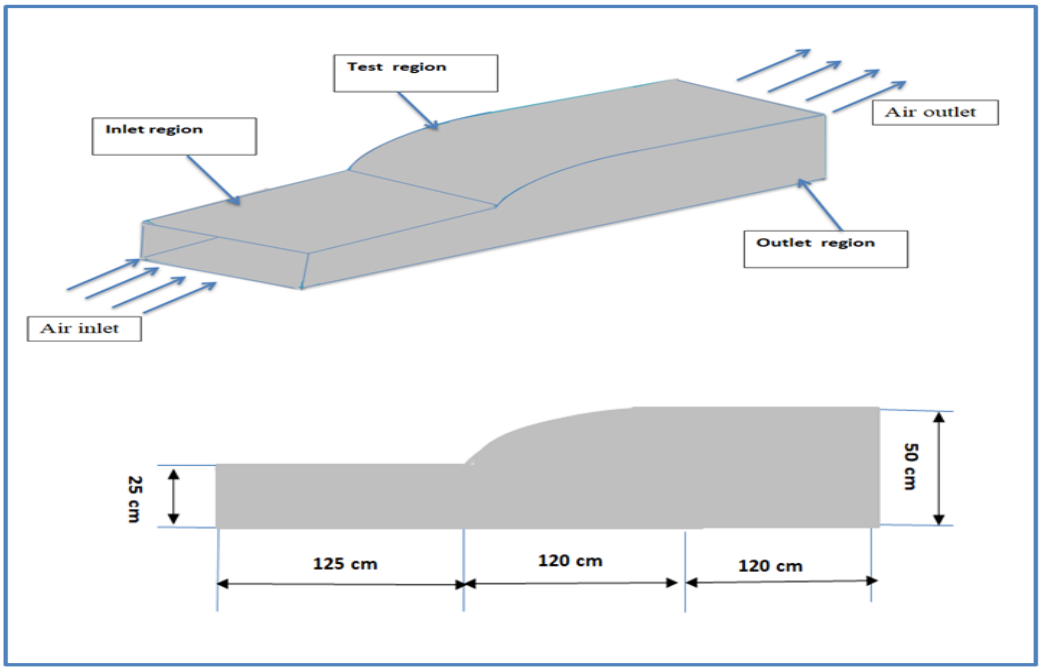

Figure (3- 1) schematic diagram of rig duct

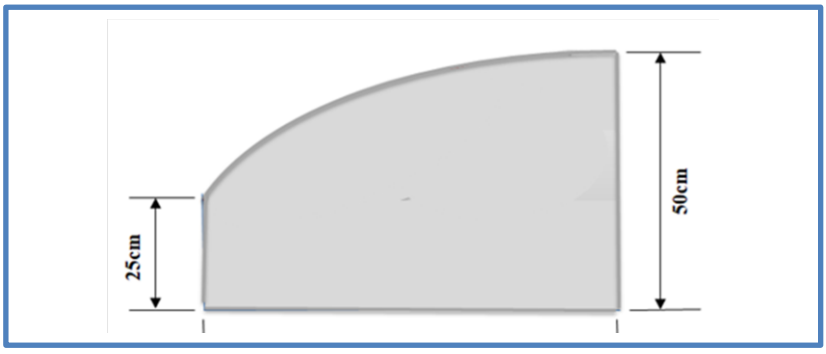

Figure (3-2) schematic diagram of test duct

3-Fan Coil

Fan coil **c**onsisting of a blower and a heater which is placed at the front of the blower to supply hot air into rig duct. The blower has an electrical motor with specifications 800 w , 220 volts ,and frequency 50 Hz . It has range velocity between (1m/s to 6m/s), and a heater has 1200 w, and 150 volts as shown in figure (3-4)

Figure (3-3) centerfugial blower

Figure (3-4) fan coil

4-Air Cooler

Air cooler is an axial of rotation to supply cooling air into rig duct. It has an electrical motor with specifications 500 w , 230 volts, 1.3A ,and frequency 50 Hz . It has range velocity between (1m/s to 6m/s) as shown in figure (3-5)

5-Heater

The electrical heater is considered the source of heat flux on the surfaces of the test section. It is made from nickel chrome alloy consist of six

turns and connected with power analyzer device to measure the power supply , as shown in figure (3-6).

Figure (3-5) air cooler

6- Voltage Variation Device

To control the value of power supply to the heater, a variable voltage device is used. This device can supply different values of voltage with range of (0 to 220) volts .This variation is controlled by changing of internal resistance until reaches the required value of voltage as shown in figure . (3-7).

7- Power Analyzer Device

Digital power analyzer type Lutron model (DW-6091) with a maximum current (10 A) and maximum voltage (600V) is used to transform the voltage (analog) signal from the power supply into a digital signal which can be read, as shown in figure (3-8).

Figure (3-7) Voltage Variation Device

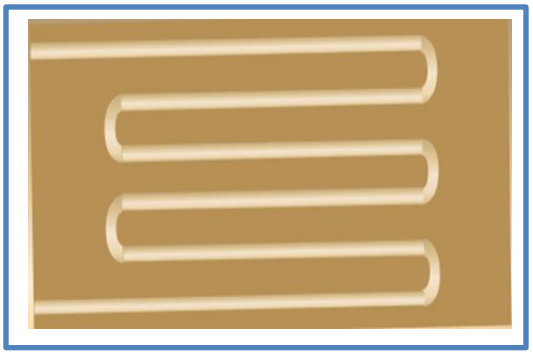

Figure (3-6) heater

Figure (3- 8) power analyzer device

3.3. Measurement Devices

3.3.1. Temperature Recording Device

The temperature recorder is a (12) channel model BTM-42085D, which is used by the paperless SD card in order to save time-related data as shown in figure (3-9). The echtzeit data logger saved (12) channel temperature that is determined by time (year, month, date, minutes, seconds) in SD memory card and downloaded to excel software.. The sampling time of the date logger varies from 1 to 3600 seconds. It has resolution degree/0.1,

size of the SD card is 1GB and 16 GB . Rs232/USB interface provides intelligent functionality and the microcomputer circuit is highly precision .

Figure (3-9) temperature recording device.

Two devices are used to measure temperature inside the rig duct. A type of thermocouple (K) is used to measure temperature. Figure (3-10) shown the thermocouples locations along the rig duct. 15 thermocouples are fixed in irregular duct (test duct) in order to measure the temperatures distribution through the air flow in irregular duct at three cases of boundary conditions.

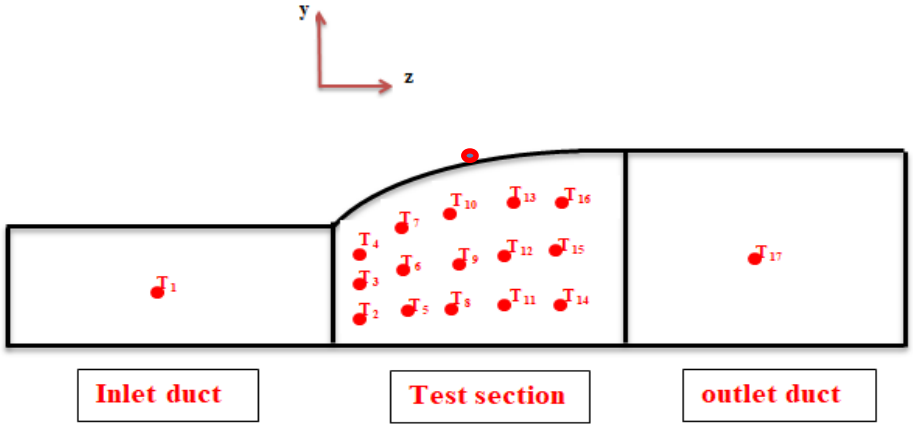

Figure (3-10) location of thermocouples in irregular duct(test duct).

3.3.1.2. Temperature Recording Calibration

Temperature measurements are calibrated with the SUMMIT SDT 150 digital thermometer as shown in figure (3-11). Chromium and aluminum thermocouple type (K) is extensively used for temperature measurement in the range -200◦C to +1250◦C, as shown in figure(3-12). **Omega [40]** gives information of thermocouple types as shown in table (3-1). The reading for both thermocouples and UMMIT SDT 150 digital are measured . The calibration method is performed by two instruments with different temperature from 19^{o}C to 80^{o}C to calculate the value of the temperature of air. The relation of temperature readings for two devices is shown in figure (3-13). Thermocouple measurement correction has been accomplished by a polynomial equation, this relation is :

$$T_{calib.} = -0.9481 + 1.0341T_{red} + 0.0002T^{2}_{red} - 0.000005\,T^{3}_{red} \quad \ldots\ldots\ldots (3.1)$$

Table (3-1) thermocouple information .

Thermocouple type	Name of Materials	Useful Application Range (◦C)
E	Chromium(+) Constant (-)	-200-900
J	Iron(+) Constant(-)	0-750
K	Chromium(+) Aluminum(-)	-200-1250
T	Copper(+) Constant(-)	-250-350

3.3.2. Hand-held Digital Anemometer

Digital anemometer measures the velocity of air . Depending on the model, an air velocity meter also can possess data logging or data recording functionality to take measurements over a period of time, as shown in figure(3-14) .

Figure (3-11) SUMMIT STD 150 device **Figure (3-12) thermocouple type (K)**

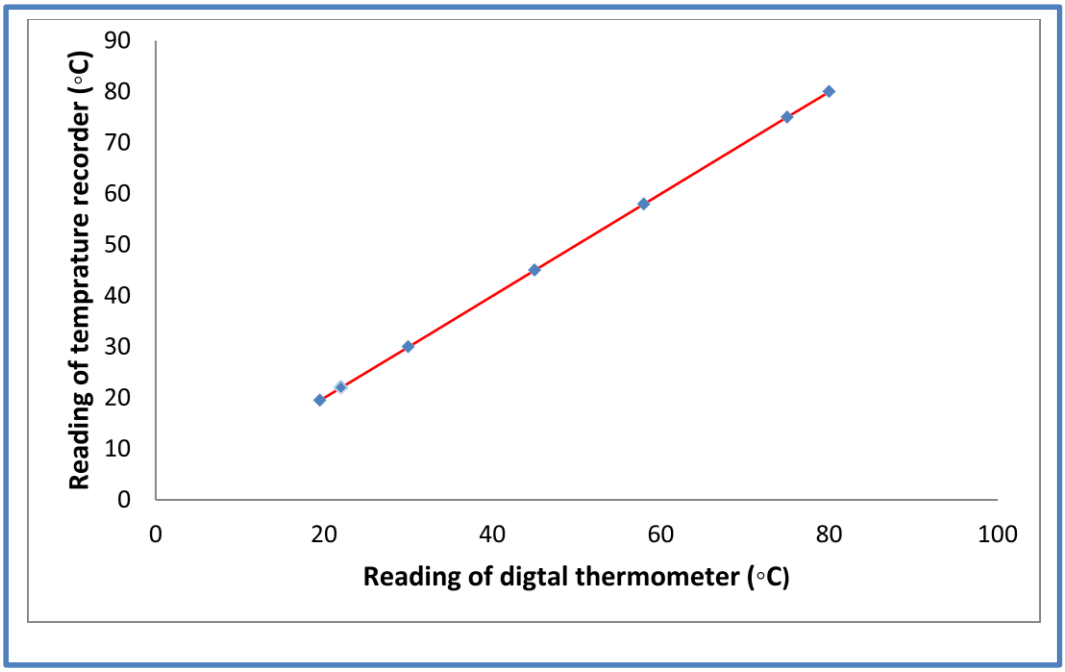

Figure (3- 13) curve of temperature calibration

3.3.2.2. Velocity Calibration

Velocity is calibrated with a digital calibration device type (Hot Wire Anemometer) as shown in figure (3-15). The hot wire anemometer device is used for measuring the velocity and direction of the fluid. This can be done by

measuring the heat loss of the wire which is placed in the fluid stream. The wire is heated by electrical current. The hot wire when placed in the stream of the fluid, in that case, the heat is transferred from wire to fluid, and hence the temperature of wire reduces. A polynomial equation is obtained to correct the velocity measurement readings as:

$$V_{cali.} = 0.2201 + 0.8926V_{red} - 0.0031\ V_{red}^2 + 0.00061\ V_{red}^3 \quad \text{.....(3.2)}$$

Figure(3-16) shows the curve of velocity calibration.

Figure (3-14) Hand-held digital anemometer

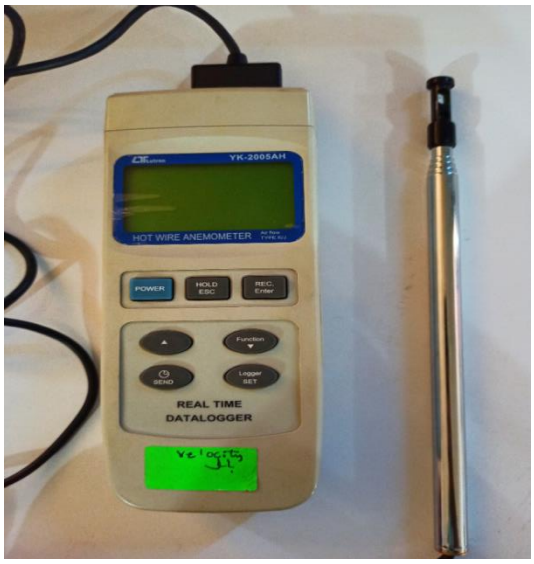

Figure (3- 15) Hot Wire Anemometer

Five digital anemometer are fixed in rig duct in order to measure the air flow velocity through the experimental work at three cases of boundary conditions. Three digital anemometer are fixed in irregular duct in different locations. Also, one anemometer fixed in inlet duct to measure the initial flow air velocity and another anemometer fixed in outlet duct to measure the outlet velocity of air, as shown in figure (3-17).

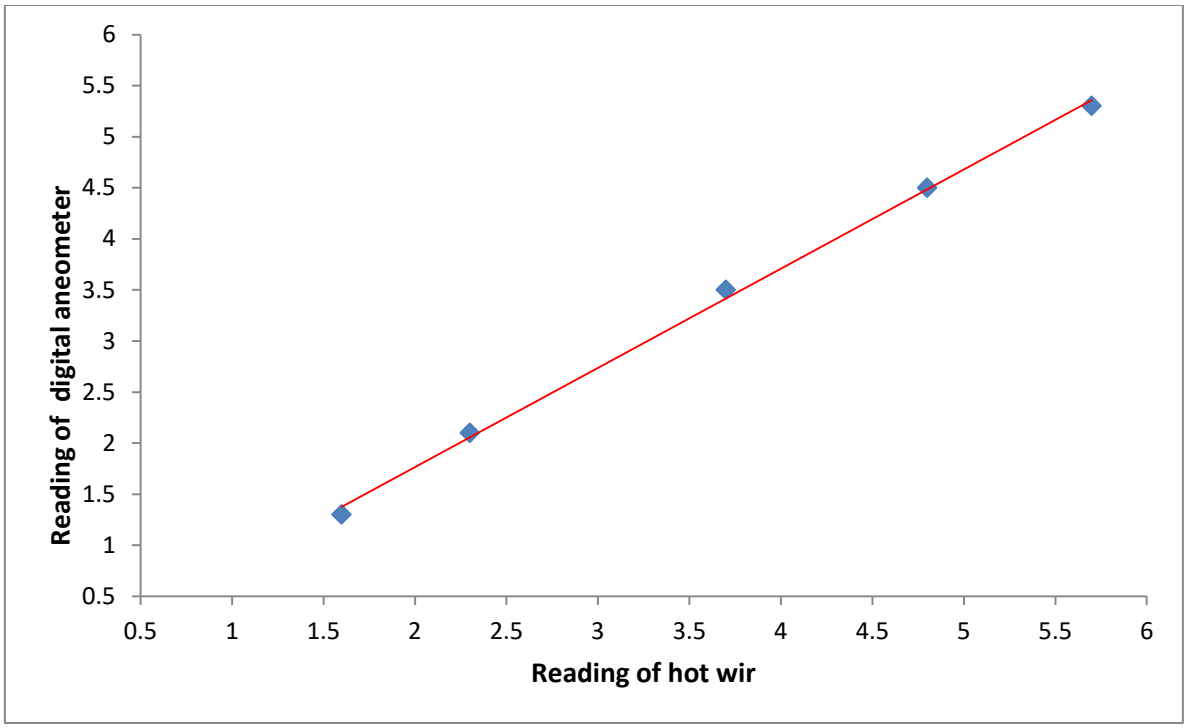

Figure (3- 16) curve of velocity calibration

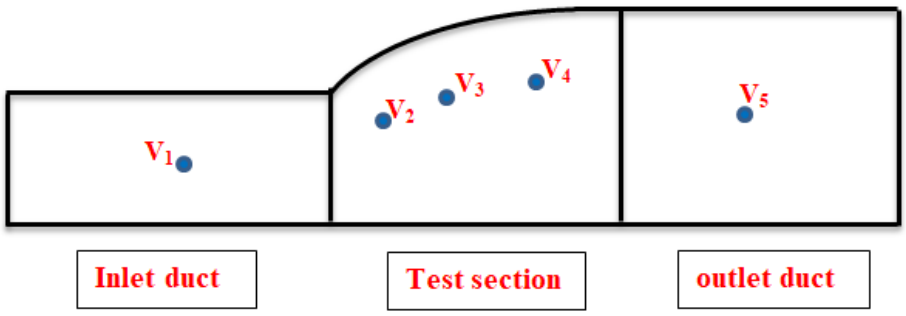

Figure (3-17) location of digital anemometer in rig duct

3.4. Experimental procedure

3.4.1. Case One

In the first case, heat flux is used as a boundary condition. The experimental procedure is comprised of the following stages:

1- Heating the air flow through the irregular duct by heat flux which is placed at the top and side wall of the test duct (irregular duct).

2- Reading the power supply for heat flux by using digital power analyzer device which is connected between heaters and voltage variation device.

3-The measurements for temperatures and velocities are recorded after 120 minutes of working time. At this time of heating of air reaches to steady state. These measurements taken with three values of inlet velocity of air which are 4.2m/s, 2.8m/s, 1.4m/s.

4-Supplying the air flow by blower which is placed at left side of rig duct, and the second part of duct remains open. The blower provides the duct with different velocity of air. A flexible pipe is used to connect between the rig duct and blower in order to reduce the effect of vibration.

5- Measuring the air velocity inside the test duct (irregular duct) in three different places by Hand-held digital anemometer. Also, at the same time, it measures the inlet and outlet velocities. These readings record with three values of inlet velocity supply.

6- (15)Thermocouples are fixed in different locations inside of the irregular duct and one thermocouple in inlet duct and another in exit duct, as shown in figure (3-11). The data logger with SD ram is operates to read and save the temperature measurements through the time of temperature recorder device. The temperature readings measure in all selection points at three values of inlet velocity supply.

7- Repeating the same processes, when supply the air from the right side of rig duct with the same values of inlet velocity of air.

3.4.2. Case Two

In the second case, it uses fan coil to supply hot air as the following stages:

1-Heating the air flow through the irregular duct by a heater which is placed at the front of the blower. It formed together as fan coil.

2- Supply a hot air for rig duct by using fan coil which is placed at left side of rig duct at the part of inlet duct. The outlet duct part remains open. The hot air supply with three values of inlet velocity. A flexible pipe also connects between the fan coil and rig duct to reduce the effect of vibration.

3- Measuring the air velocity inside irregular duct in several different places by Hand-held digital anemometer. Also, it measures the inlet and outlet velocity at the same time.

4-Readings of temperature are recorded through the irregular duct by using two devices of temperature recorder after 120 minutes of working time.

5- Repeating the same processes, when put the fan coil at right side of rig duct. These results note in table(3-7), and table(3-9) after calibrated.

3.4.3. Case Three

In the third case, it uses air cooler to supply cooling air for rig duct with three values of inlet velocity as the following stages:

1-Supply cold air to the rig duct by using air cooler which is placed at left side of the rig duct. The third part (outlet duct) of rig duct remins open. A flexible duct is used to connect between the rig duct and air cooler in order to reduce the effect of vibration.

2- Measurements of velocity are recorded at three values of inlet cold air velocity. These measurements illustrate in table(3-12) after calibrated by using equation(3.2).

3 Readings of temperature are calibrated after recorded by two devices of temperature recorder. These readings describe in table(3-10).

4- Repeating the same processes, when put the air cooler in the opposite side i.e. at the right side of rig duct. Readings value describe in table(3-11), and table (3-13) after calibrated.

Notes:

1-Using manometer in order to measure the pressure drop through the rig duct in three cases. It is not record any readings of pressure drop. This is due to the pressure drop is very small in irregular duct as pointed by **Zhang and Li [36]**

2-Readings of temperature distributions and air velocity for three cases of boundary conditions are repeating many times in each channel in order to get true result.

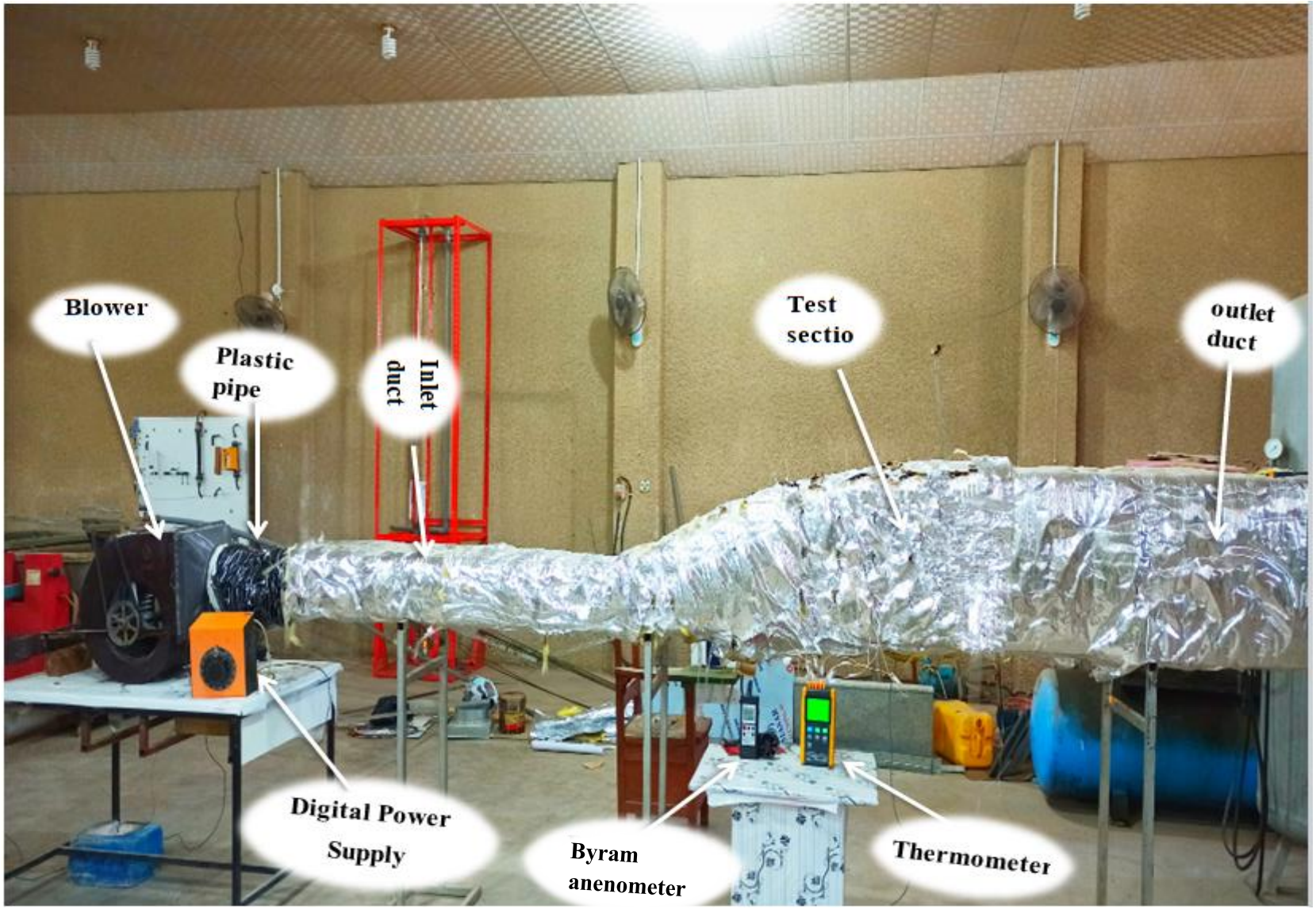

Figure (3-18) photograph of experimental rig

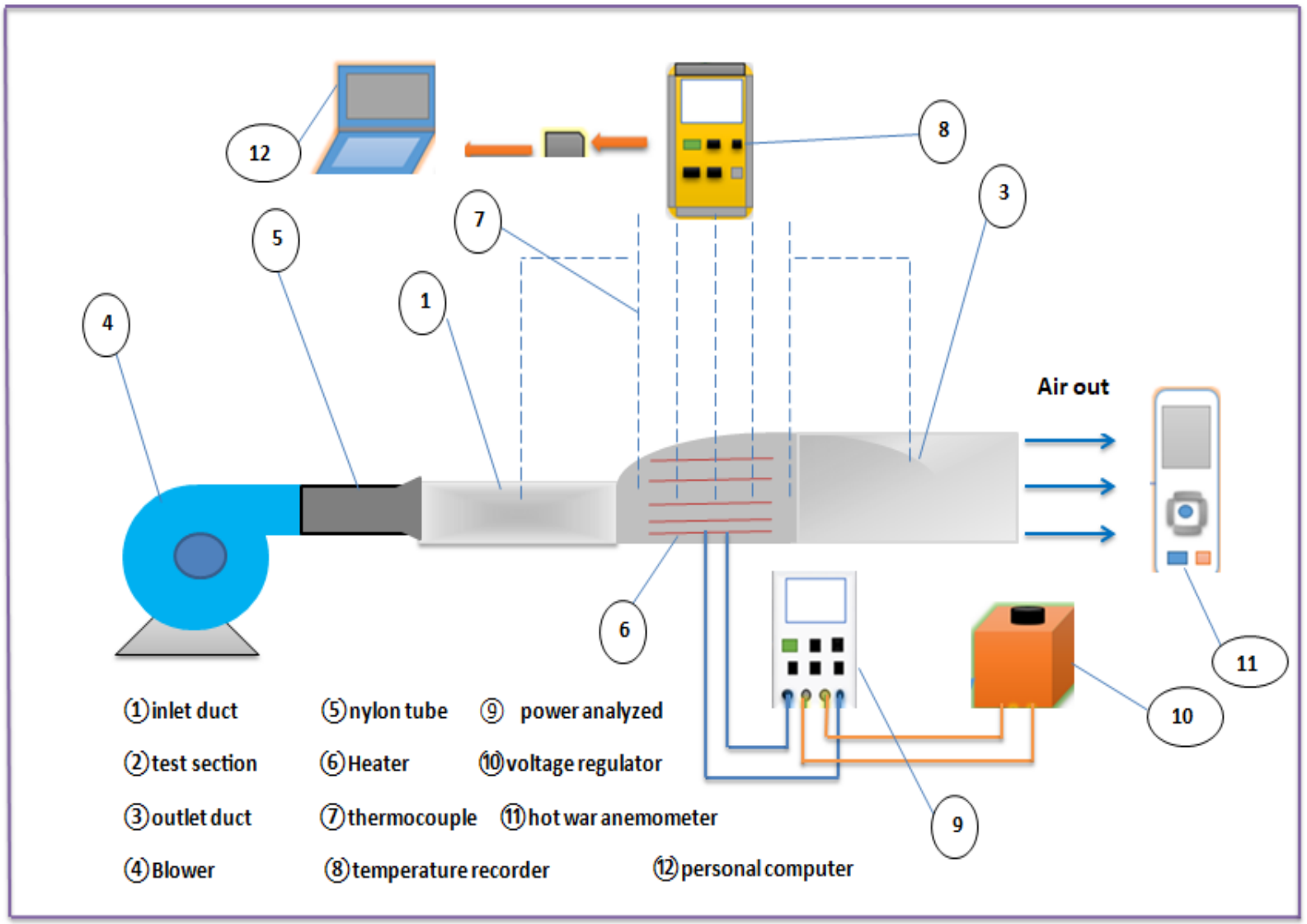

Figure (3- 19) schematic diagram of the rig test.

3.5. Experimental Analysis

These analysis are calculated in irregular duct only for three cases of boundary conditions.

1- Reynolds Number

The Reynolds number is calculated as:

$$Re = \frac{\rho U D_h}{\mu} \qquad \text{..... (3.3)}$$

Where

$$D_h = \frac{4A}{W} \qquad \text{..... (3.4)}$$

Where D_h is the hydraulic diameter .It was showed by **Holman [42]**

The hydraulic diameter, which is calculated for three sections where the velocity are measured in irregular duct. These cross section area(A) of each section is calculated by using numerical integration (trapezoidal rule). Schematic diagram below represents each one of three sections.

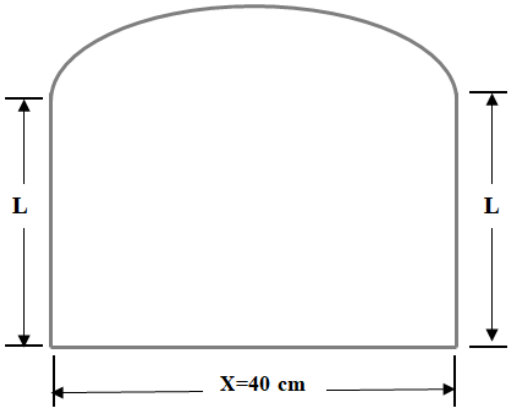

Figure(3-20) front view of irregular duct(test section)

The equation of curve in each section with different of height (L) is found by using grapher 10 program, as shown in figure (3-20). The curve equation is represented for each section as:

$y=L+0.3x-0.75x^2$ ……..(3.5)

The curve of side view of irregular duct equation is represented for each section as:

$Z=0.3L+2.5x-0.32x^2$

2-Friction Factor

Onur and Arslan [27] presents friction factor for laminar flow in duct as:

$$f = \frac{64}{Re} \quad \text{……(3-6)}$$

These values of friction factor is calculated for three cases of boundary conditions.

3- Pressure Drop

Onur and Arslan [27] describes the pressure drop in irregular duct for three cases of boundary condition is calculated as:

$$\Delta P = f * \rho * \frac{l}{Dh} * \frac{v^2}{2} \quad \text{……(3.7)}$$

4- Heat Flux

Heat flux is calculated from the electrical power which supply by electrical heat. This heater is fixed over the top curve surface, and outer left

side of duct wall. The value of electrical power analyzer device is 1116 w. Then, the heat flux is calculated as:

$$q'' = \frac{Power}{Aera} = \frac{P}{A} \qquad \text{……..(3-8)}$$

5- Coefficient of Heat Transfer

The local heat transfer coefficient is reported by **Wang et al. [44]** as :

$$h_x = \frac{q''}{T_s - T_f} \qquad \text{…….. (3.9)}$$

Where T_f is the average temperature of air flow at each five section, as shown in figure (3-10). T_s is the temperature of curve top surface of irregular duct. The heat transfer coefficient is calculated only in case one of boundary condition. This due to a significant heat exchange happens between the air passing through the test duct and upper curve top surface which heat flux is fixed.

6- Nusselt Number

Zhang and Chen [45] reports the Nusselt number which calculated as :

$$Nu = \frac{h\, D_h}{k} \qquad \text{…..... (3.10)}$$

These parameters are showed in tables in appendix[A].

3.6. Uncertainty analysis

The error in measurement is defined as the difference between its true and measured value. However, this definition is not easy to know which is the true quantity of these values. Therefore, it is necessary to compute the uncertainty

when presenting an experimental results. Generally, the uncertainty of measurement is described as the amount of errors or doubts in taking measurement. These errors or doubts are mainly due to measuring instrument, measuring process, human error(operator skills), and operating condition. For any set data, the standard uncertainty (SU) can be calculated by equation detailed by **Bell[46]** as:

$$Su = \frac{S.D}{\sqrt{N}} \qquad \text{.....(3.11)}$$

Where,

N is the total number of measurements in each channel.

S.D is the standard deviation which is calculated as:

$$S.D = \sqrt{\frac{\sum_{i=1}^{N}\left(X_i - X_{average}\right)^2}{(N-1)}} \qquad \text{.....(3.12)}$$

$X_{average}$ is the average readings of temperature or any function in channel. The average experimental values of readings in each channel which were repeating N times. The value of average readings is calculated as:

$$Xaverage = \frac{1}{N}\sum_{i=1}^{N} X_i \ldots\ldots\ldots \qquad \text{.....(3.13)}$$

Where X_i is represented the values for measurements data of temperature or any function measured in each channel.

The average error rate for all readings is 1.75

Chapter Four

Theoretical analysis

Theoretical Work

4.1. Introduction

Investigation of air laminar flow and forced heat transfer convection in irregular duct under constant heat flux is an interesting subject. The heat transfer mechanism of air flow through irregular duct (test duct) with different boundary conditions are studied. This mechanism shows the effect of air velocity and shape geometry of duct on temperature distribution.

In the present work, mathematical model is performed in a two dimensions deals with the temperatures distribution along irregular test duct by using a finite difference method which solving the energy equation. Matlab software was used to simulate the temperature distributions by a computer program. While, it was studied the flow characteristics and air flow velocity through all the test duct by using Ansys-fluent 19.2. These two models with three cases of boundary conditions simulated the temperature distribution and the velocity of air supply from the left side and right side for rig duct.

4.2. Mathematical Model

There are many steps in the implementation of mathematical model before getting the results:

4.2.1.Geometry Generation

The geometry of the system was modeled as a 2D structure for the two phase flow using Design modeler combined with Ansys Workbench 19.2 by drawing entrance section with dimensions 1.25 m length, 0.4 m width and.25 m height, this part is designed as a rectangular shape, the second part is test section which was designed irregular as curve shape with length 1.2 m, the third part is the exit duct section which is designed as a square shape with dimension 1.25 m length, and square section (0.5 x 0.5), after that, a surface

was generated from the sketch. The geometry was set to be fluid. For the purpose of obtaining an inexpensive arithmetical model, it was necessary to build it as small as possible as shown in figure(4-2).

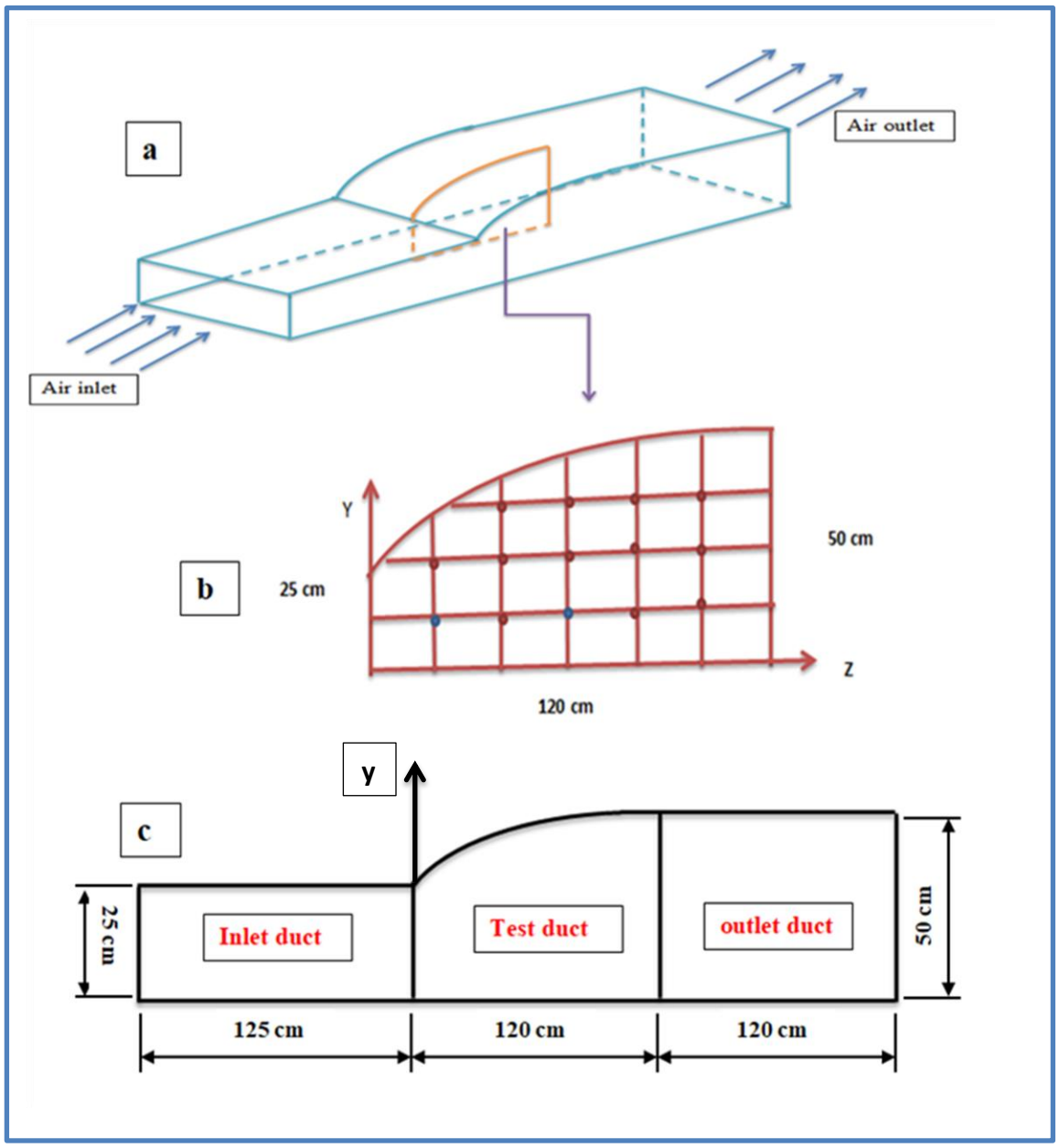

Figure(4-1) schematic diagram of rig duct a-three dimension of rig duct, b-test duct, and c-front view of rig duct

4.2.2. Mesh Generation

There are many types of mesh, such as coarse , medium , and fine mesh choosing the type of mesh depends on several factors, such as, the system geometry, the type of flow, and complexity as detailed by **Bakker[47] .** In the present work, the geometry of the duct was divided into small square element (Quadrilateral structured grid) using the meshing combined with Ansys Workbench 19.2 with maximum and minimum size equal to (0.002 m) through fine relevance center and medium smoothing mesh near the wall of channel. The model governing equations would be solved at each element of the model geometry . as shown in figure (4-3).

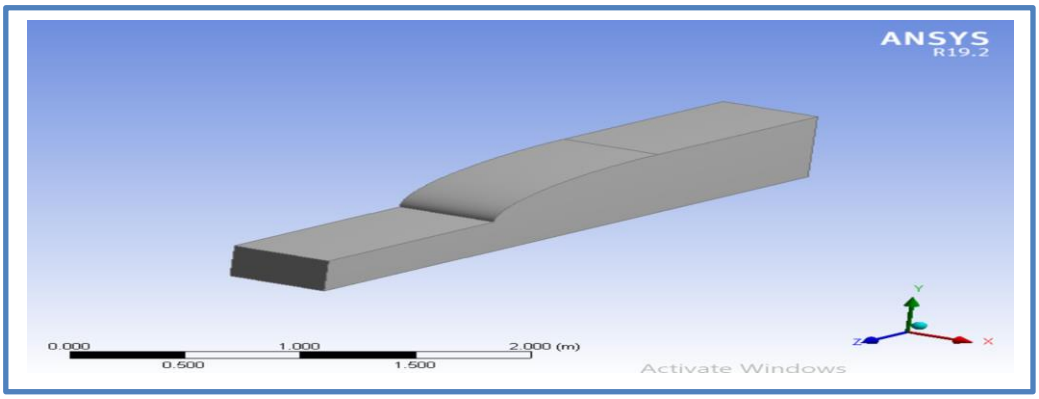

Figure (4-2) rig duct geometry by Ansys

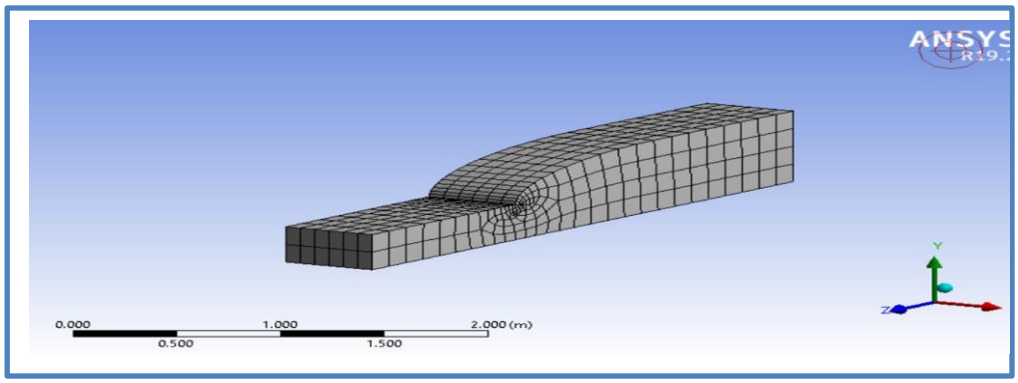

Figure (4-3) mesh of rig duct

4.2.3.Assumptions and Boundary conditions Validation

There are some assumptions of the hot and cold air flow inside the rig duct, and boundary conditions can be described in this research as shown in figure (4-4). These assumptions of hot and cold air flow through the rig duct are:

1-Incompressible fluid flow.

2-Steady state fluid flow.

3-Fluid flow with constant physical properties.

4-Newtonian fluid and fully developed.

5-Assume inlet values of inlet velocities from left side of rig duct and represented the component of velocity in z-direction (u).

1-Case One

A heat flux at the top and side wall of test duct and provided inlet values of inlet velocity by fan as shown in figure (4-5).

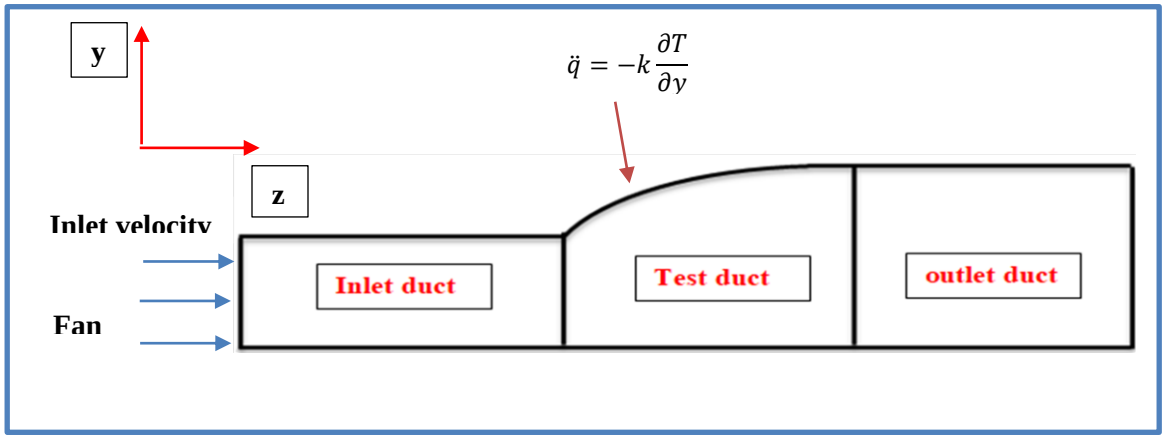

Figure(4-5) schematic diagram of rig duct for case one

2-Case Two

Supply the rig test by hot air by fan coil from the left side only with different values of inlet velocity with 36^{o}C as shown in figure (4-6).

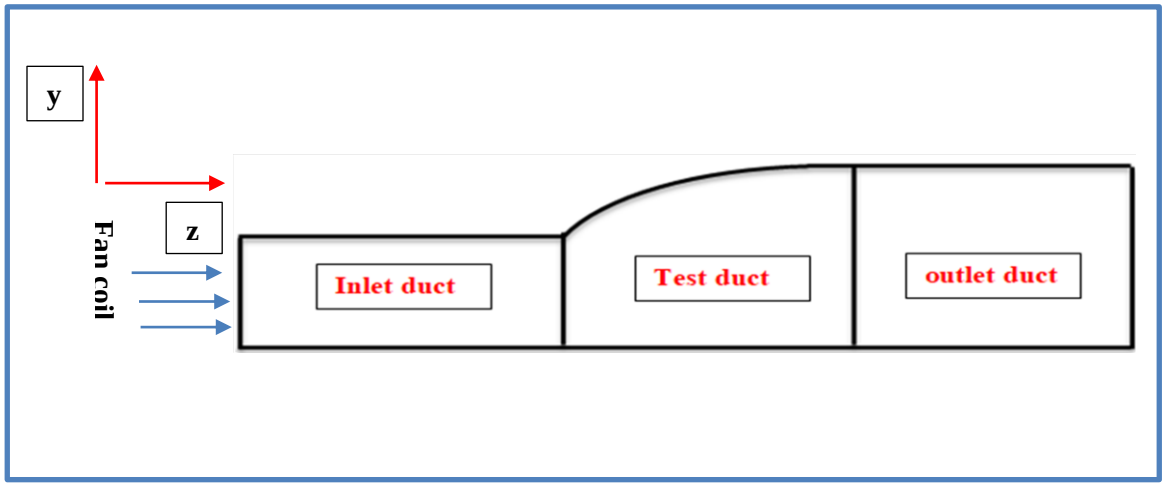

Figure(4-6) schematic diagram of rig duct for case two

3-Case Three

Supply the rig duct with cool air by using air cooler from the left side only with different values of inlet velocity as shown in figure (4-7).

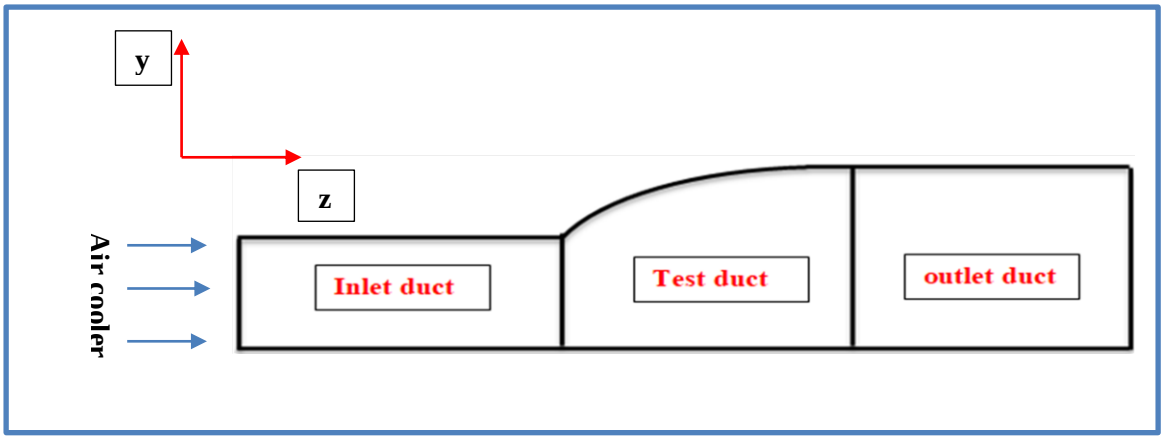

Figure(4-7) schematic diagram of rig duct for case two

4.3.Numerical Solution of Mathematical Model

It should be represented the governing equations which solved the temperatures distribution of hot and cool air by forced convection. Energy

equation was used to simulate the temperatures distribution through the irregular test duct depending upon the inlet velocity of air flow through the rig duct. This equation was reported by **Kang et al.[48]** in two dimensions as:

$$\rho C_p u \frac{\partial T}{\partial z} + v \frac{\partial T}{\partial y} = k \left(\frac{\partial^2 T}{\mathrm{dy}^2} + \frac{\partial^2 T}{\mathrm{dz}^2} \right) \qquad \text{…….(4.1)}$$

In order to solve the energy equation, it was needed the values of inlet air velocity. In experimental work, it was measured these inlet velocity with different three cases steady which were assumed. Also, the velocity of hot and cold air was measured inside irregular test duct in different positions. It was used ANSYS-Fluent 19.0 to represent the air flow characteristics and calculated the values of air flow velocities inside the rig duct through geometric duct. These velocities were calculated by using continuity and momentum equations. Using the upper assumptions of air flow and assumed the air has constant viscosity, density, and steady through all the region of rig duct. Near the wall of rig duct all the components of the velocities in z, and y directions are assumed equal zero (u=0, and v=0). Simulation velocity of hot and cold air inside rig duct by ANSYS-Fluent 19.0 was represented by the following steps of flowchart as shown in figure(4-8).

4.4. Temperature Distribution Through Irregular Test Duct

In this domain of the assumptions of rig duct of flow air and the three cases of boundary conditions were assumed. The temperatures distribution of hot and cold air in irregular test duct were calculated by solving the energy equation. Two dimensions model of partial significance is two dimensional steady state heat condition energy equation in horizontal z-axis and vertical direction y-axis. For T=T(y,z).

It is assumed that the thermal properties are independent of temperature, the air flow is taken to be homogenous and isotropic. Equation (4.4) is heat equation which is classified as elliptic partial differential equation, isotopic medium. Finite difference approximation is imperative to use for the partial differential equation. So, it has been used forward and central spaces difference to linearize the steady state energy equation . The resulting algorithm for equation (4.4) is :

$$\frac{u}{\alpha}\frac{T_{j,k+1}-T_{j,k}}{\Delta z} = \frac{T_{j+1,k}-2T_{j,k}+T_{j-1,k}}{\Delta y^2} + \frac{T_{j,k+1}-2T_{j,k}+T_{j,k-1}}{\Delta z^2} \qquad \ldots\ldots\ldots(4.5)$$

It has been considered the estimate in region over orthogonal grid with an equation dispersing (the separation between neighboring focuses). The indices j and k will be utilized for indicating the point along the y and z headings. The separation between the points in confirmed grid are Δy and Δz. The grid for this model is represented by figure (4-9), and the number of mesh nodes of irregular test duct are 250 x 600. The distances in between points in established grid are Δy and Δz=2mm. This domain was used in solving theoretically the task of temperature distribution of hot and cold air flow through the rig duct by forced convection.

Numerical analysis was done for irregular test duct as domain sample from rig duct as shown in figure(4-9). This domain mesh space was divided in number of nodes in Δy and Δz, these are 250x600.

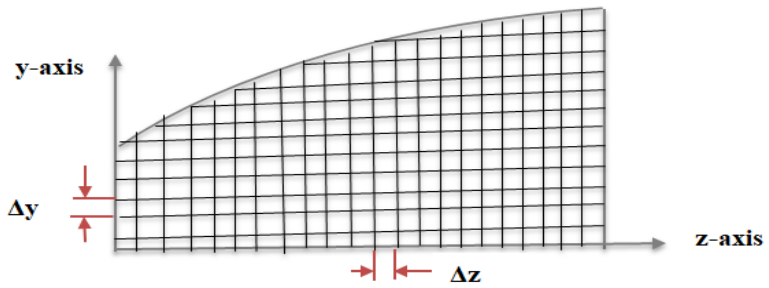

Figure(4-9) grid layout of irregular test duct

A finite-difference method was used to solve equation (4.5) for internal regular nodes which have Δy=Δz . Simulated the temperature inside the domain of test duct depending upon the boundary condition cases.

$$T_{j,k} = \frac{T_{j+1,k}+T_{j-1,k}+(1-\frac{u\Delta y}{\alpha})T_{j,k+1}+T_{j,k-1}}{\left(4-\frac{u\Delta y}{\alpha}\right)} \qquad \text{.....(4.9)}$$

Equation (4.9) calculated the temperature distribution of all internal nodes in domain which are regular. The problem involved irregular curve shape of test duct at upper wall. In this region Δy don't equal Δz, in order to use finite difference method to eliminate these errors. It should be derived equation to solve problem which involved irregular shape at upper wall of test duct as shown in figure (4-10).

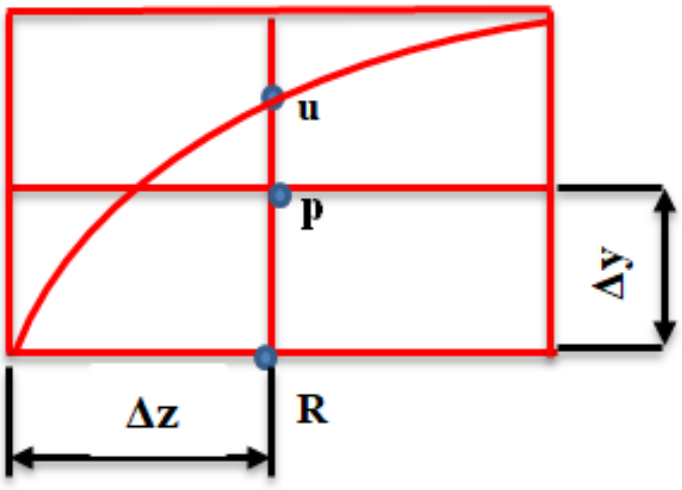

Figure(4-10) sketch of irregular node

By using Taylor's series forward assumption as:

Assume pu=λ Δy

$$T_u = T_p + \lambda \Delta y \frac{\partial T}{\partial y} + \frac{\lambda^2 \Delta y^2}{2!}\frac{\partial^2 T}{\partial y^2} \qquad \text{.....(4.10)}$$

For Taylor's series backward, thus:

$$T_R = T_p - \Delta y \frac{\partial T}{\partial y} + \frac{\Delta y^2}{2!} \frac{\partial^2 T}{\partial y^2} \quad \text{.....(4.11)}$$

From equation (4.11)

$$\Delta y \frac{\partial T}{\partial y} = T_p - T_R + \frac{\Delta y^2}{2!} \frac{\partial^2 T}{\partial y^2} \quad \text{.....(4.12)}$$

Substitute in equation (4.10), then

$$T_u = T_p + \lambda \left[T_p - T_R + \frac{\Delta y^2}{2!} \frac{\partial^2 T}{\partial y^2}\right] + \frac{\lambda^2 \Delta y^2}{2!} \frac{\partial^2 T}{\partial y^2} \quad \text{.....(4.13)}$$

Thus,

$$\frac{\partial^2 T}{\partial y^2} = \frac{T_u - T_p(\lambda+1) + \lambda T_R}{\lambda(\lambda+1)\frac{\Delta y^2}{2}} \quad \text{.....(4.14)}$$

This is the form of second space derivative for irregular nodes

A-Temperature Distribution at Boundary Conditions Case One

The boundary condition in this case as pointed in figure (4-11) which were represented as:

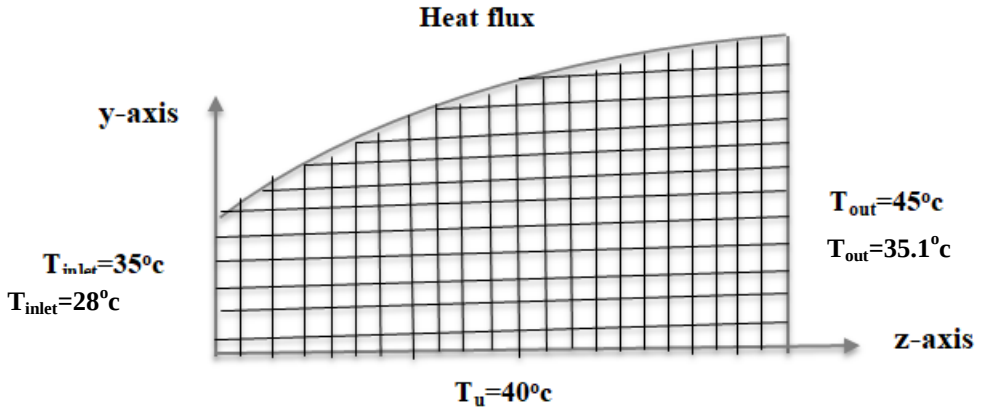

Figure (4-11) boundary condition of case one

1-T(y,0)=T_{in} =28^{o}c

2- T(0,z)=T_{u}=40^{o}c

3- T(y,z)=heat flux

$$-k\frac{\partial T}{\partial y} = \ddot{q}$$

$$-k\frac{T_{j+1,k}-T_{j,k}}{\Delta y} = \ddot{q}$$

Thus,

$$T_{j+1,k} = T_{j,k} - \frac{\ddot{q}\,\Delta y}{k} \qquad \text{……(4.15)}$$

4- T(y,120)=To=35.1^{o}c

These four boundary conditions feeding in equation number (4.9) to solve all the regular nodes inside the domain of test duct. The irregular nodes at the wall using equation (4.5) substitute the second space derivative $\frac{\partial^2 T}{\partial y^2}$ only by using equation (4.14)

B- Temperature Distribution at Boundary Conditions Case Two

The boundary conditions in this case supply hot air only from the inlet of rig duct by fan coil as illustrated in figure(4-12).

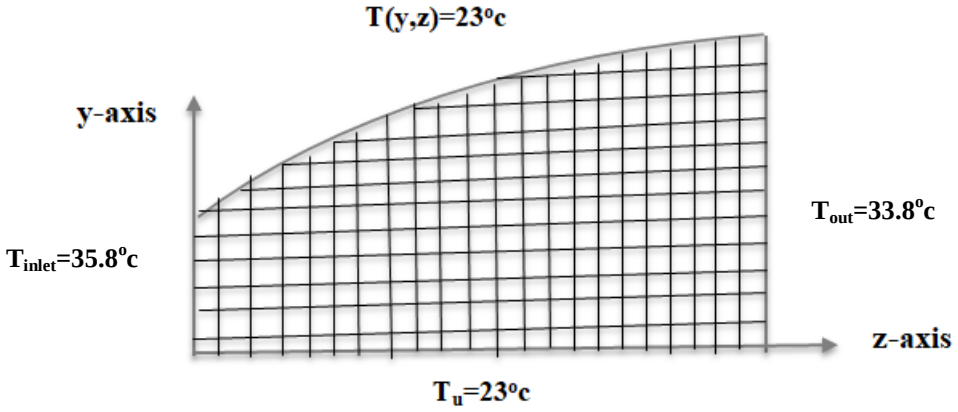

Figure (4-12) boundary condition of case two

1- $T(y,0)=T_h=35.8^oc$

2- $T(0,z)=T_u=23^oc$

3- $T(y,z)= 23^oc$

4- $T(y,120)=33.8^oc$

C- Temperature Distribution at Boundary Conditions Case Three

The boundary conditions in the case supply cold air by air cooler from the inlet of rig duct as described in figure (4-13).

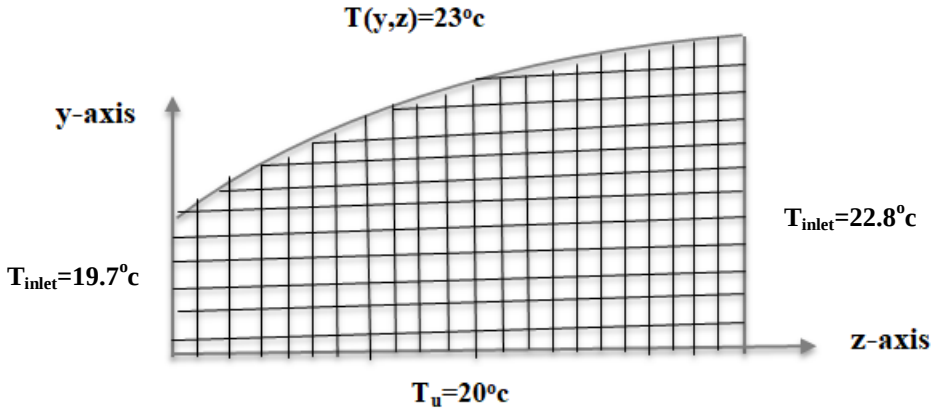

Figure (4-13) boundary condition of case three

1- $T(y,0)=T_c=19.7^oC$

2- $T(0,z)=T_u=20^oC$

3- $T(y,z)= 23^oC$

4- $T(y,120)=T_{out}=22.8^oC$

For these two cases using the same equations which were used in case one in order to simulate the temperature distribution in the irregular test duct through the flow of hot and cold air by forced convection.

It was simulated a computer program in Matlab software to solve these equations in order to calculate the temperatures distribution in irregular test duct by different cases of boundary conditions. This flowchart of a computer program was pointed in figure(4-14).

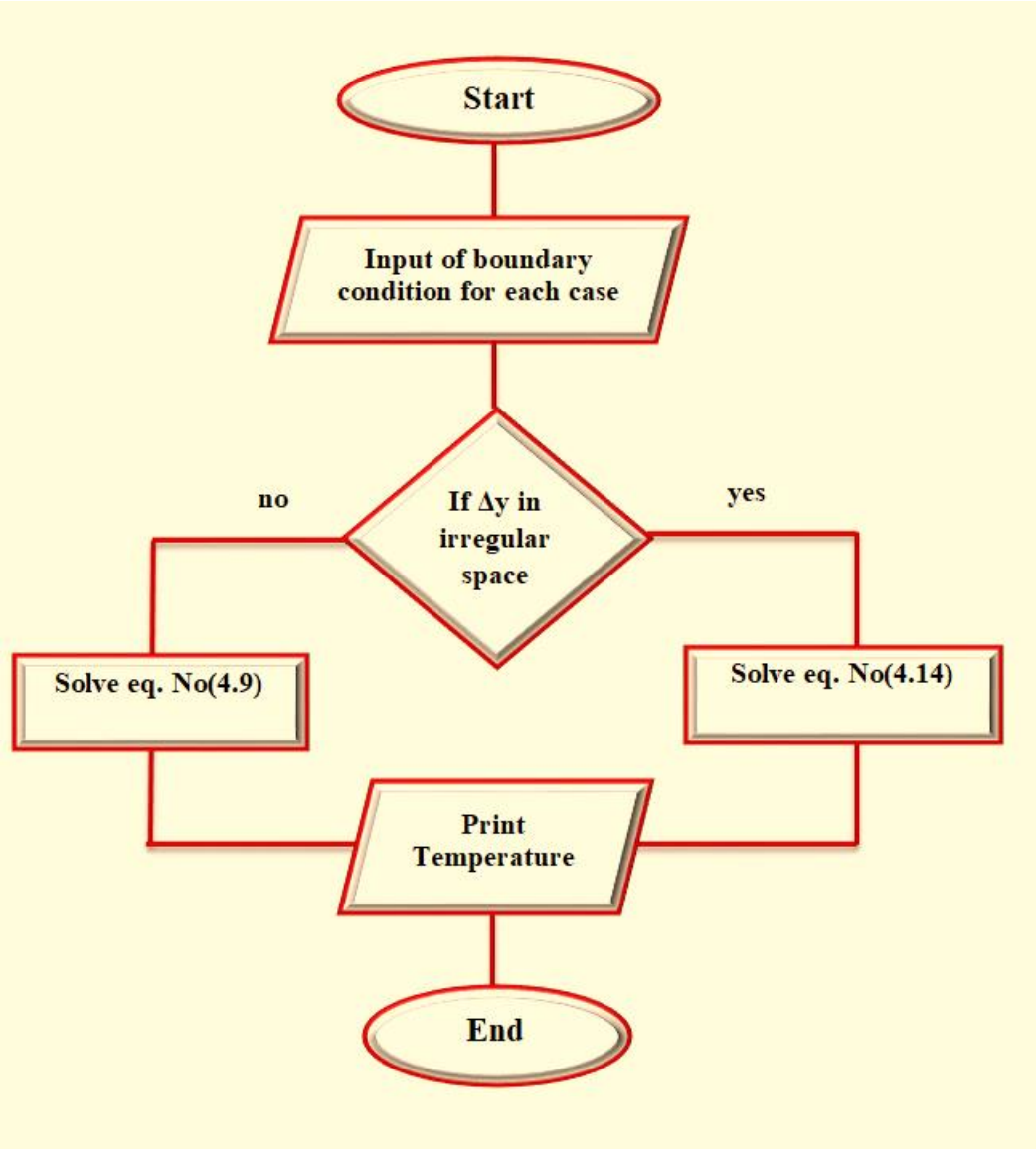

Figure(4-14) flowchart of Matlab program

Chapter Five

Results and Discussion

Results and Discussion

5.1. Experimental Work

The experimental work describes the results for measuring temperature and velocity distribution of air through an irregular duct with different cases study of boundary conditions as shown in figure (5-1).

Case One

1-Temperature Distribution

In the first case, it was fixed a heat flux as a boundary condition at top and side wall of test duct. The measurements of air temperatures distribution were represented after 120 minutes of working time. These values of results are taken with different values of air velocity (4.2 m/s, 2.8m/s, and 1.4m/s).

A-The fan placed at left side of rig duct:

Figure (5-2) represents the temperature distribution through y-axis at value of z-axis =0.2 m inside the test section (irregular duct). The air flow is heated through the irregular duct by heat flux which is placed at the top and side of the test duct. This curve shows the temperature increasing through the y-axis with different values of air velocity supply. It is found the temperature increases a little with increasing the values of air velocity. The highest value for temperature is 63.5^{o}C at 4.2m/s, and the lowest value for temperature is 39.4^{o}Cat 1.4m/s. That means, the air flow was heating by the heat flux at top and side wall of test duct.

Figure (5-4) shows the temperature distribution through y-axis at value of z-axis =0.4 m inside the test section. This curve shows the temperature increasing through the y-axis with different values of air velocity supply. It is

found the temperature value increasing around the top and side wall of irregular duct. This is due the heat flux was fixed around these places as a boundary condition. The highest value for temperature is 58.7^{o}C at 4.2m/s, and the lowest value for temperature is 34.7 ^{o}C at 1.4m/s.

Figure (5-6) points the temperature distribution through y-axis at value of z-axis =0.6 m inside the irregular duct. This curve shows the temperature increases through the y-axis with different values of air velocity supply. It is found the temperature increasing a little with increases the values of air velocity. The highest value for temperature is 71.6^{o}C at 4.2m/s, and the lowest value for temperature is 35.8^{o}C at 1.4m/s.

Figure (5-8) indicates the temperature distribution through y-axis at value of z-axis =0.8m inside the test section. This curve shows the temperature increasing through the y-axis with different values of air velocity supply. It is found the temperature value increasing around the top and side wall of irregular duct. This is due the heat flux was fixed around these places as a boundary condition. The highest value for temperature is72.3^{o}C at 4.2m/s, and the lowest value for temperature is 36.5^{o}C at 1.4m/s.

Figure (5-10) notes the temperature distribution through y-axis at value of z-axis =1m inside the test section of irregular duct. This curve shows the temperature increasing through the y-axis with different values of air velocity supply. It is found the temperature increasing a little with increases the values of air velocity. The highest value for temperature is 41.8^{o}C at 4.2m/s, and the lowest value for temperature is 34.6^{o}C at 1.4m/s .

Figure (5-12) shows isothermal contour of the temperature distribution through irregular duct at different velocity of air flow when, it used a heat

flux as boundary condition, and the air flow from the left side of test duct. The air flow was simulated along the z-axis. The temperature near the heater in the above wall is found higher than inlet temperature

From these curves, it was pointed maximum value of temperature record is 72.3^{o}C through y-axis at value of z-axis is 0.8 m with velocity value 4.2m/s These results consistent with experimented results of **[48].**

B-The fan placed at right side of rig duct:

Figure (5-2) dominates the temperature distribution through y-axis at value of z-axis =1 m inside the test section of irregular duct. The air flow supplies by fan which is placed at right side of rig duct. The air flow is heated through the irregular duct by heat flux which was placed at the top and side of the test duct. This curve shows the temperature increases through the y-axis with different values of air velocity supply. It is found the temperature increases a little with increasing the values of air velocity. The highest value for temperature is 53 ^{o}C at 4.2m/s, and the lowest value for temperature is 35.5 ^{o}C at 1.4m/s .

Figure (5-4) illustrates the temperature distribution through y-axis at value of z-axis =0.8 m inside the test section of irregular duct. The air flow is heated through the irregular duct by heat flux which was placed at the top and side of the test duct. This curve shows the temperature increases through the y-axis with different values of air velocity supply. It is found the temperature increases a little with increasing the values of air velocity. The highest value for temperature is 52.3 ^{o}C at 4.2m/s, and the lowest value for temperature is 36.7 ^{o}C at 1.4m/s .

Figure (5-6) points the temperature distribution through y-axis at value of z-axis =0.6 m inside the test section of irregular duct. The air flow supplies by fan which is placed at right side of rig duct. The air flow was heated through the irregular

duct by heat flux which is placed at the top and side of the test duct. This curve shows the temperature increases through the y-axis with different values of air velocity supply. It is found the temperature increases a little with increasing the values of air velocity. The highest value for temperature is 47.1^{o}C at 4.2m/s, and the lowest value for temperature is 40.8 ^{o}C at 1.4m/s .

Figure (5-8) indicates the temperature distribution through y-axis at value of z-axis =0.4 m inside the test section of irregular duct. The air flow supplies by fan which is placed at right side of rig duct. The air flow is heated through the irregular duct by heat flux which was placed at the top and side of the test duct. This curve shows the temperature increases through the y-axis with different values of air velocity supply. It is found the temperature increases a little with increasing the values of air velocity. The highest value for temperature is 53.8 ^{o}C at 4.2m/s, and the lowest value for temperature is 35.9 ^{o}C at 1.4m/s .

Figure (5-10) describes the temperature distribution through y-axis at value of z-axis =0.2 m inside the test section of irregular duct. The air flow supplies by fan which is placed at right side of rig duct. The air flow is heated through the irregular duct by heat flux which was placed at the top and side of the test duct. This curve shows the temperature increases through the y-axis with different values of air velocity supply. It is found the temperature increases a little with increasing the values of air velocity. The highest value for temperature is 55.6 ^{o}C at 4.2m/s, and the lowest value for temperature is 35.9 ^{o}C at 1.4m/s .

Figure (5-13) shows isothermal contour of the temperature distribution through irregular duct at different velocity of air flow, when, it used a heat flux as boundary condition, and the air flow from the right side of test duct. The air flow was simulated

along the z-axis. The temperature near the heater in the above wall is found higher than inlet temperature.

These result indicated the values of temperature at upper of y-axis are approximately similar. That manes, the position of fan is affected on heating the duct by external boundary condition.

Figure (5-16) points variation of average Nusselt number with z-axis in the irregular duct from the left and right side of rig duct for case one. The variation of Nusselt number along the length is plotted in the graph. From analyzing the results at left side, it is found that the Nusselt number value was very high at the beginning and it reduces, but in the right side, it is found that the Nusselt number value was increasing.

Figure (5-17) point's variation of average Nusselt number with Reynolds number in the irregular duct from the left and right side of rig duct for case one. The variation of Nusselt number along the length is plotted in the graph. From analyzing the results, it is found that the Nusselt number value was very high at the beginning and it reduces. The value reaches a minimum, when the reduction diminishes and the number remains almost a constant value, but in the right side, it is found that the Nusselt number value was increasing. These results consistent with experimented results of **[36]**.

Figure (5-18) points relationship between coefficient of heat transfer and Reynolds number in the irregular duct through the left side and right side of rig duct for case one. The variation of coefficient of heat transfer along the length is plotted in the graph. From analyzing the results, it is found that coefficient of heat transfer value was very high at the beginning. The value reaches a minimum, when the reduction

diminishes and the number remains almost a constant value. These results are consistent with experimented results of **[37]**.

Figure (5-19) shows variation of average friction factor with Reynolds number in the irregular duct at left and right side of rig duct for case one at velocity (4.2 m/s, 2.8m/s, and 1.4m/s), that the value of the Reynolds number is affected by an increase in the velocity of air, as it increases as the value of the velocity increases. The value of the fraction factor is inversely proportional to the value of the Reynolds number, that the friction factor f decreases as Re increases with the same slope. The effects of modified Reynolds number and eccentricity on friction factor respectively. From figure, it is seen that the increase in modified Reynolds number results to a decrease in friction factor and that the geometry of the duct has a pronounced effect on the friction factor. These results consistent with experimented results of **[36]**.

Figure (5-20) illustrates variation of average pressure drop with Reynolds number in the irregular duct at left and right side of rig duct for case one at velocity (4.2 m/s, 2.8m/s, and 1.4m/s). that the value of the Reynolds number is affected by an increase in the velocity of air, as it increases as the value of the velocity increases. The value of the pressure drop is inversely proportional to the value of the Reynolds number, that pressure drop Reynolds number and eccentricity on pressure drop respectively. From Figure, it is seen that the increase in modified Reynolds number results to a decrease in pressure drop and that the geometry of the duct has a pronounced effect on the pressure drop. It was showed by **[6]**

Case Two

1-Temperature Distribution

In the second case, using fan coil to supply hot air and it was placed at the front of rig duct. The results were comprised in the figures:

Figure (5-21) represents the temperature distribution through y-axis at value of z-axis =0.2 m inside the irregular duct. The hot air supply by fan coil which is placed at left side of rig duct. These value of results are taken with different values of air velocity (4.2 m/s, 2.8m/s, and 1.4m/s). This curve shows the temperature increases through the y-axis with different values of air velocity supply. It is found the temperature increases a little with increasing the values of air velocity.

Figure (5-23) points the temperature distribution through y-axis at value of z-axis =1m inside the irregular duct. The hot air supply by fan coil which is placed at right side of rig duct. These value of results are taken with different values of air velocity (4.2 m/s, 2.8m/s, and 1.4m/s). This curve shows the temperature increases through the y-axis with different values of air velocity supply. It is found the temperature increasing a little with increasing the values of air velocity. It is sufficient only at z = 1, but at the values of (0.8,0.6,0.4, and 0.2m/s) it will be the same as the first value due to the absence of a significant change in temperature.

Figure (5-25) describes the temperature distribution through y-axis at value of z-axis =0.4 m inside the irregular duct. These value of results were taken with different values of air velocity (4.2 m/s, 2.8m/s, and 1.4m/s). This curve shows the temperature increases through the y-axis with different values of air velocity supply. It is found the temperature increasing a little with increasing the values of air velocity.

Figure (5-27) represents the temperature distribution through y-axis at value of z-axis =0.6 m inside irregular duct.. These value of results were taken with different values of air velocity (4.2 m/s, 2.8m/s, and 1.4m/s). This curve shows the temperature

increases through the y-axis with different values of air velocity supply. It was found the temperature increasing a little with increasing the values of air velocity.

Figure (5-29) points the temperature distribution through y-axis at value of z-axis =0.8 m inside the test section of irregular duct. These value of results were taken with different values of air velocity (4.2 m/s, 2.8m/s, and 1.4m/s). This curve shows the temperature increases through the y-axis with different values of air velocity supply. It is found the temperature increasing a little with increasing the values of air velocity.

Figure (5-31) represents the temperature distribution through y-axis at value of z-axis =1 m inside the test section of irregular duct. These value of results were taken with different values of air velocity (4.2 m/s, 2.8m/s, and 1.4m/s). This curve shows the temperature increases through the y-axis with different values of air velocity supply. It is found the temperature increasing a little with increasing the values of air velocity.

Figure (5-33) induces isothermal contour of the temperature distribution through irregular duct at different velocity of air flow, when it used a heater in the front blower as a fan coil, and the flow from the left side of test duct. from the figure, the temperature in the main flow zone near the intermediate fluid domain is relatively high, and the temperature near the wall surface is low.

Figure (5-35) illustrate isothermal contour of the temperature distribution through irregular duct at different velocity of air flow, when it used a heater in the front blower as a fan coil, and the flow from the right side of test duct from the figure, the temperature in the main flow zone near the intermediate fluid domain is relatively high, and the temperature near the wall surface is low

Figure (5-35) points variation of average friction factor with Reynolds number in the test duct at left and right side of rig duct for case two at velocity (4.2 m/s, 2.8m/s, and 1.4m/s), that the value of the Reynolds number is affected by an increase in the velocity of air, as it increases as the value of the velocity increases. The value of the fraction factor is inversely proportional to the value of the Reynolds number, that the friction factor f decreases as Re increases with the same slope. The effects of modified Reynolds number and eccentricity on friction factor respectively. From figure, it is seen that the increase in modified Reynolds number results to a decrease in friction factor and that the geometry of the duct has a pronounced effect on the friction factor. These results consistent with experimented results of **[36]**.

Figure (5-36) illustrates variation of average pressure drop with Reynolds number in the test duct at left and right side of rig duct for case two at velocity (4.2 m/s, 2.8m/s, and 1.4m/s). that the value of the Reynolds number is affected by an increase in the velocity of air, as it increases as the value of the velocity increases. The value of the pressure drop is inversely proportional to the value of the Reynolds number, that pressure drop decreases as Re increases with the same slope. The effect of modified Reynolds number and eccentricity on pressure drop respectively. These results are consistent with experimented results of **[6]**.

Case Three

1-Temperature Distribution

In the third case, using air cooler to supply cooling air and it was placed at the front of rig duct. The results were comprised in the figures:

Figure (5-37) describes the temperature distribution through y-axis at value of z-axis =0.2 m inside the irregular duct. The cooling air supplies by air cooler which is

placed from right side of rig duct. These value of results were taken with different values of air velocity (4.2 m/s, 2.8m/s, and 1.4m/s). This curve shows the temperature increasing through the y-axis with different values of air velocity supply. It was found the temperature increases a little with increasing the values of air velocity.

Figure (5-39) represents the temperature distribution through y-axis at value of z-axis =1 m inside the irregular duct. The cooling air supplies by air cooler which is placed at right side of rig duct. These values of results were taken with different values of air velocity (4.2 m/s, 2.8m/s, and 1.4m/s). This curve shows the temperature increasing through the y-axis with different values of air velocity supply. It was found the temperature increasing a little with increasing the values of air velocity. It is sufficient only at z = 1, but at the values of (0.8,0.6,0.4, and 0.2m/s) it will be the same as the first value due to the absence of a significant change in temperature.

Figure (5-41) illustrates the temperature distribution through y-axis at value of z-axis =0.4 m inside the irregular duct. The cooling air supplies by air cooler which is placed at left side of rig duct. These value of results were taken with different values of air velocity (4.2 m/s, 2.8m/s, and 1.4m/s). This curve shows the temperature increasing through the y-axis with different values of air velocity supply. It was found the temperature increasing a little with increasing the values of air velocity.

Figure (5-43) represents the temperature distribution through y-axis at value of z-axis =0.6 m inside the irregular duct. The cooling air supplies by air cooler which is placed at left side of rig duct. These values of results were taken with different values of air velocity (4.2 m/s, 2.8m/s, and 1.4m/s). This curve shows the temperature increasing through the y-axis with different values of air velocity supply. It was found the temperature increasing a little with increasing the values of air velocity.

Figure (5-45) describes the temperature distribution through y-axis at value of z-axis =0.8 m inside the irregular duct. The cooling air supplies by air cooler which is placed at left side of rig duct. These value of results were taken with different values of air velocity (4.2 m/s, 2.8m/s, and 1.4m/s). This curve shows the temperature increasing through the y-axis with different values of air velocity supply. It was found the temperature increasing a little with increasing the values of air velocity.

Figure (5-47) points the temperature distribution through y-axis at value of z-axis =1m inside the irregular duct. The cooling air supplies by air cooler which is placed at left side of rig duct. These values of results were taken with different values of air velocity (4.2 m/s, 2.8m/s, and 1.4m/s). This curve shows the temperature increasing through the y-axis with different values of air velocity supply.

Figure (5-49) induces isothermal contour of the temperature distribution through irregular duct at different velocity of air flow. The air flow supplies by fan which is placed at right-left side and left-right side of rig duct, when it used an air-cooler, and the flow from the left side of rig duct. from the figure, the temperature in the main flow zone near the intermediate fluid domain is relatively high, and the temperature near the wall surface is low.

Figure (5-50) shows isothermal contour of the temperature distribution through irregular duct at different velocity of air flow. The air flow supplies by fan which is placed at right-left side and left-right side of rig duct, when it used an air-cooler, and the flow from the right side of rig duct from the figure, the temperature in the main flow zone near the intermediate fluid domain is relatively high, and the temperature near the wall surface is low.

Figure (5-51) points variation of average friction factor with Reynolds number in the test duct at left and right side of rig duct for case three at velocity (4.2

m/s, 2.8m/s, and 1.4m/s), that the value of the Reynolds number is affected by an increase in the velocity of air, as it increases as the value of the velocity increases. The value of the fraction factor is inversely proportional to the value of the Reynolds number, that the friction factor f decreases as Re increases with the same slope. The effects of modified Reynolds number and eccentricity on friction factor respectively. From Figure, it is seen that the increase in modified Reynolds number results to a decrease in friction factor and that the geometry of the duct has a pronounced effect on the friction factor. These results consistent with experimented results of **[36]**.

Figure (5-52) illustrates variation of average pressure drop with Reynolds number in the test duct at left and right side of rig duct for case three at velocity (4.2 m/s, 2.8m/s, and 1.4m/s). That, the value of the Reynolds number is affected by an increase in the velocity of air, as it increases as the value of the velocity increases. The value of the pressure drop is inversely proportional to the value of the Reynolds number, that pressure drop decreases as Re increases with the same slope. The effect of modified Reynolds number and eccentricity on pressure drop respectively. These results are consistent with experimented results of **[6]**.

5.2. Theoretical Work

Case One

In the first case, using heat flux as a boundary condition at top and side wall of test duct. The measurements of air temperature distribution were represented after 120 minutes of working time. These values of results are taken with different values of air inlet velocity (4.2 m/s, 2.8m/s, and 1.4m/s).

1. Temperature Distributions

The following results of temperature distribution are obtained from the analysis after completing the calculations by a computer program in Matlab software.

A-The fan placed at left side of rig duct:

Figure (5-3) describes the temperature distribution through y-axis at value of z-axis =0.2 m inside the test section of left side of irregular duct for case one. These value of results are taken with different values of air velocity (4.2 m/s,2.8m/s, and 1.4 m/s). This curve shows the temperature increasing through the y-axis with different values of air velocity supply. It is found the temperature increasing a little with increasing the values of air velocity. The highest value for temperature is 63.5^{o}C at 4.2m/s, and the lowest value for temperature is 39.4^{o}C at 1.4m/s.. That means the air flow heating by the heat flux at top and side wall of duct.

Figure (5-5) represents the temperature distribution through y-axis at value of z-axis =0.4 m inside the test section of irregular duct. These value of results are taken with different values of air velocity (4.2 m/s,2.8m/s, and 1.4 m/s). This curve shows the temperature increasing through the y-axis with different values of air velocity supply. It is found the temperature increases a little with increasing the values of air velocity. The highest value for temperature is 63.5^{o}C at 4.2m/s, and the lowest value for temperature is 39.4^{o}Cat 1.4m/s.

Figure (5-7) points the temperature distribution through y-axis at value of z-axis =0.6 m inside the test section of irregular duct. These value of results were taken with different values of air velocity (4.2 m/s,2.8m/s, and 1.4 m/s). This curve shows the temperature increasing through the y-axis with different values of air velocity supply. It is found the temperature increases a little with increasing the values of air

velocity. The highest value for temperature is 63.5^{o}C at 4.2m/s, and the lowest value for temperature is 39.4^{o}Cat 1.4m/s.

Figure (5-9) shows the temperature distribution through y-axis at value of z-axis =0.8m inside the test section of irregular duct. These value of results are taken with different values of air velocity (4.2 m/s,2.8m/s, and 1.4 m/s). This curve shows the temperature increasing through the y-axis with different values of air velocity supply. It is found the temperature increases a little with increasing the values of air velocity. The highest value for temperature is 63.5^{o}C at 4.2m/s, and the lowest value for temperature is 39.4^{o}Cat 1.4m/s.

Figure (5-11) illustrates the temperature distribution through y-axis at value of z-axis =1 m inside the test section of irregular duct. These value of results were taken with different values of air velocity (4.2 m/s,2.8m/s, and 1.4 m/s). This curve shows the temperature increasing through the y-axis with different values of air velocity supply. It is found the temperature increases a little with increasing the values of air velocity. The highest value for temperature is 63.5^{o}C at 4.2m/s, and the lowest value for temperature is 39.4^{o}Cat 1.4m/s.

From these curves, it was pointed maximum value of temperature record 72.3^{o}C is through y-axis at value of z-axis is 0.8 m with velocity value 4.2m/s These results consistent with experimented results of **[48].**

B-The fan placed at right side of rig duct:

Figure (5-3) represents the temperature distribution through y-axis at value of z-axis =1 m inside the test section of irregular duct. The air flow supplies by fan which is placed at right side of rig duct. The air flow is heated through the irregular duct by heat flux which was placed at the top and side of the test duct. These value of results are taken with different values of air velocity (4.2 m/s,2.8m/s, and 1.4 m/s).

This curve shows the temperature increasing through the y-axis with different values of air velocity supply. It is found the temperature increases a little with increases the values of air velocity. The highest value for temperature is 63.5^{o}C at 4.2m/s, and the lowest value for temperature is 39.4^{o}Cat 1.4m/s.

Figure (5-5) points the temperature distribution through y-axis at value of z-axis =0.8 m inside the test section of irregular duct. The air flow supply by fan which is placed at right side of rig duct. The air flow is heated through the irregular duct by heat flux which was placed at the top and side of the test duct. These value of results were taken with different values of air velocity (4.2 m/s,2.8m/s, and 1.4 m/s). This curve shows the temperature increasing through the y-axis with different values of air velocity supply. It is found the temperature increases a little with increases the values of air velocity. The highest value for temperature is 63.5^{o}C at 4.2m/s, and the lowest value for temperature is 39.4^{o}Cat 1.4m/s.

Figure (5-7) induces the temperature distribution through y-axis at value of z-axis =0.6 m inside the test section of irregular duct. The air flow supply by fan which is placed at right side of rig duct. The air flow is heated through the irregular duct by heat flux which is placed at the top and side of the test duct. These value of results are taken with different values of air velocity (4.2 m/s,2.8m/s, and 1.4 m/s). This curve shows the temperature increasing through the y-axis with different values of air velocity supply. It is found the temperature increases a little with increases the values of air velocity. The highest value for temperature is 63.5^{o}C at 4.2m/s, and the lowest value for temperature is 39.4^{o}Cat 1.4m/s.

Figure (5-9) illustrates the temperature distribution through y-axis at value of z-axis =0.4 m inside the test section of irregular duct. The air flow supply by fan which is placed at right side of rig duct. The air flow is heated through the irregular

duct by heat flux which is placed at the top and side of the test duct. These value of results were taken with different values of air velocity (4.2 m/s,2.8m/s, and 1.4 m/s). This curve shows the temperature increasing through the y-axis with different values of air velocity supply. It is found the temperature increases a little with increases the values of air velocity. The highest value for temperature is 63.5^{o}C at 4.2m/s, and the lowest value for temperature is 39.4^{o}Cat 1.4m/s.

Figure (5-11) describes the temperature distribution through y-axis at value of z-axis =0.2 m inside the test section of irregular duct. The air flow supply by fan which is placed at right side of rig duct. The air flow is heated through the irregular duct by heat flux which was placed at the top and side of the test duct. These value of results were taken with different values of air velocity (4.2 m/s,2.8m/s, and 1.4 m/s). This curve shows the temperature increasing through the y-axis with different values of air velocity supply. It is found the temperature increases a little with increases the values of air velocity. The highest value for temperature is 63.5^{o}C at 4.2m/s, and the lowest value for temperature is 39.4^{o}Cat 1.4m/s.

These result indicated the values of temperature at upper of y-axis are approximately similar. That manes, the position of fan is effected on heating the duct by external boundary condition.

Figure (5-13) shows isothermal contour of the temperature distribution through irregular test of duct at different velocity of air flow, when it used a heat flux as boundary condition, and the flow from the left side of test duct. The flow is simulated along the z-axis. The temperature near the heater in the above wall is found higher than inlet temperature.

Case Two

In the second case, it use fan coil to supply hot air and it was placed at the front of rig duct. The results are comprised in the figures:

1. Temperature Distributions

The following results of temperature distribution are obtained from the analysis after completing the calculations by a computer program in Matlab software.

Figure (5-22) shows the temperature distribution through y-axis at value of z-axis =0.2m inside the test section of irregular duct. The hot air supply by fan coil which is placed at left side of rig duct. These value of results were taken with different values of air velocity (4.2 m/s,2.8m/s, and 1.4 m/s). This curve shows the temperature increasing through the y-axis with different values of air velocity supply. It is found the temperature increasing a little with increasing the values of air velocity.

Figure (5-24) points the temperature distribution through y-axis at value of z-axis =1m inside the test section of irregular duct. The hot air supply by fan coil which is placed at right side of rig duct. These value of results were taken with different values of air velocity (4.2 m/s,2.8m/s, and 1.4 m/s). This curve shows the temperature increasing through the y-axis with different values of air velocity supply. It is found the temperature increasing a little with increases the values of air velocity.

Figure (5-26) describes the temperature distribution through y-axis at value of z-axis =0.4 m inside the test section of irregular duct. The hot air supply by fan coil which is placed at left side of rig duct. These values of results were taken with different values of air velocity (4.2 m/s,2.8m/s, and 1.4 m/s). This curve shows the temperature increases through the y-axis with different values of air velocity supply. It is found the temperature increasing a little with increasing the values of air velocity.

Figure (5-28) indicates the temperature distribution through y-axis at value of z-axis =0.6 m inside the test section of irregular duct. The hot air supply by fan coil which is placed at left side of rig duct. These value of results were taken with different values of air velocity (4.2 m/s,2.8m/s, and 1.4 m/s). This curve shows the temperature increasing through the y-axis with different values of air velocity supply. It is found the temperature increasing a little with increasing the values of air velocity.

Figure (5-30) shows the temperature distribution through y-axis at value of z-axis =0.8 m inside the test section of irregular duct. The hot air supply by fan coil which is placed at left side of rig duct. These value of results were taken with different values of air velocity (4.2 m/s,2.8m/s, and 1.4 m/s). This curve shows the temperature increasing through the y-axis with different values of air velocity supply. It is found the temperature increasing a little with increasing the values of air velocity.

Figure (5-32) points the temperature distribution through y-axis at value of z-axis =1 m inside the test section of irregular duct. The hot air supply by fan coil which is placed at left side of rig duct. These value of results were taken with different values of air velocity (4.2 m/s,2.8m/s, and 1.4 m/s). This curve shows the temperature increasing through the y-axis with different values of air velocity supply. It is found the temperature increasing a little with increasing the values of air velocity.

Figure (5-36) illustrates isothermal contour of the temperature distribution through irregular test of duct at different velocity of air flow, when it used a heater in the front blower as a fan coil, and the flow from the left side of test duct. from the

figure, the temperature in the main flow zone near the intermediate fluid domain is relatively high, and the temperature near the wall surface is low.

Case Three

In the third case, using air cooler to supply cooling air and it is placed at the front of rig duct. The results was comprised in the figures:

1. Temperature Distributions

The following results of temperature distribution are obtained from the analysis after completing the calculations by a computer program in Matlab software.

Figure (5-38) illustrates the temperature distribution through y-axis at value of z-axis =0.2 m inside the test section of irregular duct. The cooling air supplies by air cooler which is placed at left side of rig duct. These values of results were taken with different values of air velocity (4.2 m/s,2.8m/s, and 1.4 m/s). This curve shows the temperature increasing through the y-axis with different values of air velocity supply. It is found the temperature increasing a little with increases the values of air velocity.

Figure (5-40) points the temperature distribution through y-axis at value of z-axis =1 m inside the test section of irregular duct. The cooling air supplies by air cooler which is placed at right side of rig duct. These value of results were taken with different values of air velocity (4.2 m/s, 2.8m/s, and 1.4 m/s). This curve shows the temperature increasing through the y-axis with different values of air velocity supply. It is found the temperature increasing a little with increasing the values of air velocity.

Figure (5-42) shows the temperature distribution through y-axis at value of z-axis =0.4 m inside the test section of irregular duct. The cooling air supplies by air

cooler which is placed at left side of rig duct. These values of results were taken with different values of air velocity (4.2 m/s,2.8m/s, and 1.4 m/s). This curve shows the temperature increasing through the y-axis with different values of air velocity supply. It is found the temperature increasing a little with increasing the values of air velocity.

Figure (5-44) induces the temperature distribution through y-axis at value of z-axis =0.6 m inside the test section of irregular duct. The cooling air supplies by air cooler which is placed at left side of rig duct. These value of results were taken with different values of air velocity (4.2 m/s, 2.8m/s, and 1.4 m/s). This curve shows the temperature increasing through the y-axis with different values of air velocity supply. It is found the temperature increasing a little with increasing the values of air velocity.

Figure (5-46) describes the temperature distribution through y-axis at value of z-axis =0.8 m inside the test section of irregular duct. The cooling air supplies by air cooler which is placed at left side of rig duct. These value of results were taken with different values of air velocity (4.2 m/s, 2.8m/s, and 1.4 m/s). This curve shows the temperature increasing through the y-axis with different values of air velocity supply. It is found the temperature increasing a little with increasing the values of air velocity.

Figure (5-48) describes the temperature distribution through y-axis at value of z-axis =1m inside the test section of irregular duct. The cooling air supplies by air cooler which is placed at left side of rig duct. These value of results were taken with different values of air velocity (4.2 m/s, 2.8m/s, and 1.4 m/s). This curve shows the temperature increasing through the y-axis with different values of air velocity supply.

It is found the temperature increasing a little with increasing the values of air velocity.

Figure (5-50) points isothermal contour of the temperature distribution through irregular test of duct at different velocity of air flow, when it used an air-cooler, and the flow from the left side of test duct. from the figure, the temperature in the main flow zone near the intermediate fluid domain is relatively high, and the temperature near the wall surface is low.

2. Velocity Distribution

The following results are obtained from the ANSYS - Fluent 19.2, which used to study the flow characteristics of air velocity through irregular duct.

Case one

Figure (5-53) illustrates the relationship of air velocity passing inside the duct and z-axis of left side of duct for case one. It was found the air inlet velocity was (4.2, 2.8, and 1.4 m/s) and decreasing inside the irregular duct the flow is through the front duct due to the effect of the duct shape. it has an increase in the air velocity in the middle of the duct at the beginning of entry, and the speed gradually decreases when passing in the second irregular zone.

Figure (5-54) describes the relationship of air velocity passing in the opposite side inside the duct through the z- axis of right side of duct for case one. That it has an increase in the air velocity in the middle of the duct at the beginning of entry, and the speed gradually increases when passing through the second irregular zone due. Where the shape of the duct affects the velocity, which will increase when the flow is through reversing the duct.

Case two

Figure (5-55) illustrates the relationship of air velocity passing inside the duct and z-axis of left side of duct for case two. It was found that the air velocity was (4.2, 2.8, and 1.4 m/s)and decreases when the flow is through the front duct due to the effect of the duct shape. it has an increase in the air velocity in the middle of the duct at the beginning of entry, and the speed gradually decreases when passing in the second irregular zone.

Figure(5-56) describes the relationship of air velocity passing in the opposite side inside the duct through the z- axis of right side of duct for case two. That it has an increase in the air velocity in the middle of the duct at the beginning of entry, and the speed gradually increases when passing through the second irregular zone. This is due the shape of the duct affects the velocity, which will increase when the flow is through reversing the duct.

Case three

Figure (5-57) illustrates the relationship of air velocity passing inside the duct and z-axis of left side of duct for case three. It was found that the air velocity was (4.2, 2.8, and 1.4 m/s) and decreases when the flow is through the front duct due to the effect of the duct shape. it has an increase in the air velocity in the middle of the duct at the beginning of entry, and the speed gradually decreases when passing in the second irregular zone.

Figure(5-58) describes the relationship of air velocity passing in the opposite side inside the duct through the z- axis of right side of duct for case three. That it has an increase in the air velocity in the middle of the duct at the beginning of entry, and the speed gradually increases when passing through the second irregular zone. This is

due the shape of the duct affects the velocity, which will increase when the flow is through reversing the duct.

Zhang and Chen[8]] showed velocity streamline for different angle b at the same Reynolds number. In Figure(5-59), some zones which appear in the center of the computational domain with high air velocity and others of stagnation due to the fins and the wall can be observed. The hydraulic diameter of flow channel gradually expanded along the flow direction. The flow velocity decreased gradually with increasing cross section, which will restrain the convection heat transfer. In fact, this movement decreases the flow intensity in channel and weakens the heat transfer. From these figures, more number of recirculation zones and a destabilization of boundary layer can be found when b 30. As seen, the stream wise flows are disturbed at the near wall showing recirculation flow and separation/reattachment while b 30. The results indicate that there is a low heat transfer region at the wall. It can be also seen that streamline is nearly parallel to the flow direction in the middle domain. And with the increase of b, the values of velocity are getting smaller and smaller. It is noteworthy that the boundary layer separation happening on the wall when b = 30; However, b = 40 is a turning point to evaluate the performance of the two ducts, instead of b = 30. The thermal-hydraulic characteristics for trapezoidal ducts are better than in a rectangular duct When b 40. On the contrary, the rectangular duct has a better performance when b 40.

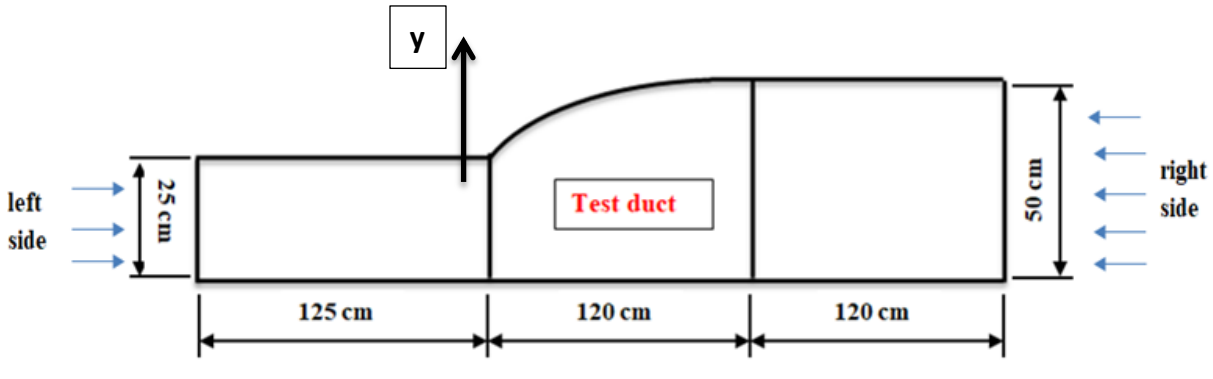

Figure (5-1)schematic diagram of rig duct

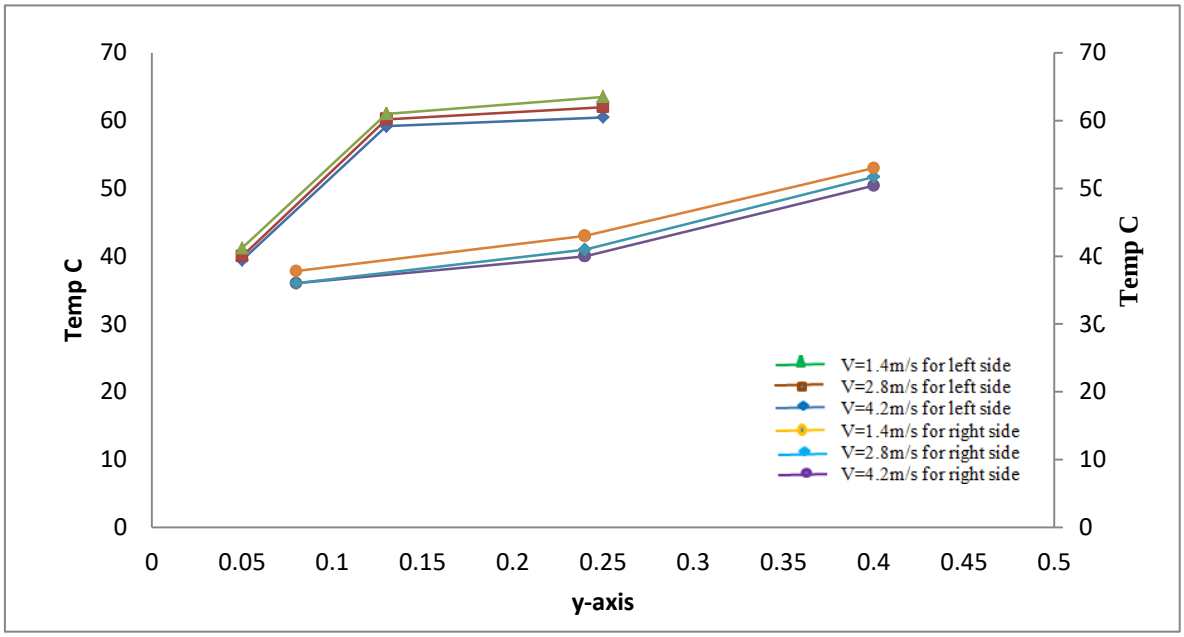

Figure(5-2) experimentally temperature distribution with y-axis in the test duct at z=0.2 m from the left-right side and z=1 m from the right-left side of rig duct for case one.

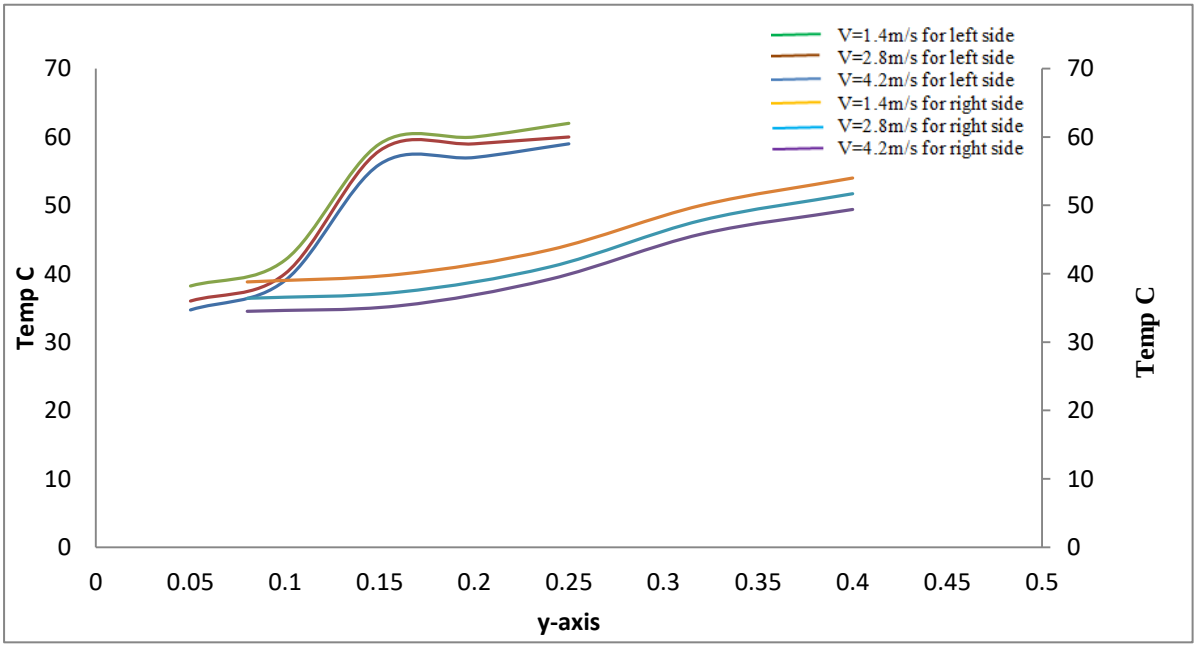

Figure(5-3) theoretically temperature distribution with y-axis in the test duct at z=0.2 m from the left-right side and z=1 m from the right-left side of rig duct for case one.

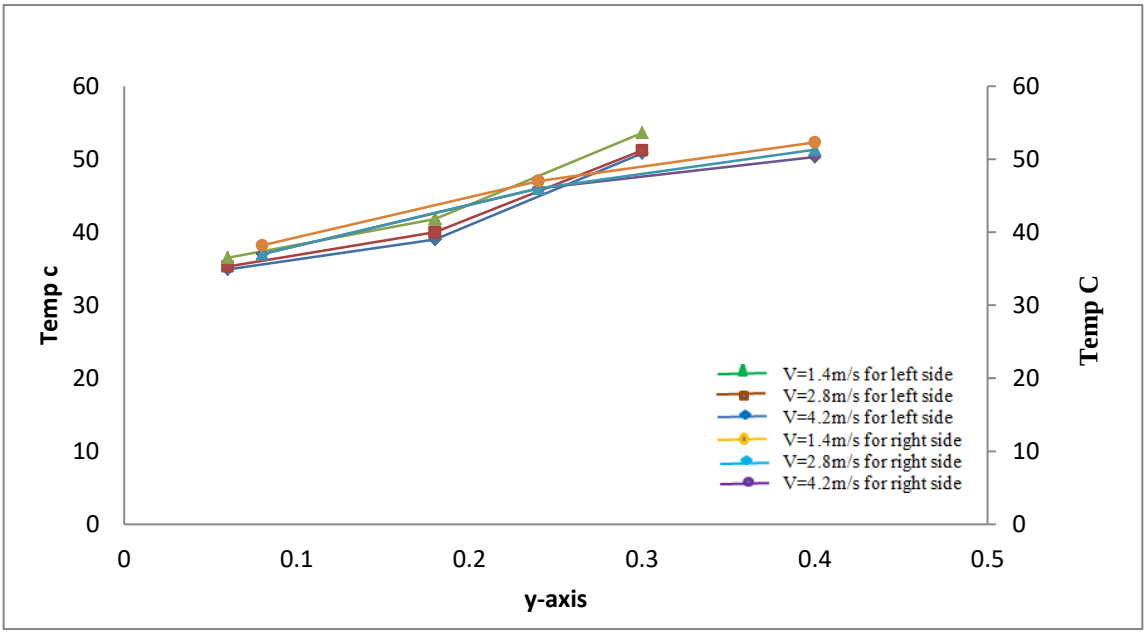

Figure(5-4) experimentally temperature distribution with y-axis in the test duct at z=0.4 m from the left-right side and z=0.8 m from the right-left side of rig duct for case one.

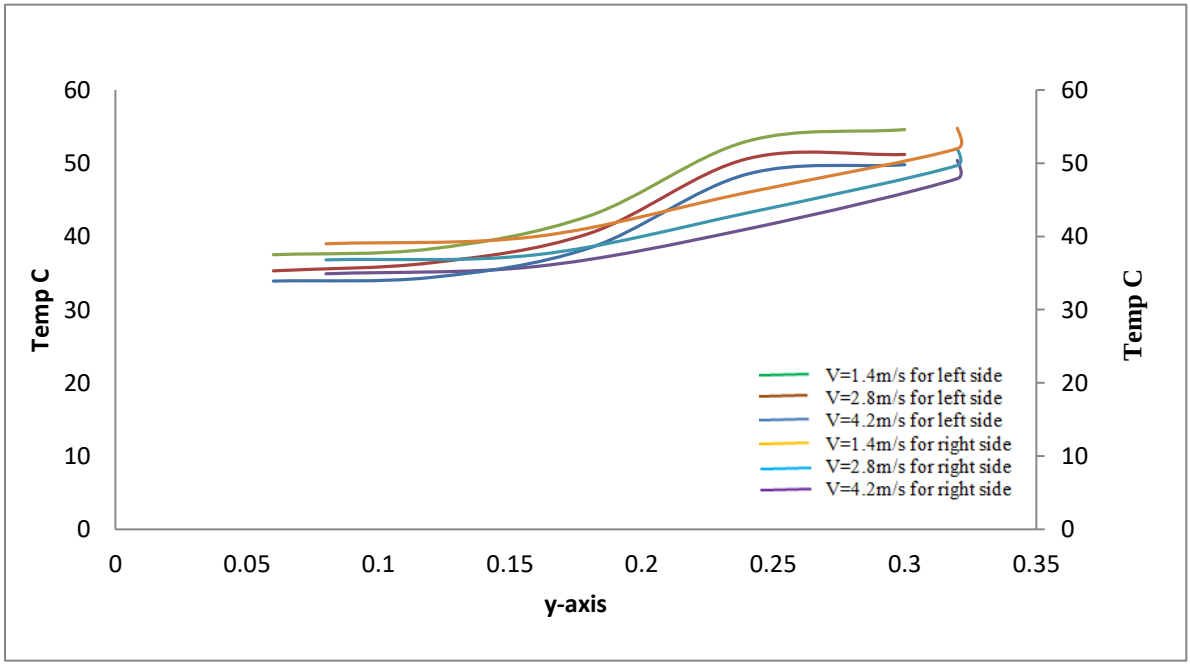

Figure(5-5) theoretically temperature distribution with y-axis in the test duct at z=0.4m from the left-right side and z=0.8 m from the right-left side of rig duct for case one.

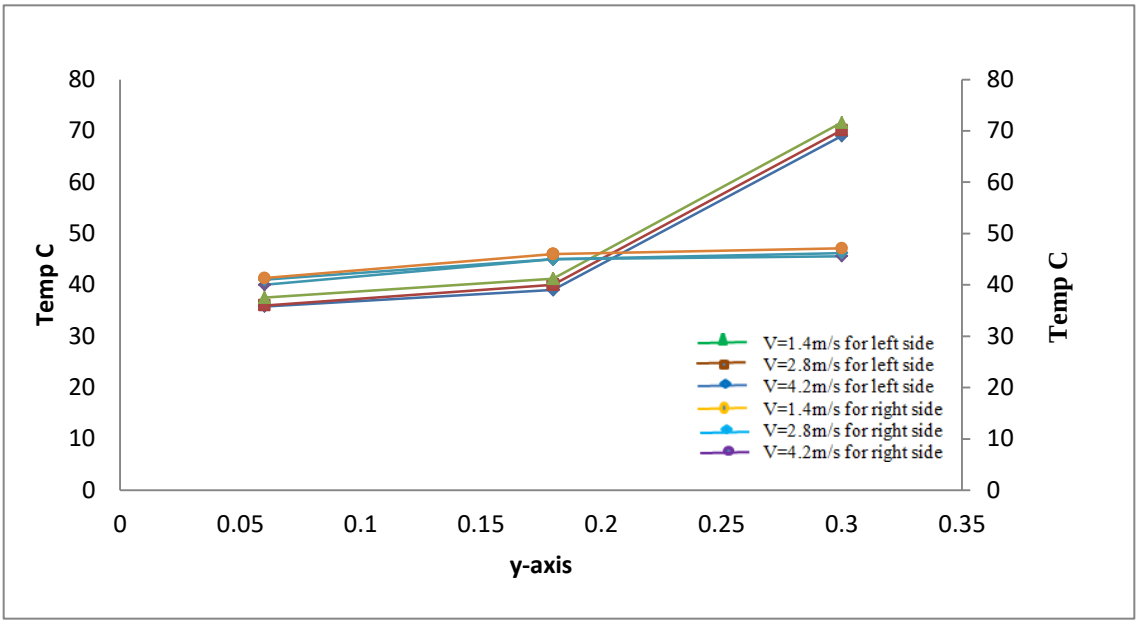

Figure(5-6) experimentally temperature distribution with y-axis in the test duct at z=0.6 m from the left-right side and z=0.6 m from the right-left side of rig duct for case one.

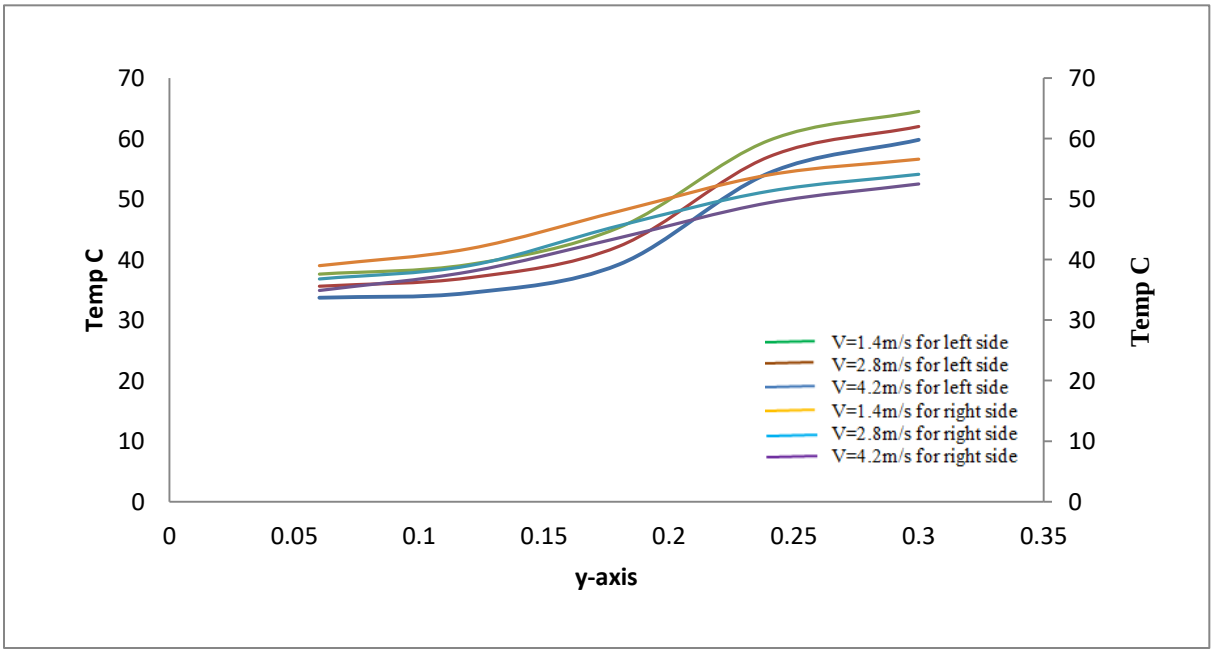

Figure(5-7) theoretically temperature distribution with y-axis in the test duct at z=0.6m from the left-right side and z=0.6 m from the right-left side of rig duct for case one.

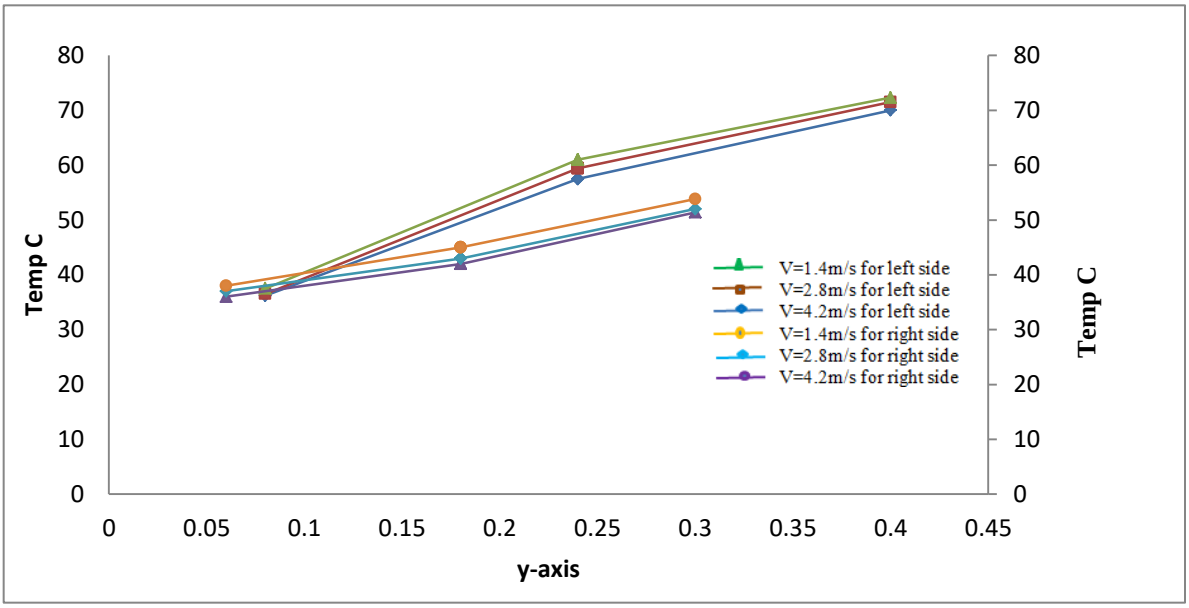

Figure(5-8) experimentally temperature distribution with y-axis in the test duct at z=0.8 m from the left-right side and z=0.4 m from the right-left side of rig duct for case one.

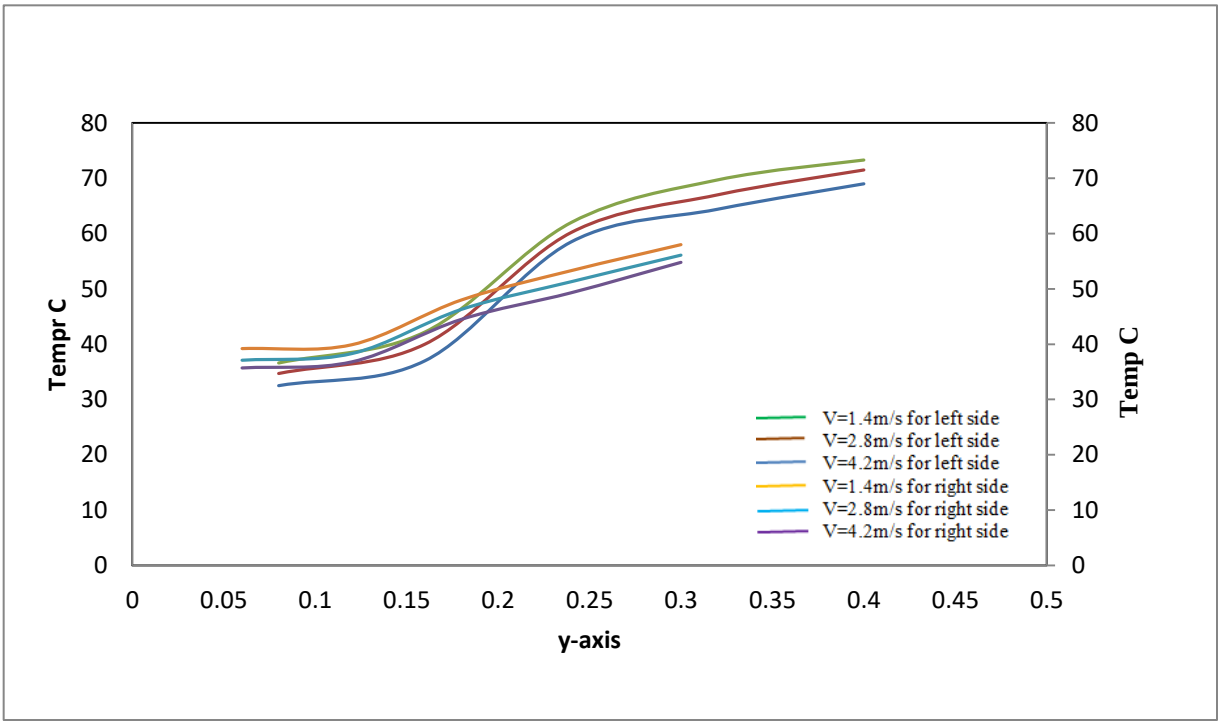

Figure(5-9) theoretically temperature distribution with y-axis in the test duct at z=0.8 m from the left-right side and z=0.4 m from the right-left side of rig duct for case one.

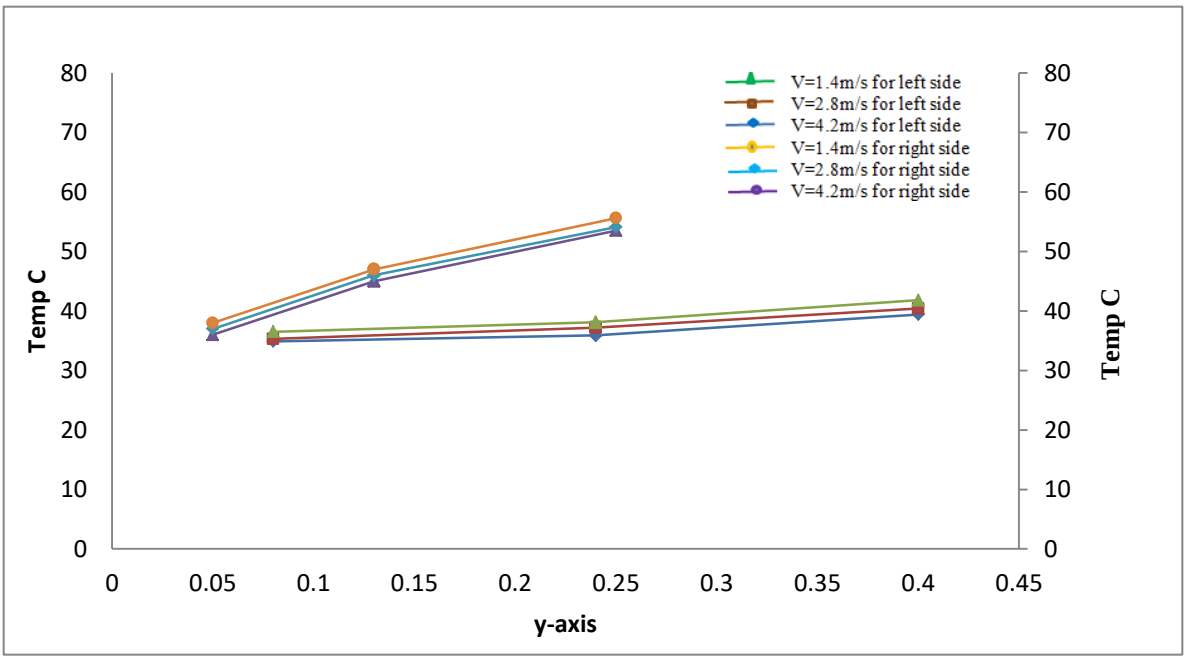

Figure(5-10) experimentally temperature distribution with y-axis in the test duct at z=1 m from the left-right side and z=0.2 m from the right-left side of rig duct for case one.

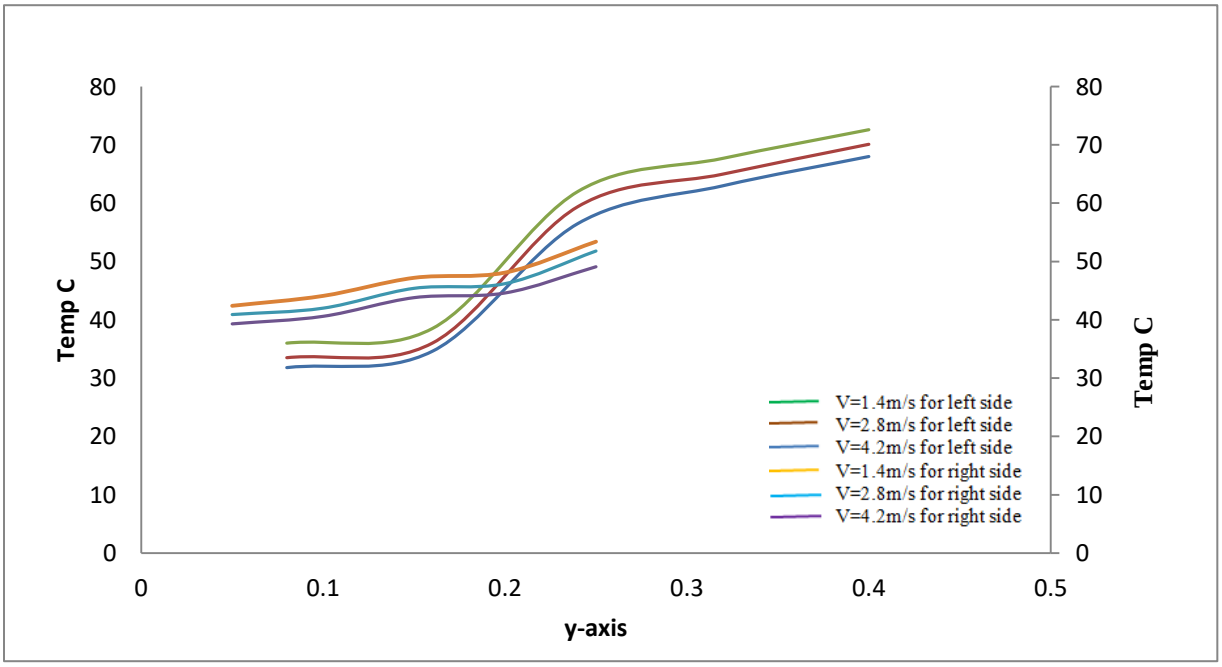

Figure(5-11) theoretically temperature distribution with y-axis in the test duct at z=1 m from the left-right side and z=0.2 m from the right-left side of rig duct for case one.

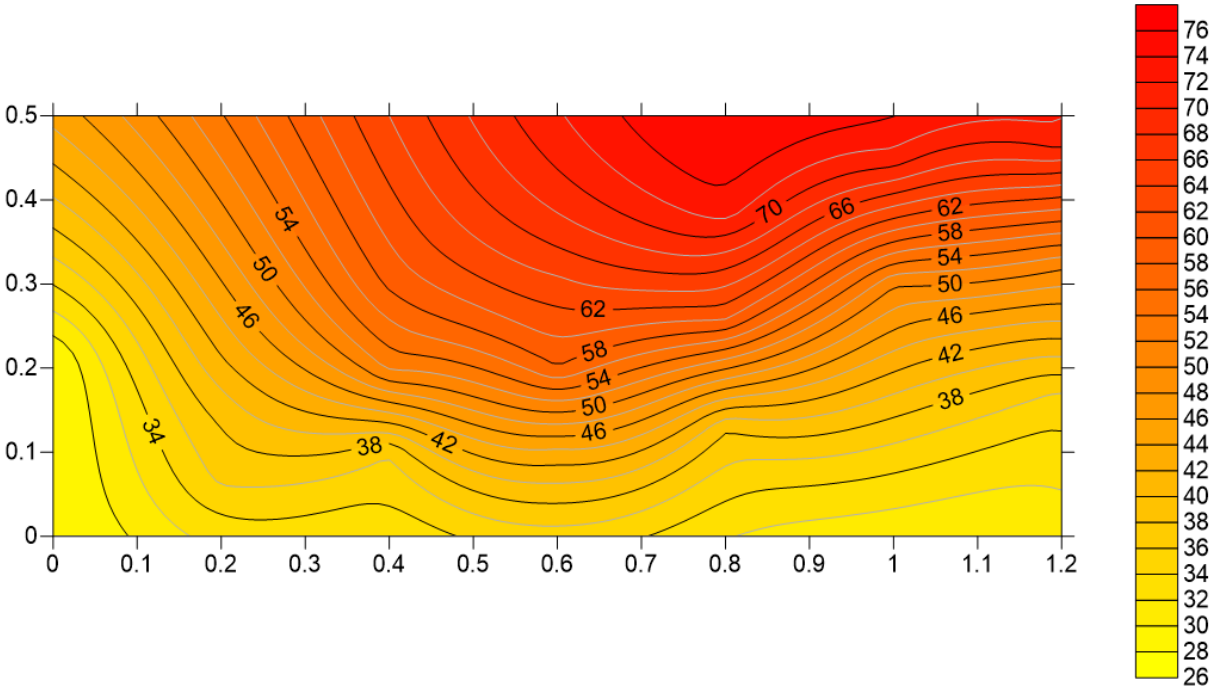

one.

Figure (5-12) experimental results of isothermal contour temperature distribution in the irregular duct through (y-z) plane from left side of rig duct for case one at 4.2m/s .

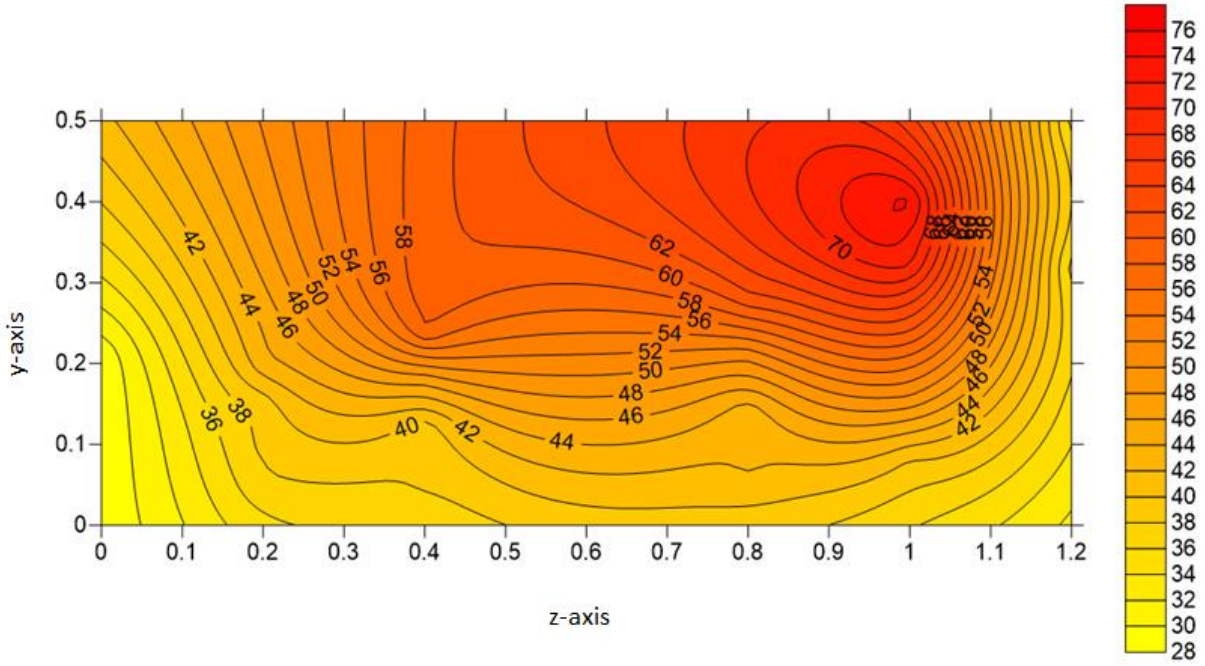

Figure (5-13) theoretical results of isothermal contour temperature distribution in the test duct through (y-z) plane from left side of rig duct for case one at 4.2m/s.

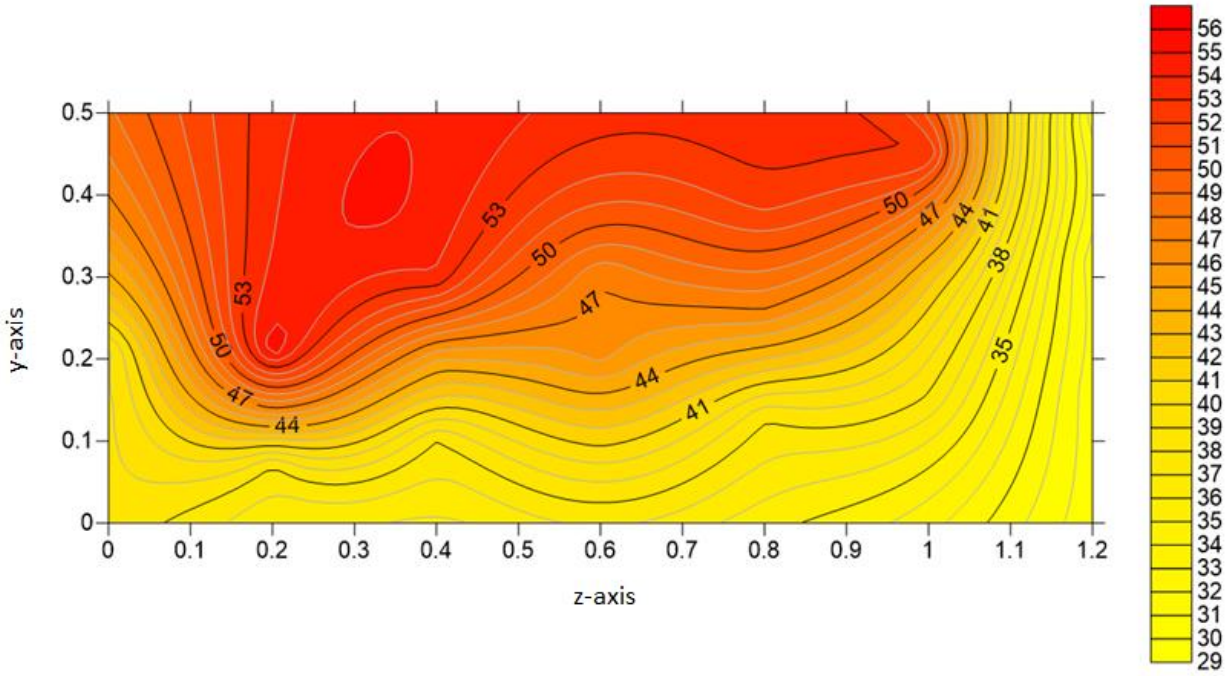

Figure (5-14) experimental results of isothermal contour temperature distribution in the irregular duct through (y-z) plane from right side of rig duct for case one at 4.2m/s.

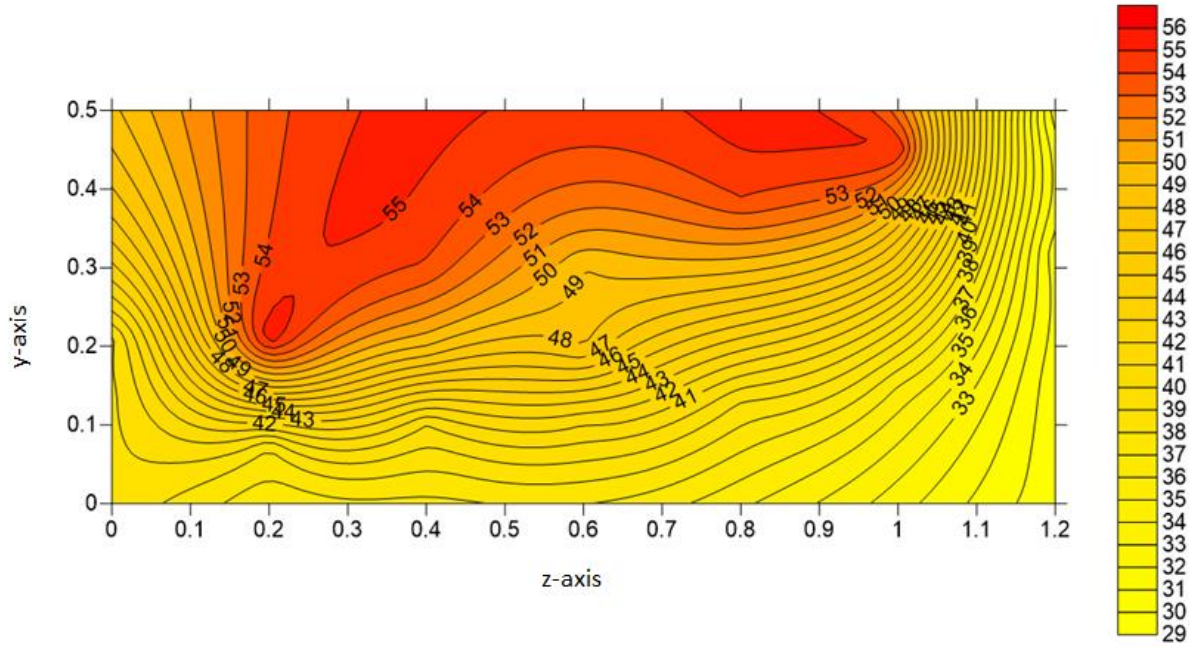

Figure (5-15) theoretical results of isothermal contour temperature distribution in the test duct through (y-z) plane from right side of rig duct for case one at 4.2m/s.

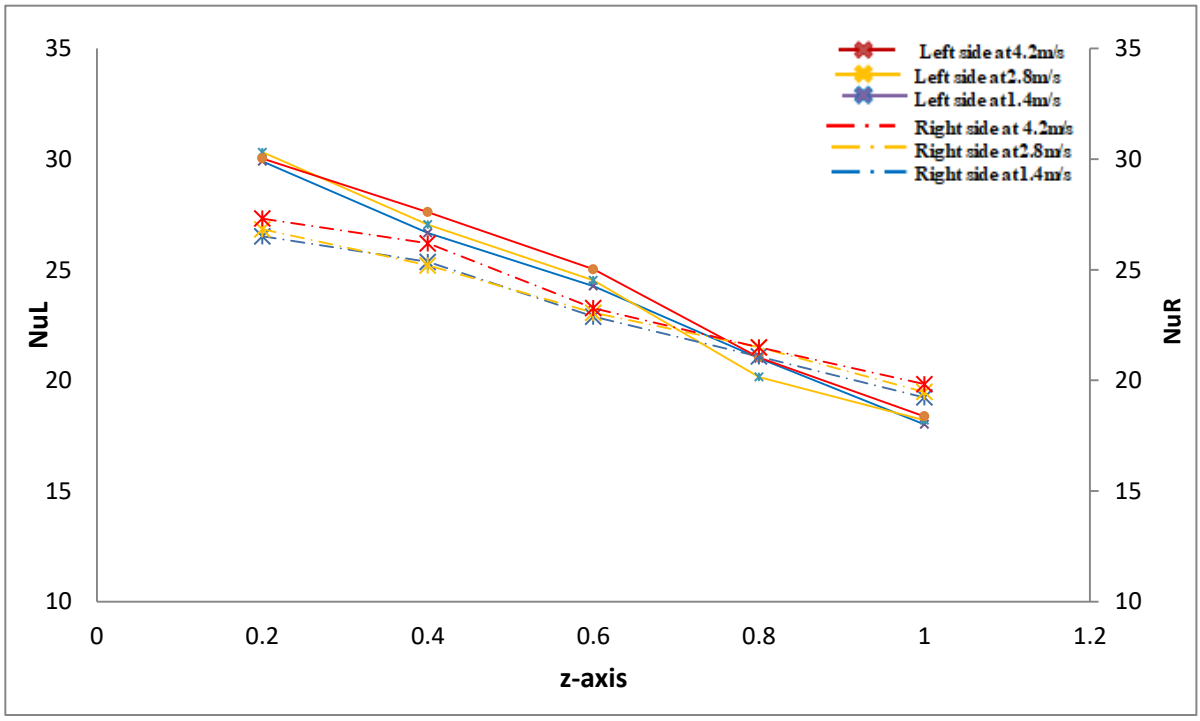

Figure(5-16) variation of Nusselt number through z-axis from left side and right side of test duct for case one.

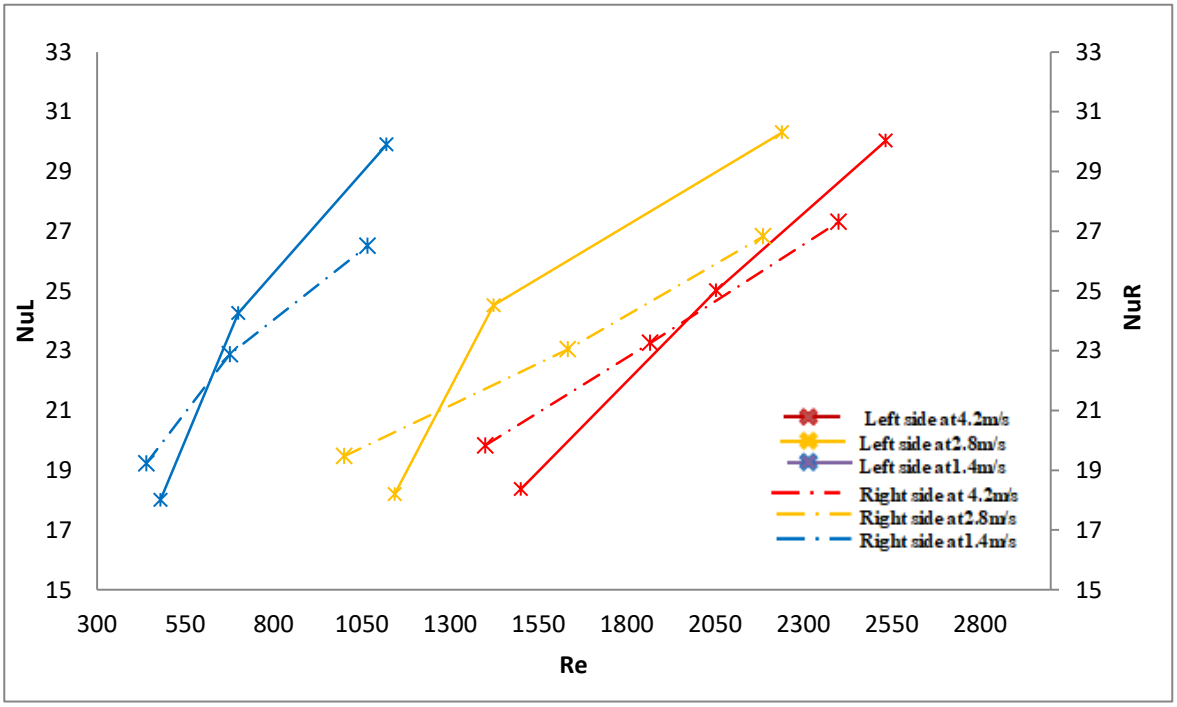

Figure(5-17) relationship between the Nusselt and Reynolds number from the left side, and right side of test duct for case one.

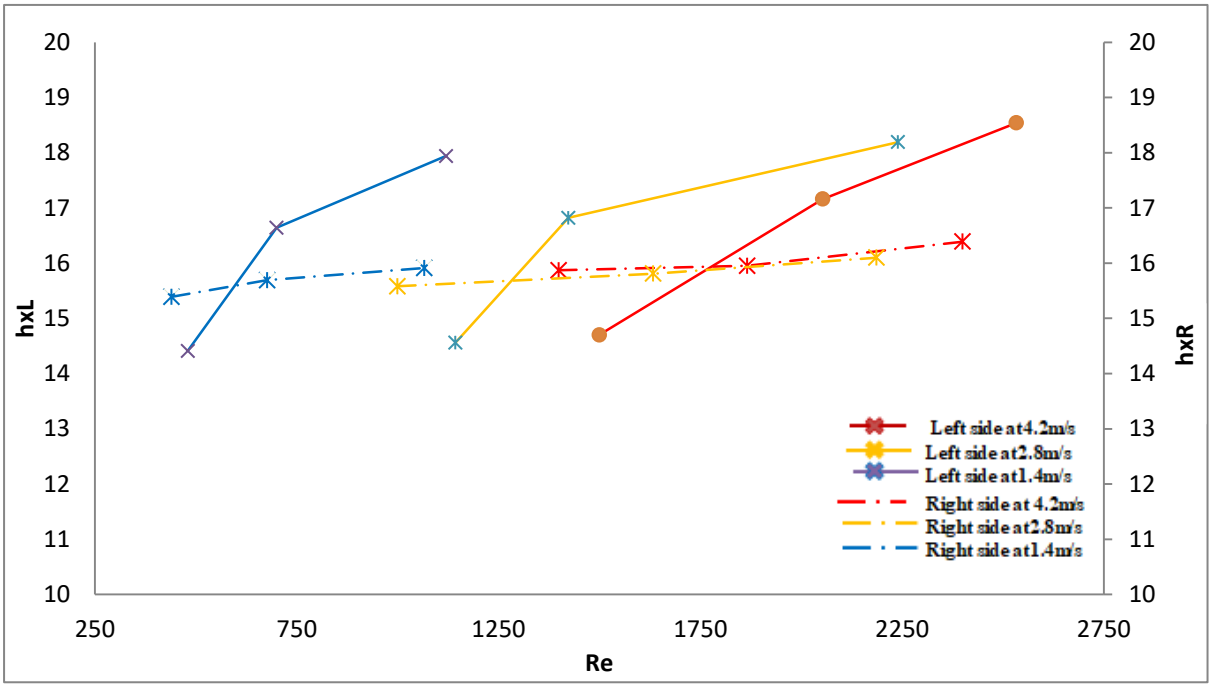

Figure(5-18) relationship between coefficient of heat transfer and Reynolds number from the left side and right side of test duct for case one.

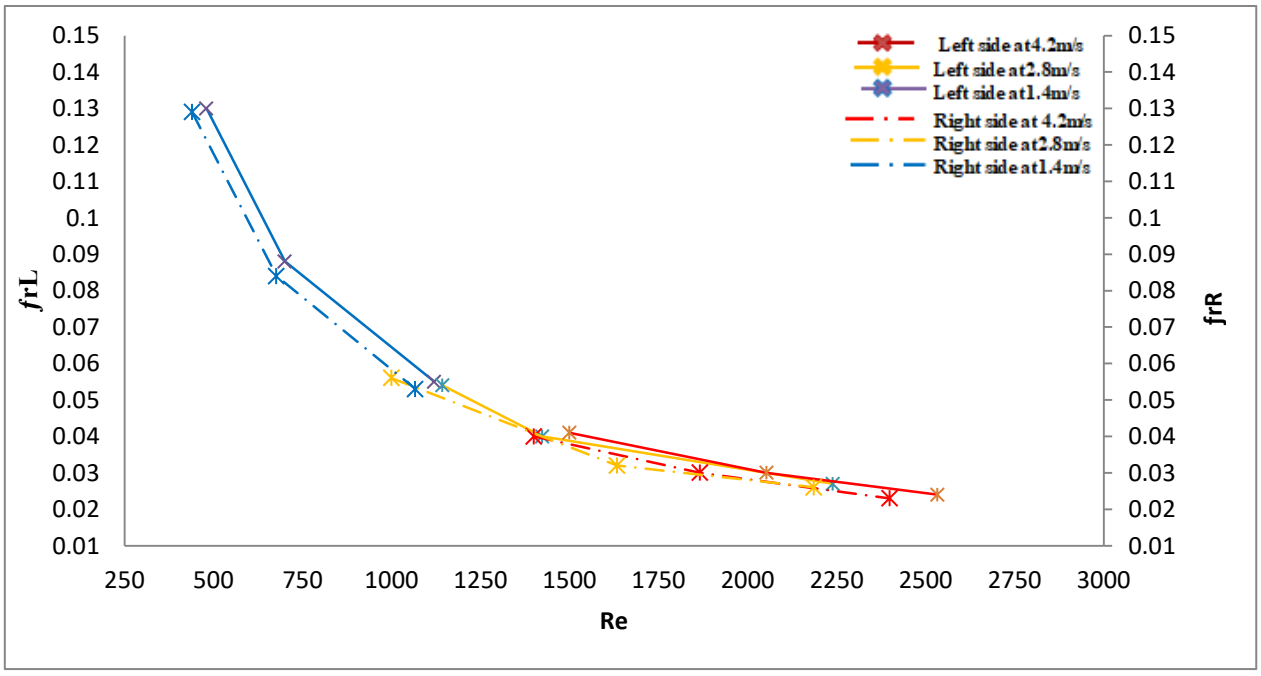

Figure(5-19) variation of friction factor with Reynolds number from left side and right side of test duct for case one.

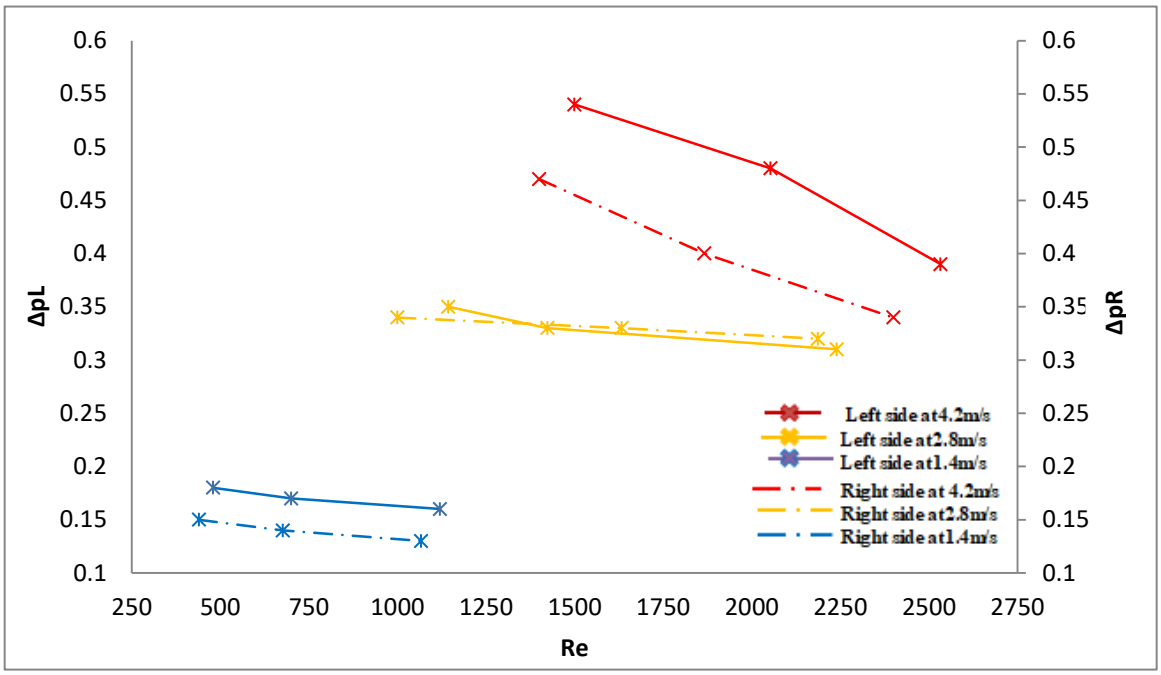

Figure(5-20) variation of pressure drop with Reynolds number from left side and right side of test duct for case one.

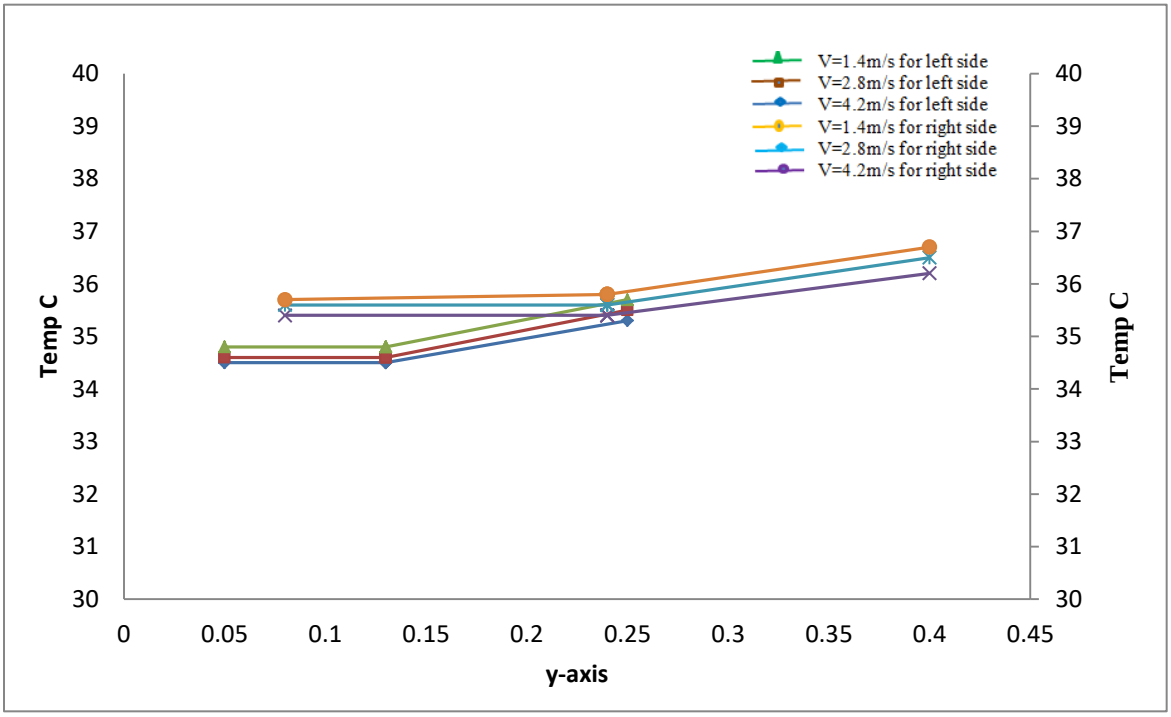

Figure(5-21) experimentally temperature distribution with y-axis in the test duct at z=0.2 m from the left-right side and z=1 m from the right-left side of rig duct for case two.

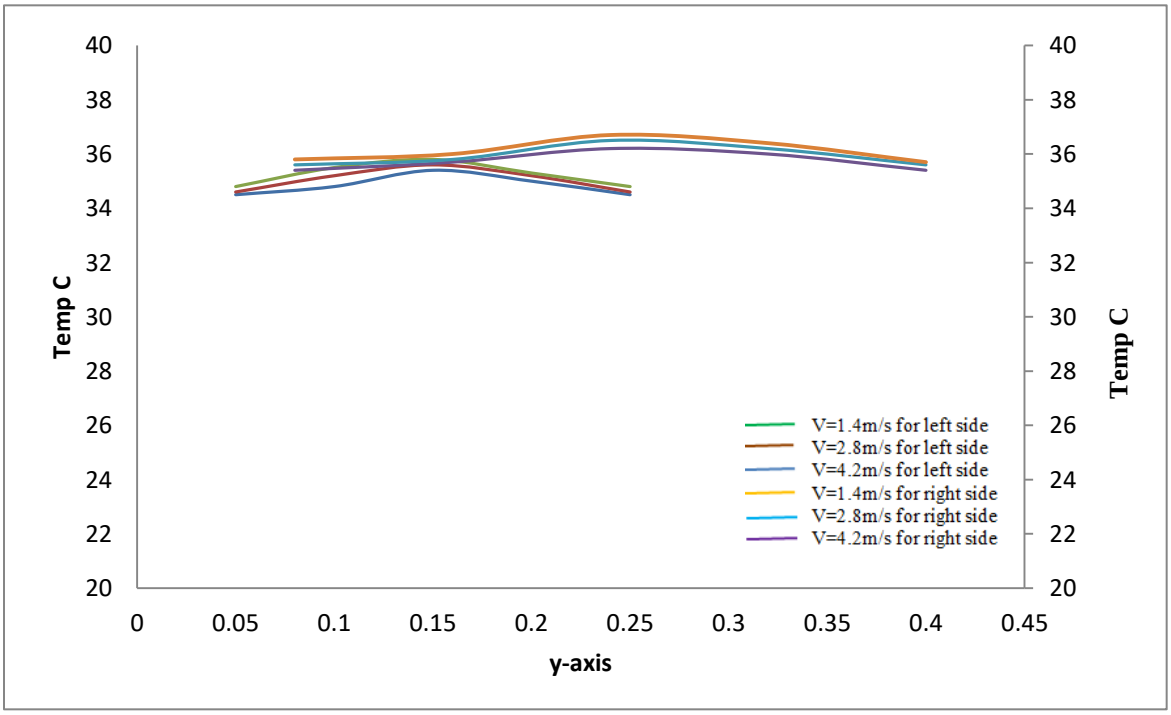

Figure(5-22) theoretically temperature distribution with y-axis in the test duct at z=0.2 m from the left-right side and z=1 m from the right-left side of rig duct for case two.

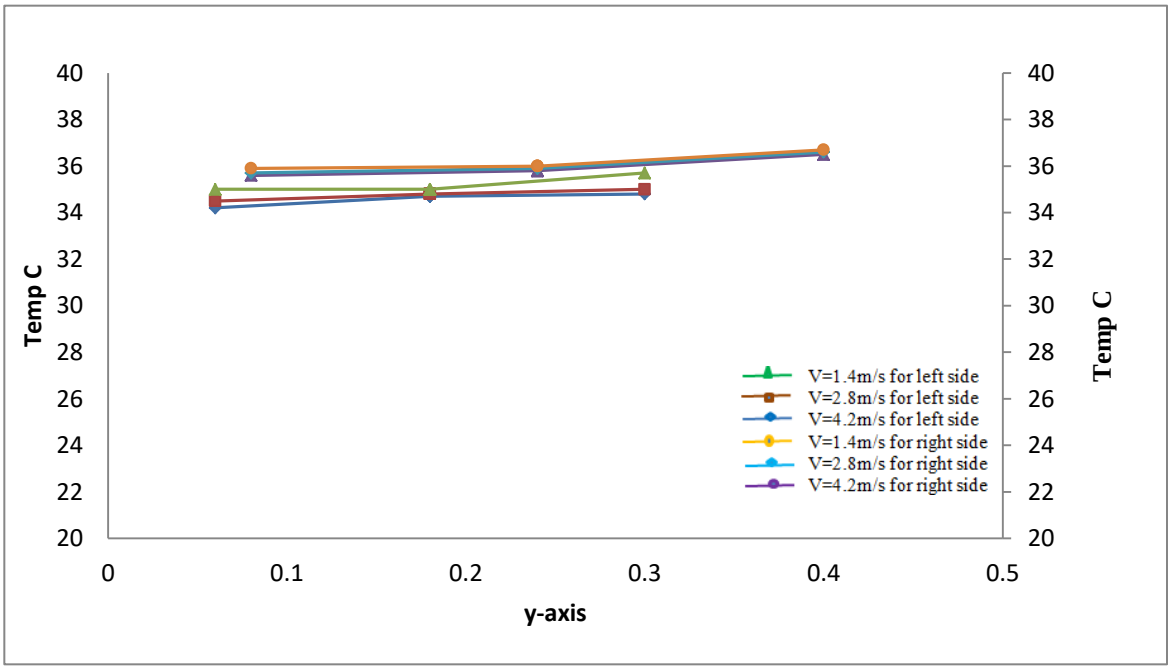

Figure(5-23) experimentally temperature distribution with y-axis in the test duct at z=0.4 m from the left-right side and z=0.8 m from the right-left side of rig duct for case two.

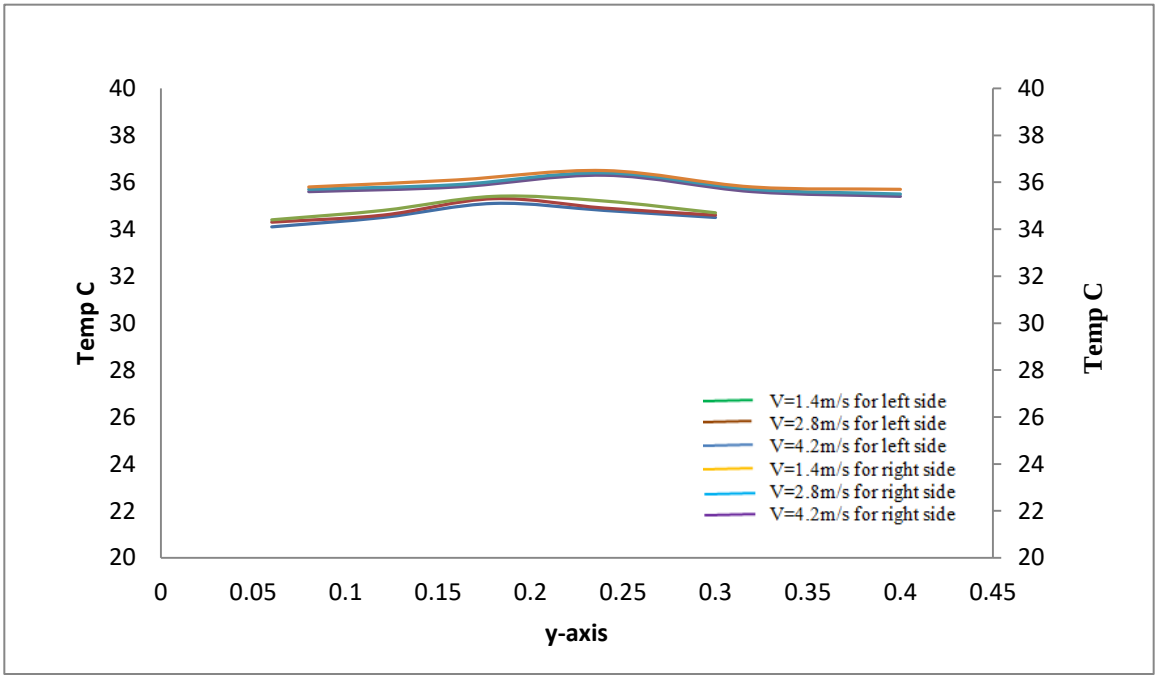

Figure(5-24) theoretically temperature distribution with y-axis in the test duct at z=0.4 m from the left-right side and z=0.8 m from the right-left side of rig duct for case two.

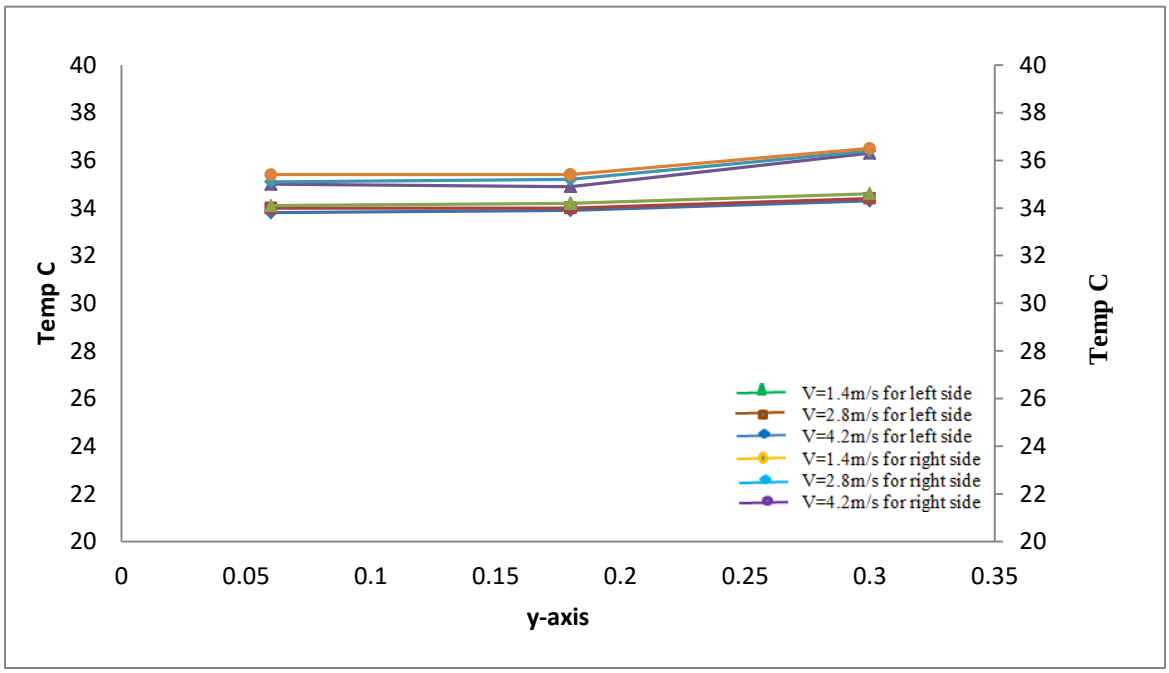

Figure(5-25) experimentally temperature distribution with y-axis in the test duct at z=0.4 m from the left-right side and z=0.8 m from the right-left side of rig duct for case two.

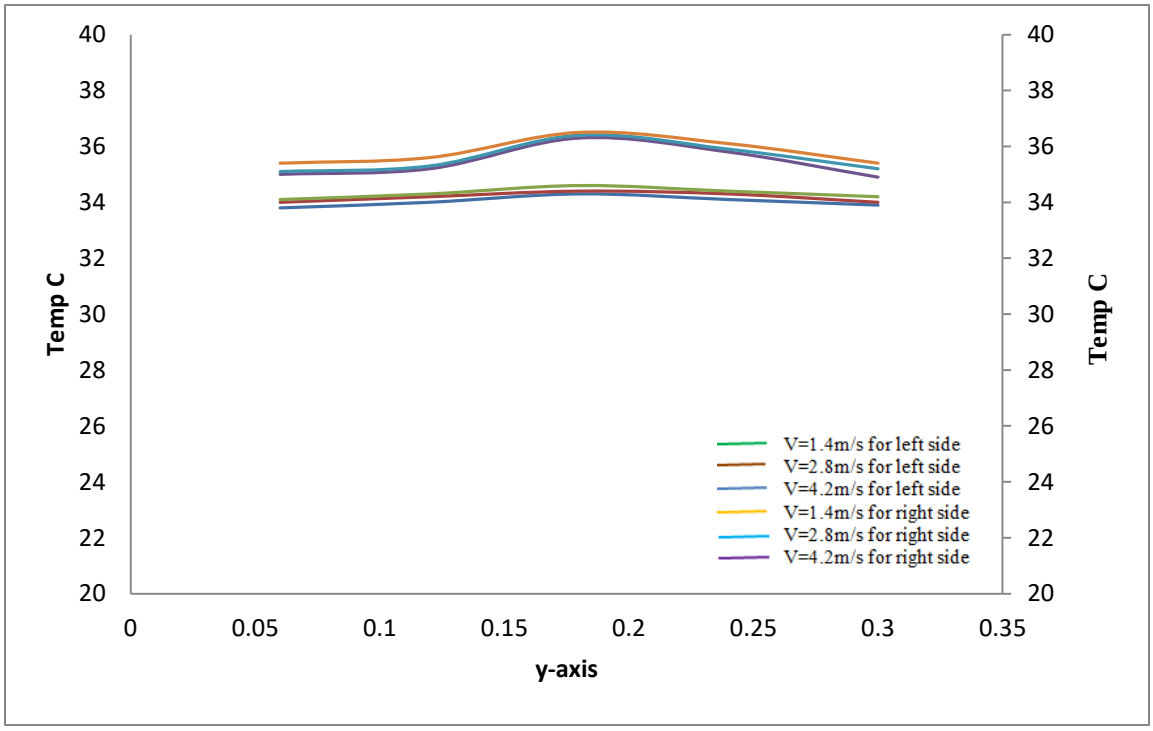

Figure(5-26) theoretically temperature distribution with y-axis in the test duct at z=0.6 m from the left-right side and z=0.6 m from the right-left side of rig duct for case two.

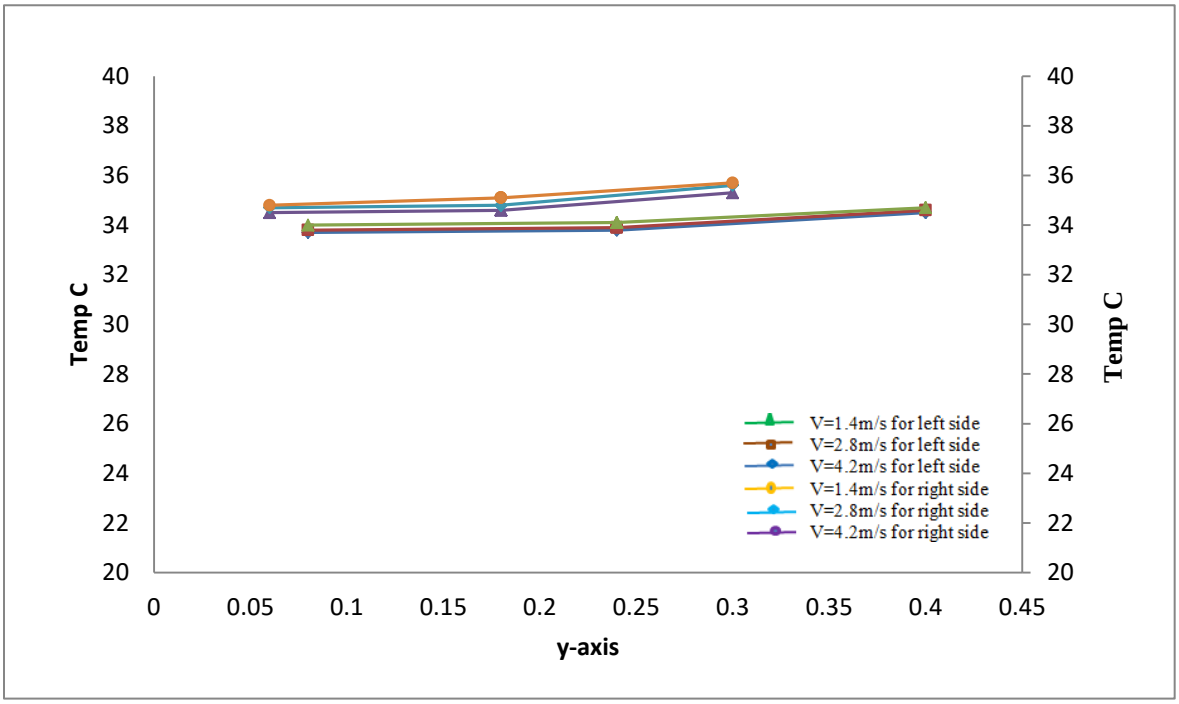

Figure(5-27) experimentally temperature distribution with y-axis in the test duct at z=0.8 m from the left-right side and z=0.4 m from the right-left side of rig duct for case two.

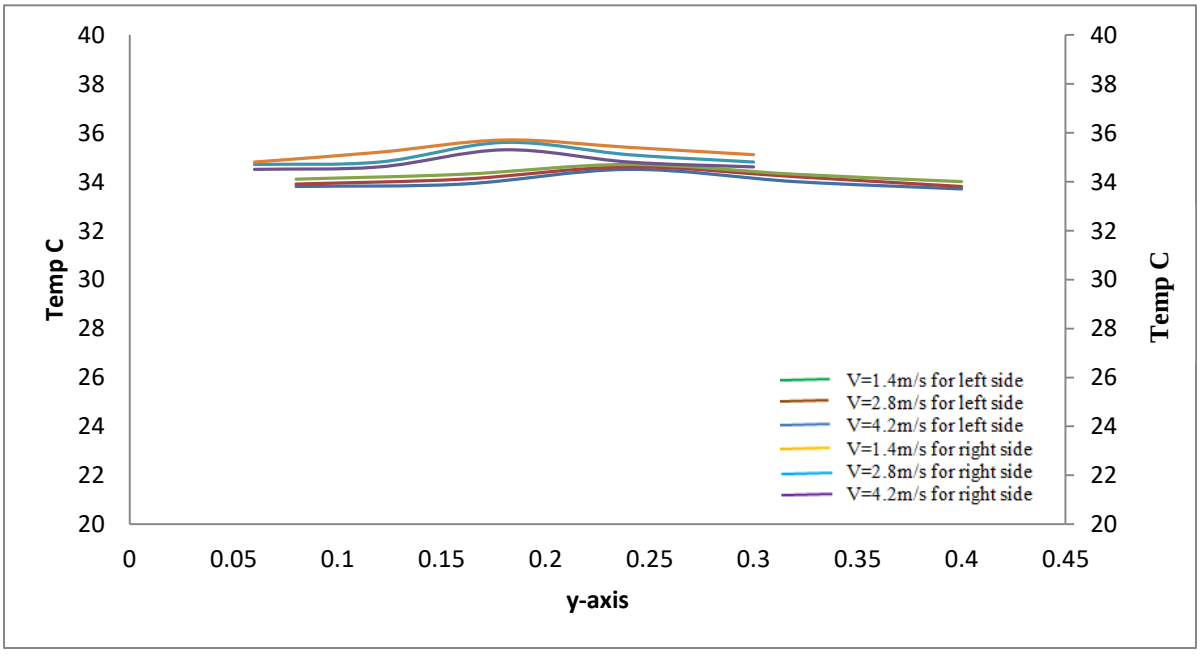

Figure(5-28) theoretically temperature distribution with y-axis in the test duct at z=0.8 m from the left-right side and z=0.4 m from the right-left side of rig duct for case two.

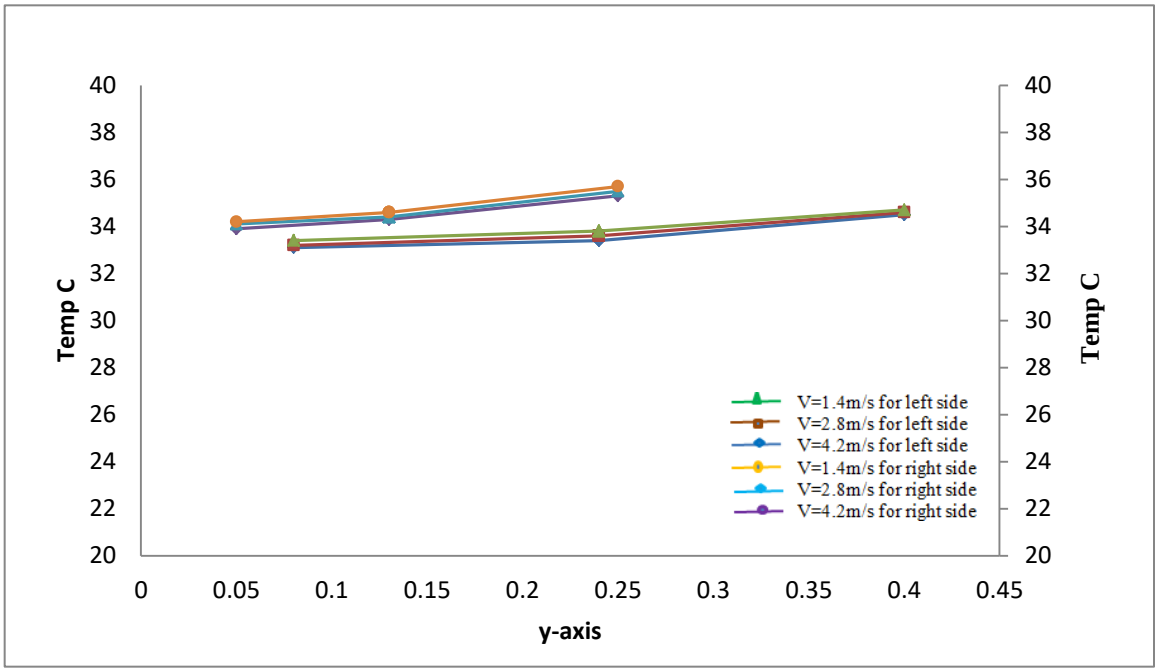

Figure(5-29) experimentally temperature distribution with y-axis in the test duct at z=1 m from the left-right side and z=0.2 m from the right-left side of rig duct for case two.

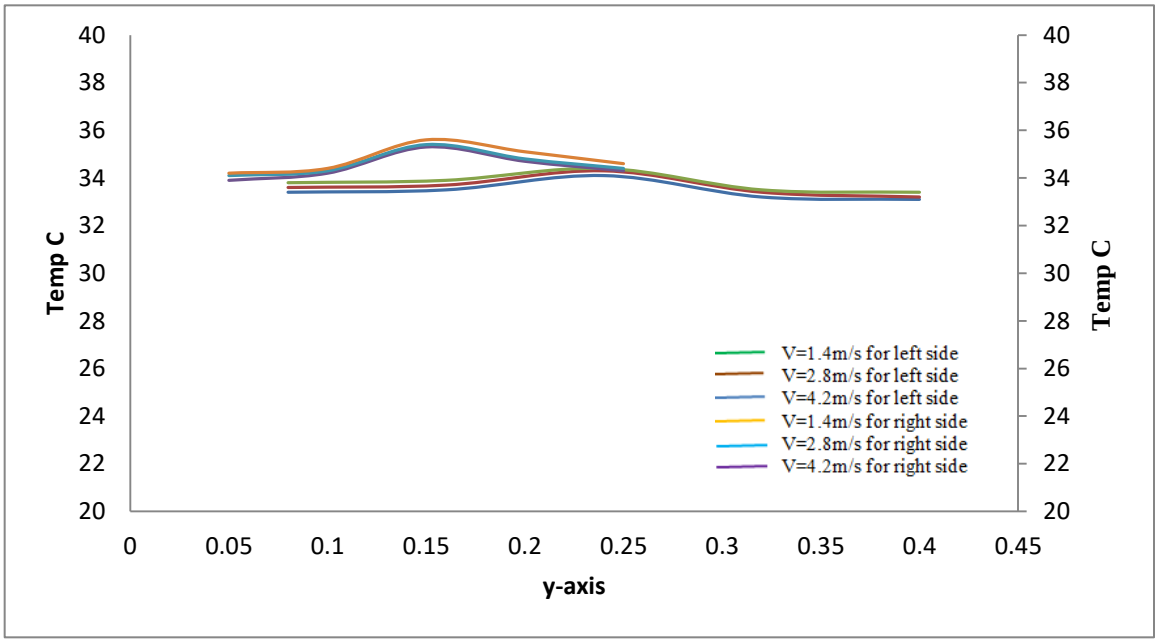

Figure(5-30) theoretically temperature distribution with y-axis in the test duct at z=1 m from the left-right side and z=0.2 m from the right-left side of rig duct for case two.

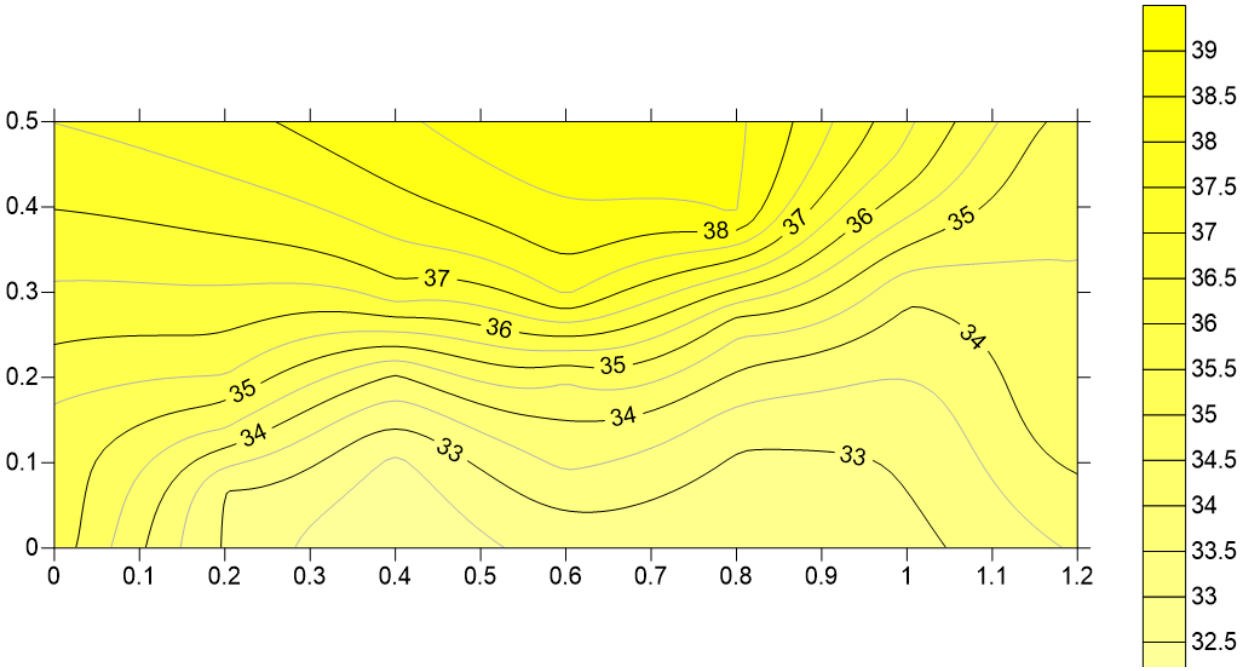

Figure (5-31) experimental results of isothermal contour temperature distribution in the irregular duct through (y-z) plane from left side of rig duct for case two at 2.8m/s.

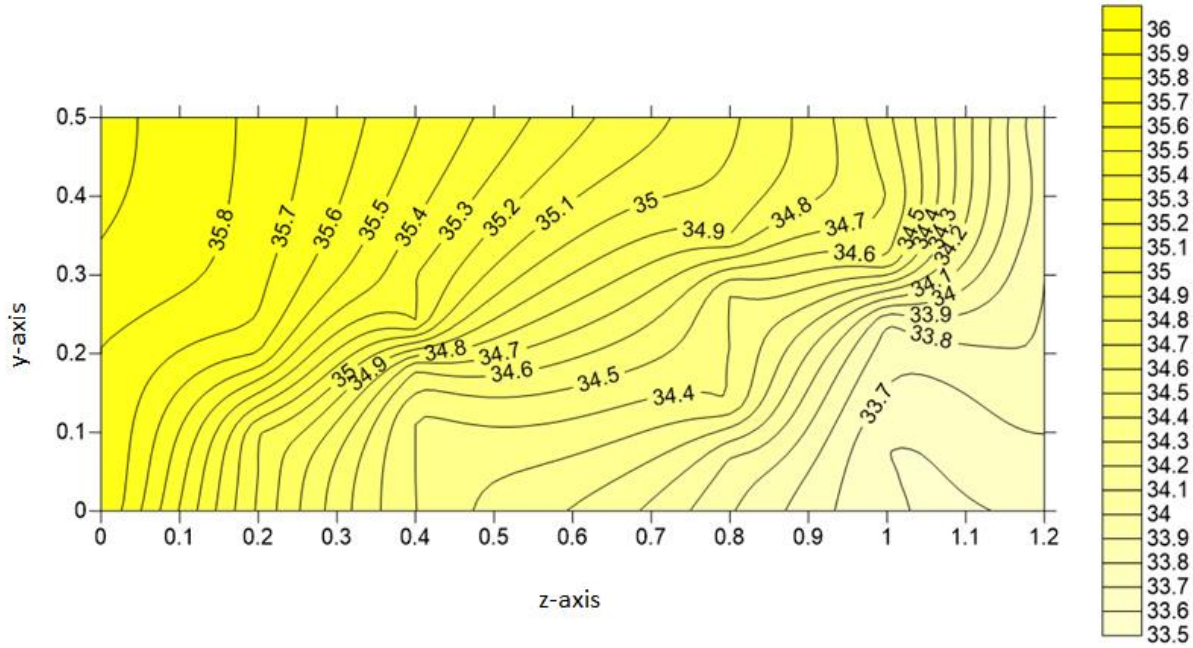

Figure (5-32) theoretical results of isothermal contour temperature distribution in the test duct through (y-z) plane from left side of rig duct for case two at 2.8m/s.

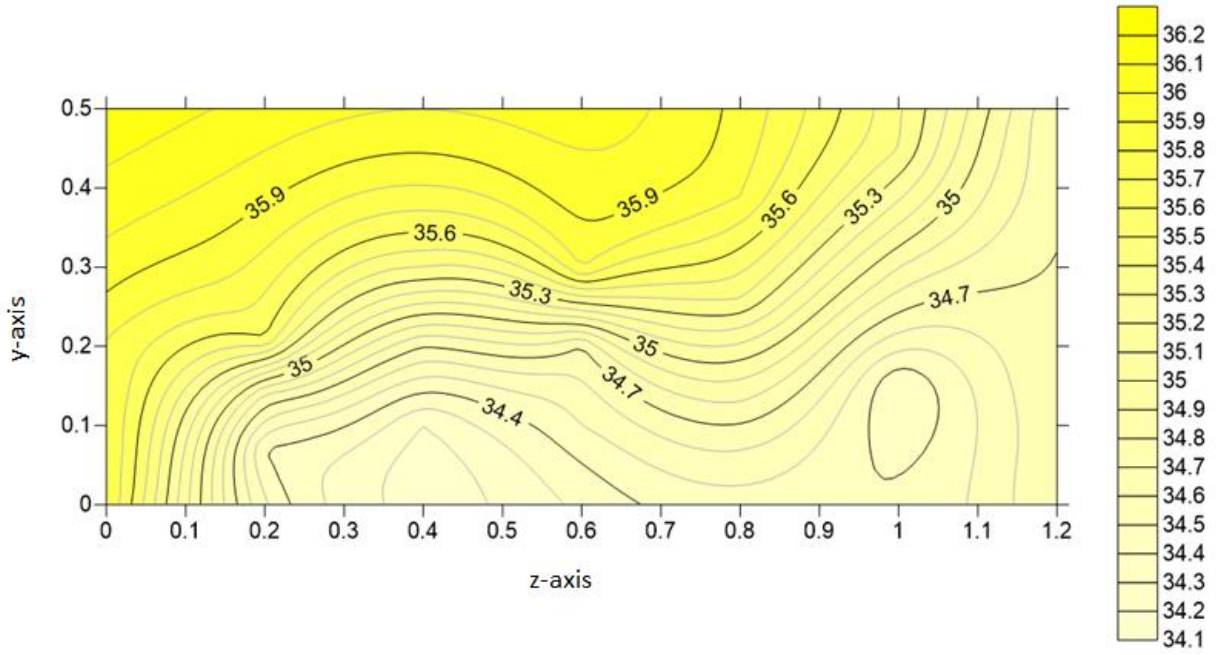

Figure (5-33) experimental work of isothermal contour temperature distribution in the irregular duct through (y-z) plane from right side of rig duct for case two at 2.8m/s.

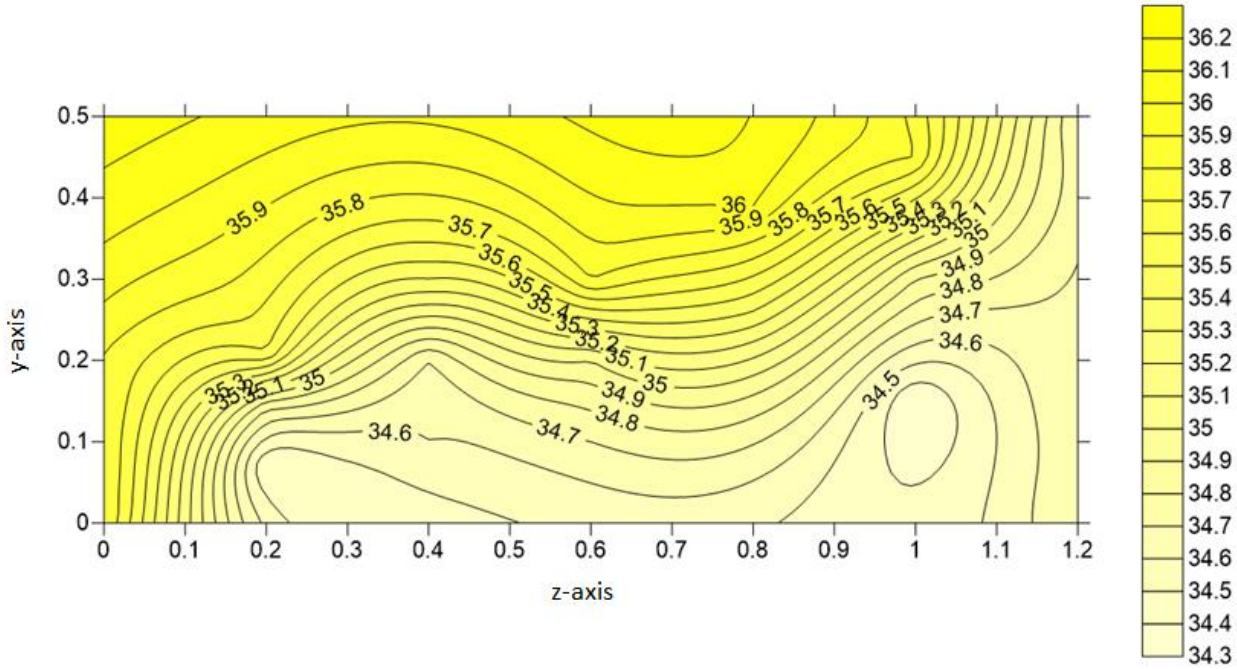

Figure (5-34) theoretical work of isothermal contour temperature distribution in the test duct through (y-z) plane from right side of rig duct for case two at 2.8 m/s

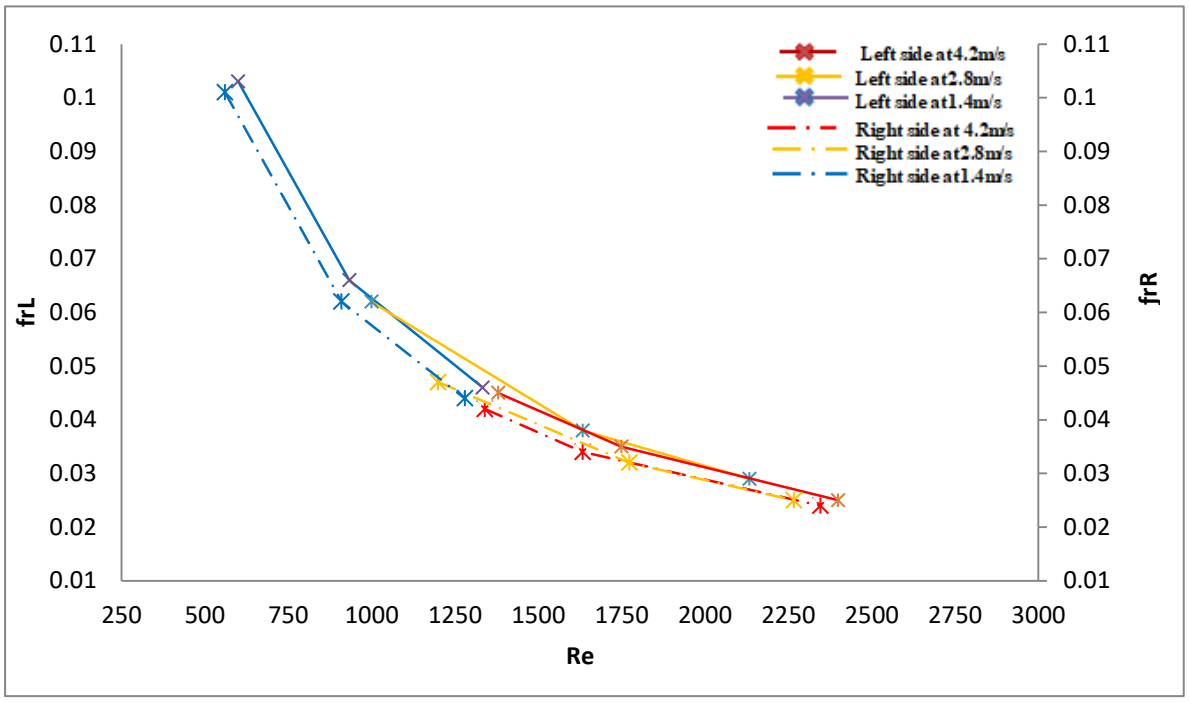

Figure(5-35) variation of friction factor with Reynolds number from left side of test duct for case two.

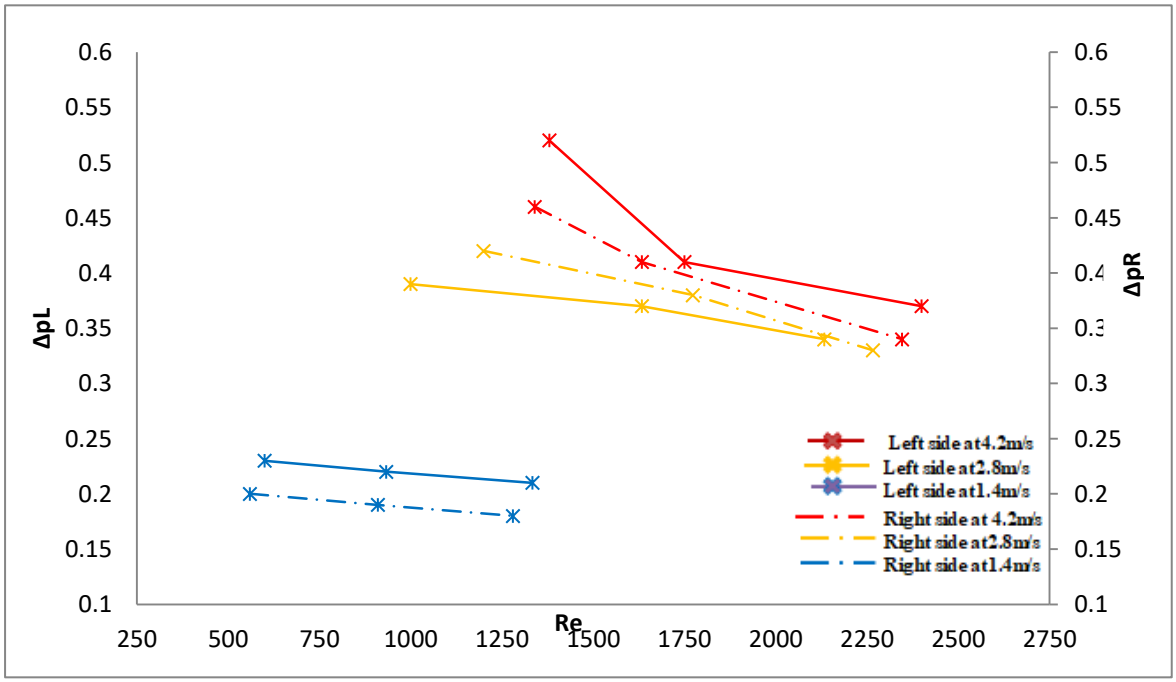

Figure(5-36) variation of pressure drop with Reynolds number from left side and right side of test duct for case two.

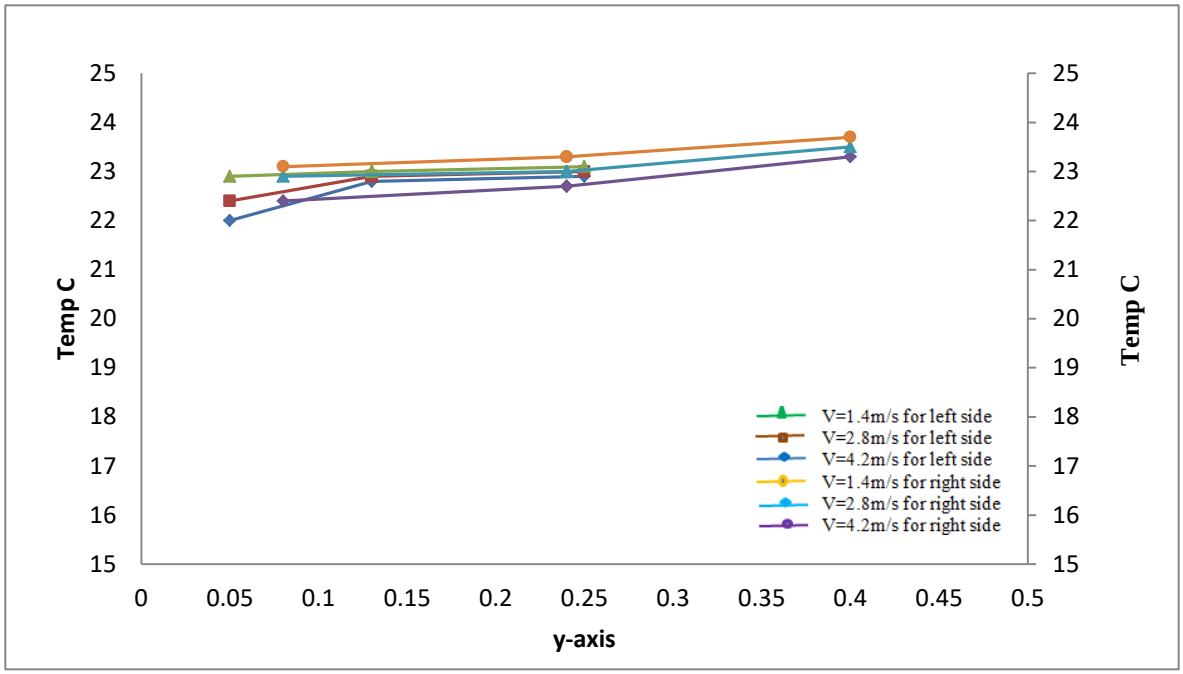

Figure(5-37) experimentally temperature distribution with y-axis in the test duct at z=0.2 m from the left-right side and z=1 m from the right-left side of rig duct for case three.

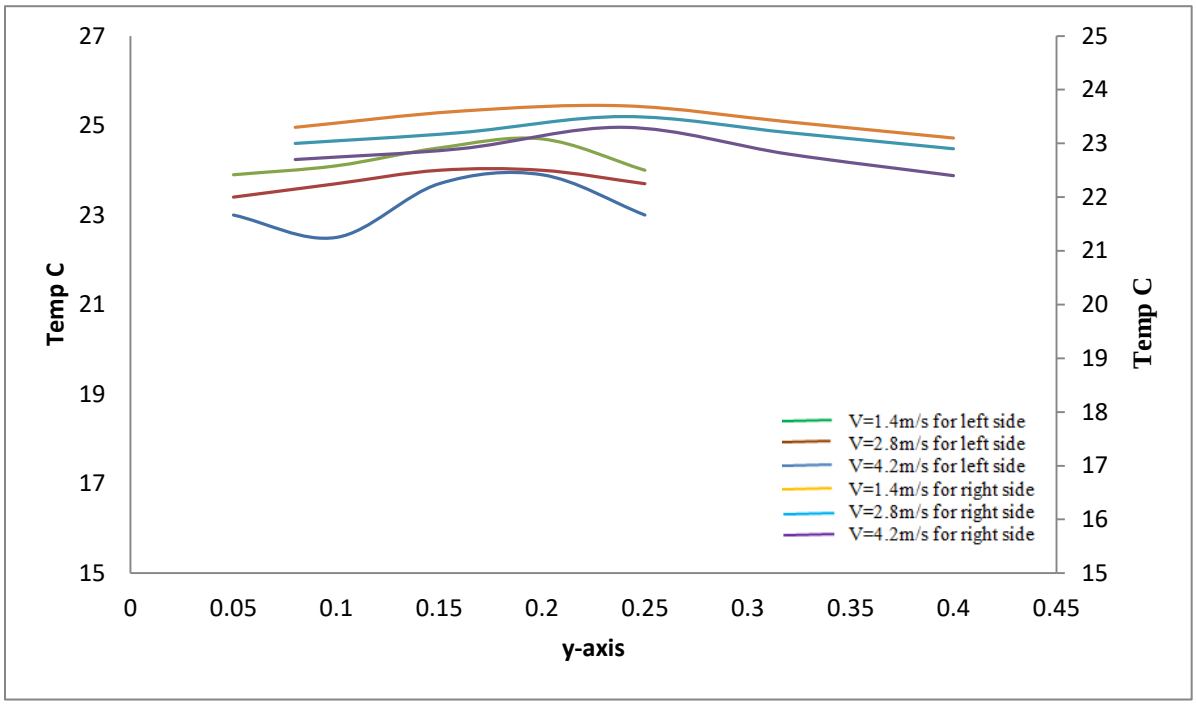

Figure(5-38) theoretically temperature distribution with y-axis in the test duct at z=0.2 m from the left-right side and z=1 m from the right-left side of rig duct for case three.

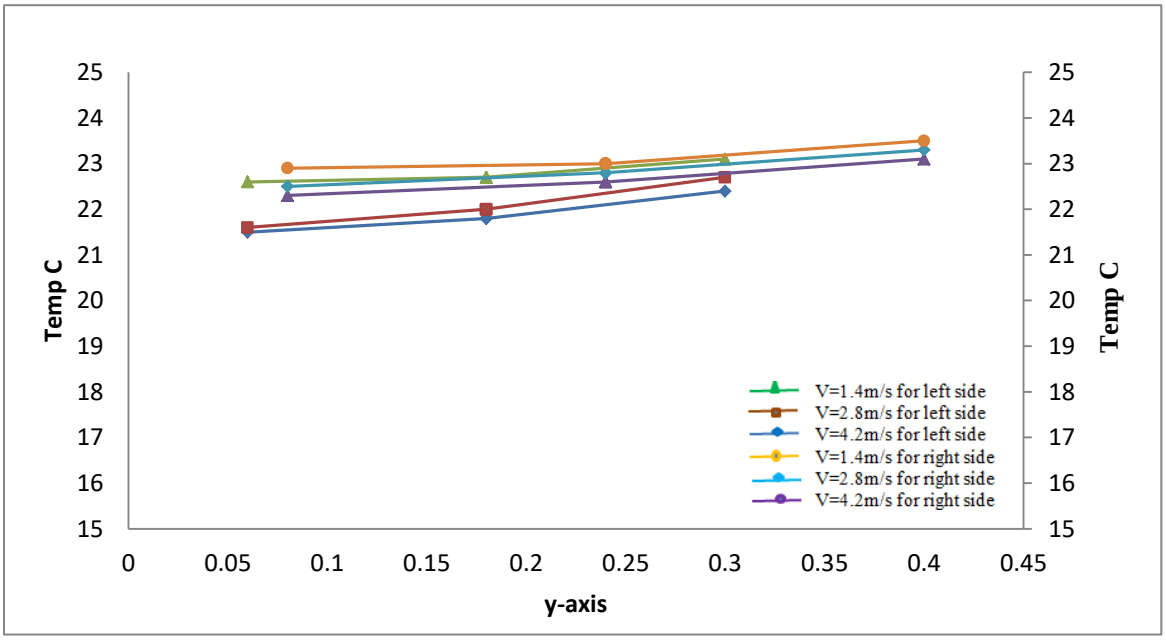

Figure(5-39) experimentally temperature distribution with y-axis in the test duct at z=0.4 m from the left-right side and z=0.8 m from the right-left side of rig duct for case three.

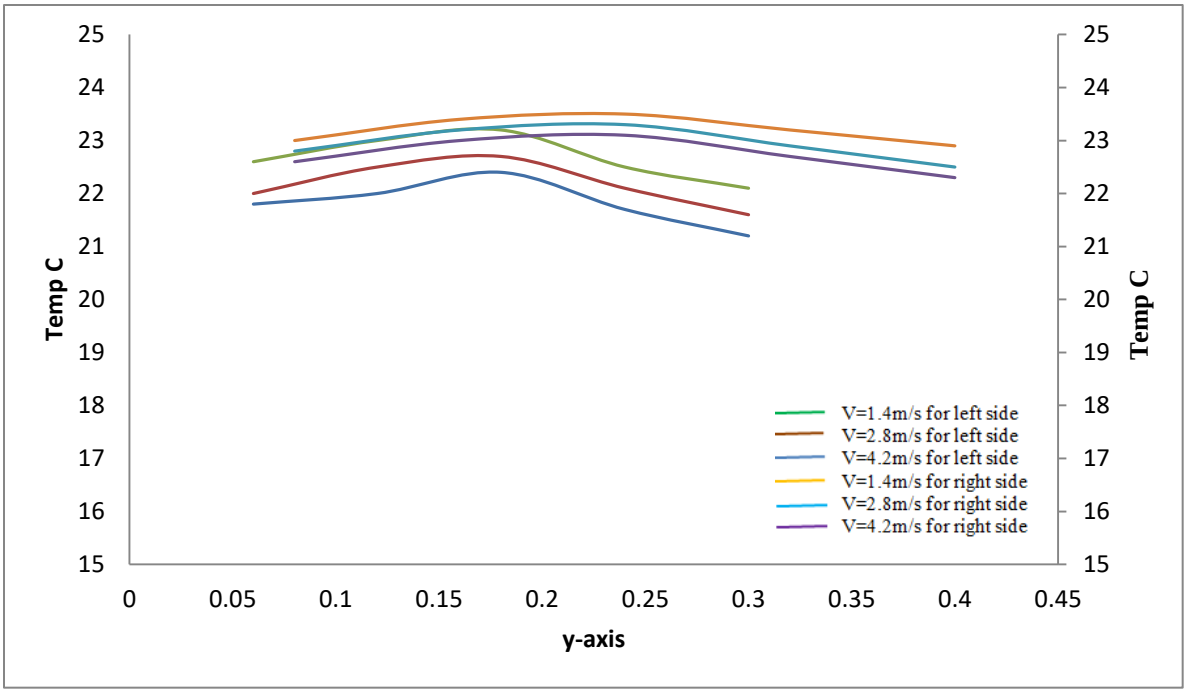

Figure(5-40) theoretically temperature distribution with y-axis in the test duct at z=0.4 m from the left-right side and z=0.8 m from the right-left side of rig duct for case three.

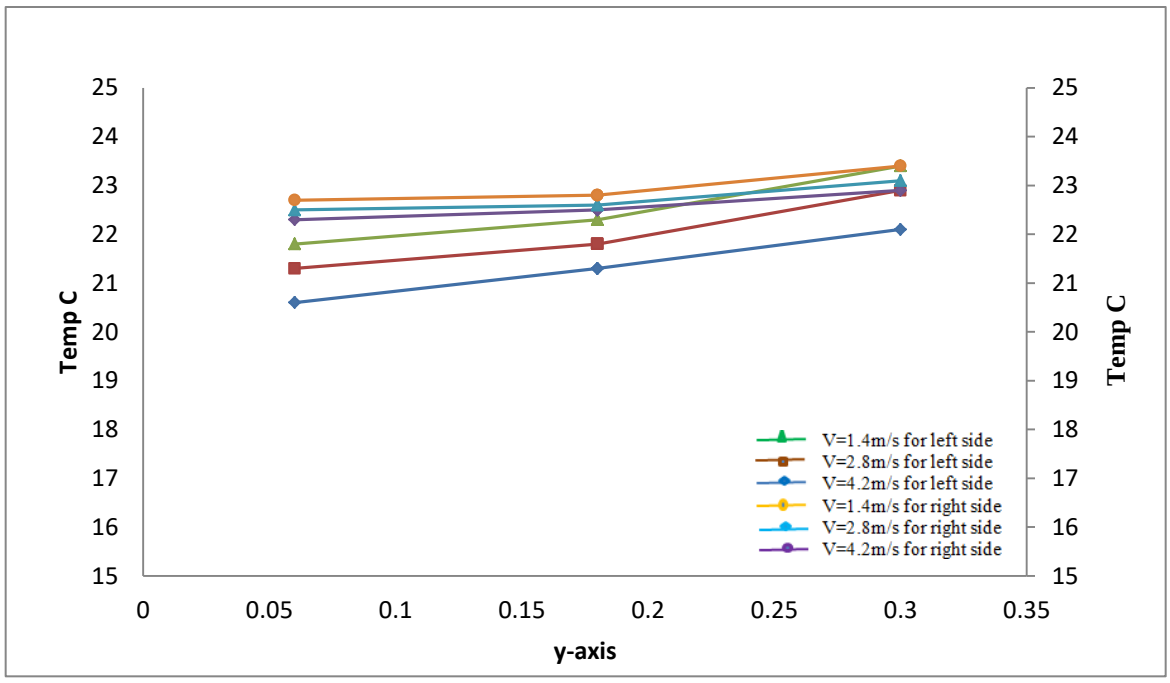

Figure(5-41) experimentally temperature distribution with y-axis in the test duct at z=0.6 m from the left-right side and z=0.6 m from the right-left side of rig duct for case three.

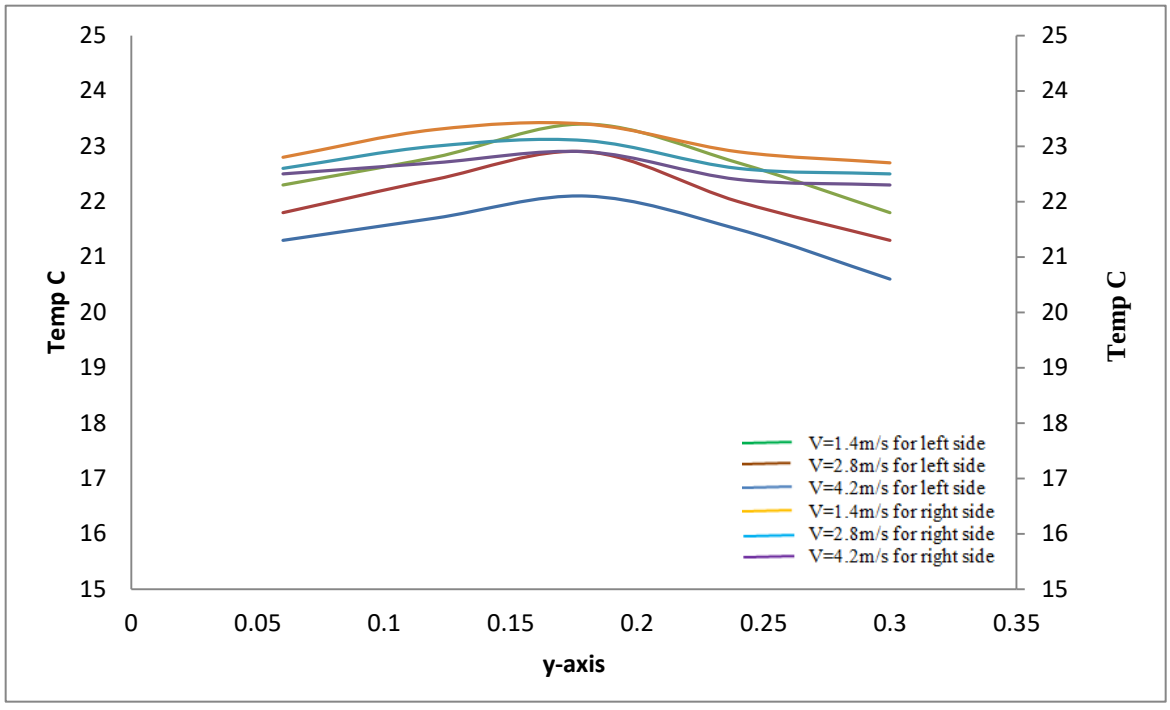

Figure(5-42) theoretically temperature distribution with y-axis in the test duct at z=0.8m from the left-right side and z=0.4 m from the right-left side of rig duct for case three.

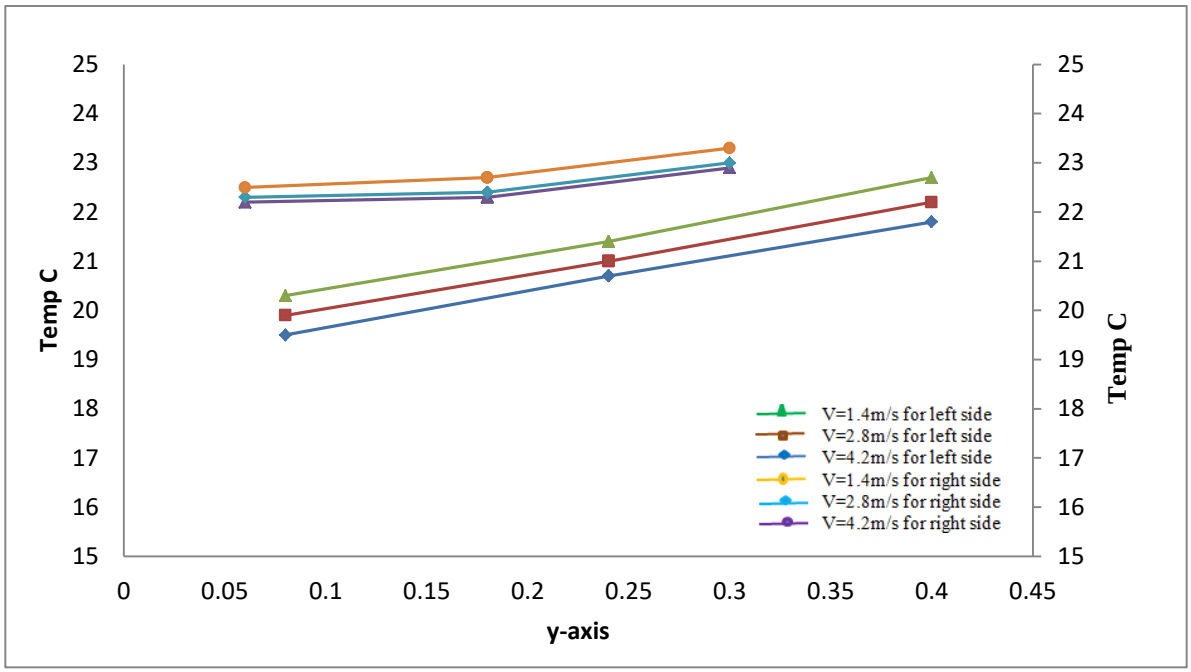

Figure(5-43) experimentally temperature distribution with y-axis in the test duct at z=0.8 m from the left-right side and z=0.4 m from the right-left side of rig duct for case three.

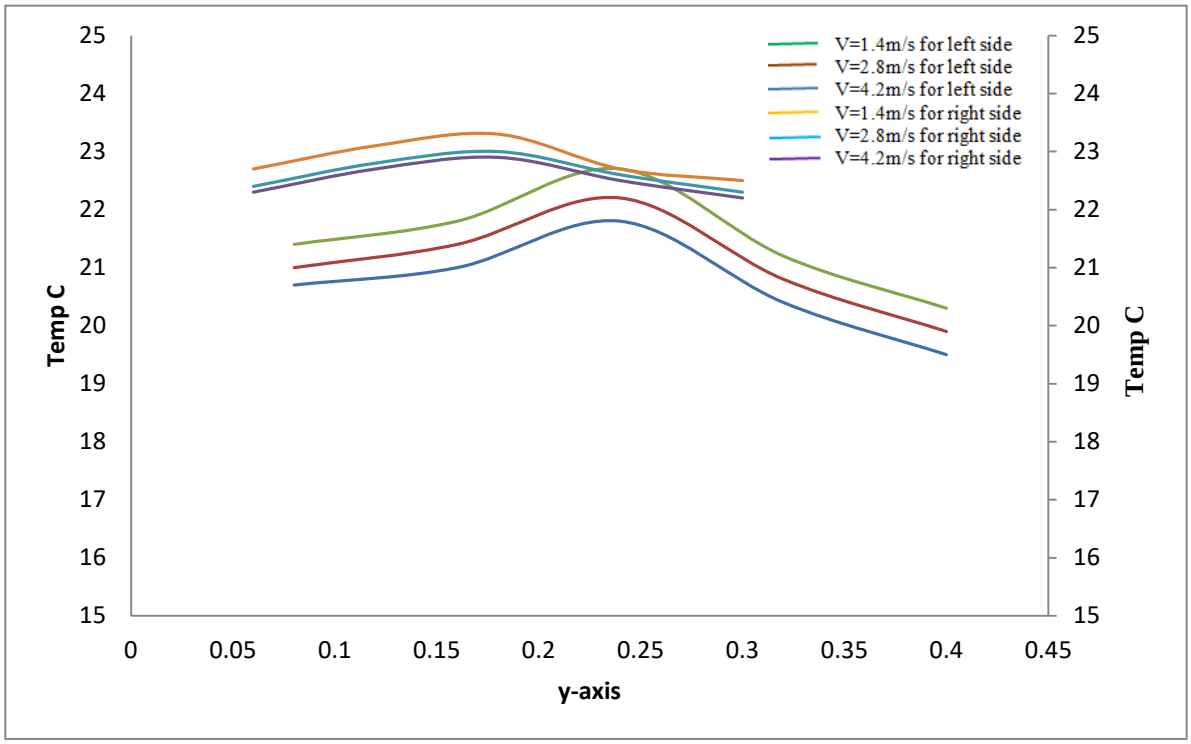

Figure(5-44) theoretically temperature distribution with y-axis in the test duct at z=0.8 m from the left-right side and z=0.4 m from the right-left side of rig duct for case three.

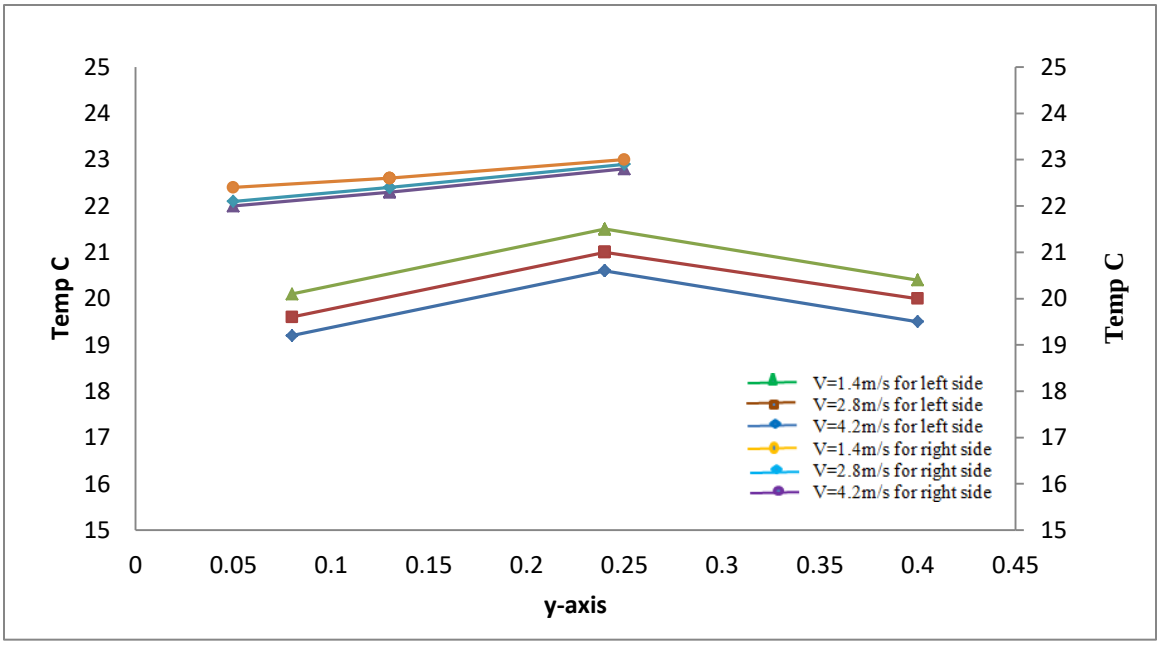

Figure(5-45) experimentally temperature distribution with y-axis in the test duct at z=1 m from the left-right side and z=0.2 m from the right-left side of rig duct for case three.

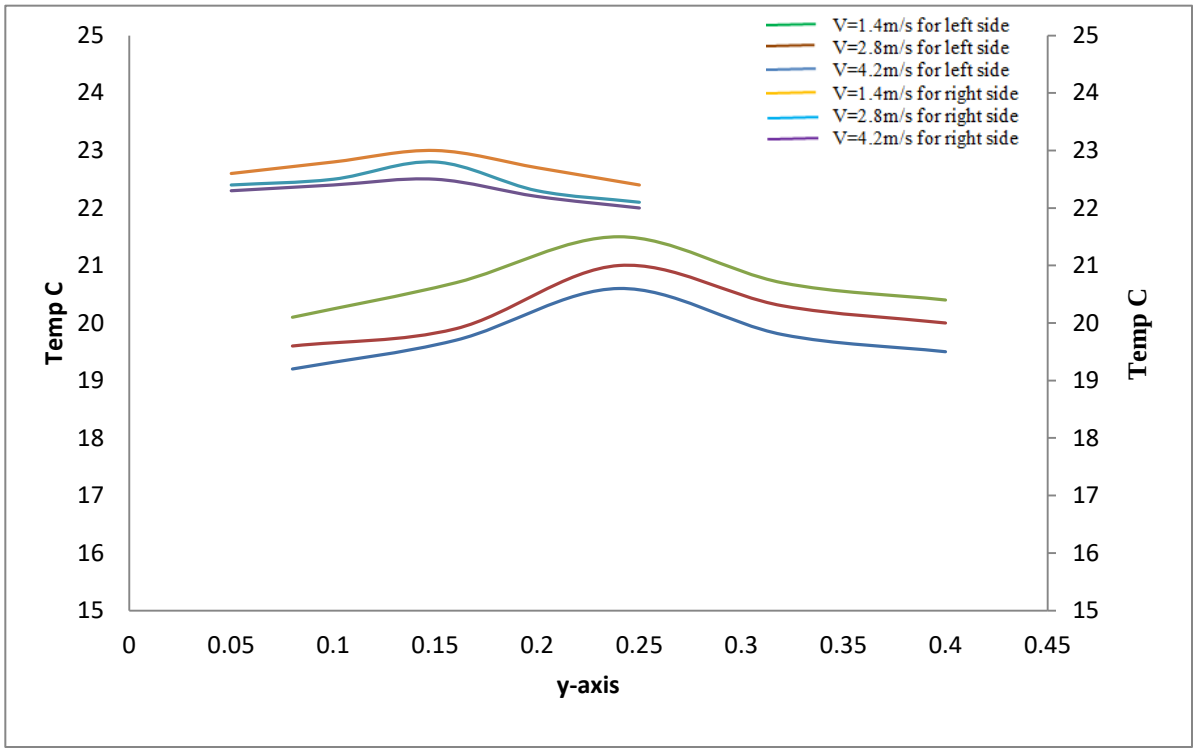

Figure(5-46) theoretically temperature distribution with y-axis in the test duct at z=1 m from the left-right side and z=0.2 m from the right-left side of rig duct for case three.

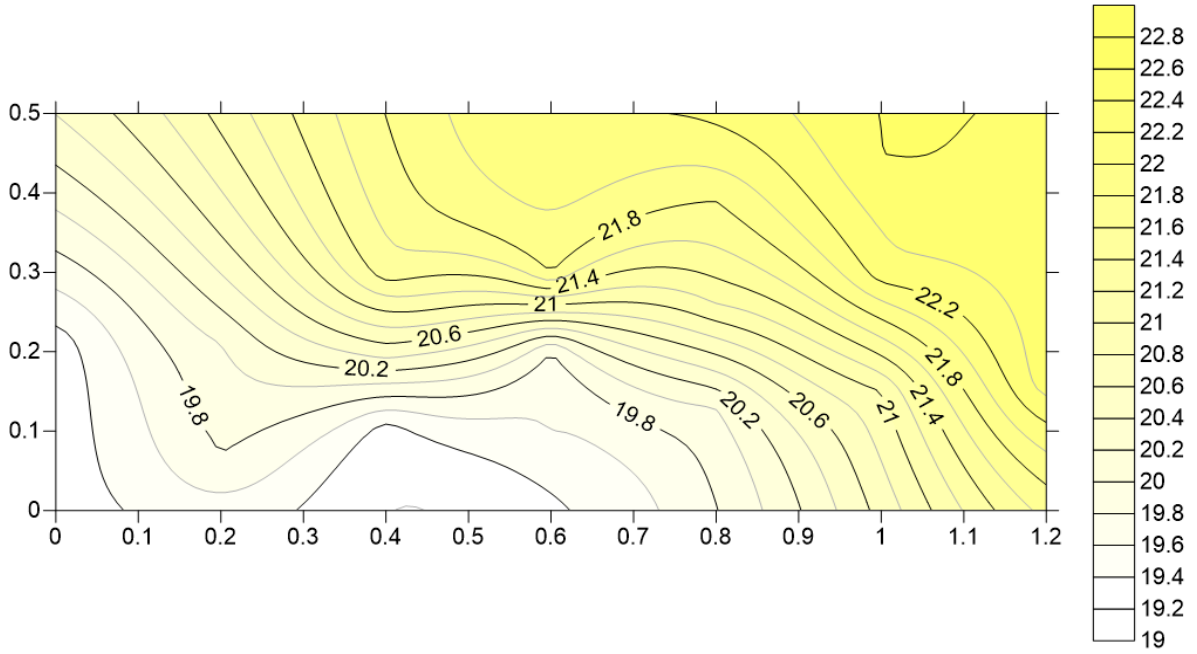

Figure (5-47) experimental work for isothermal contour of temperature distribution in the irregular duct through (y-z) plane from left side of rig duct for case three at 1.4m/s.

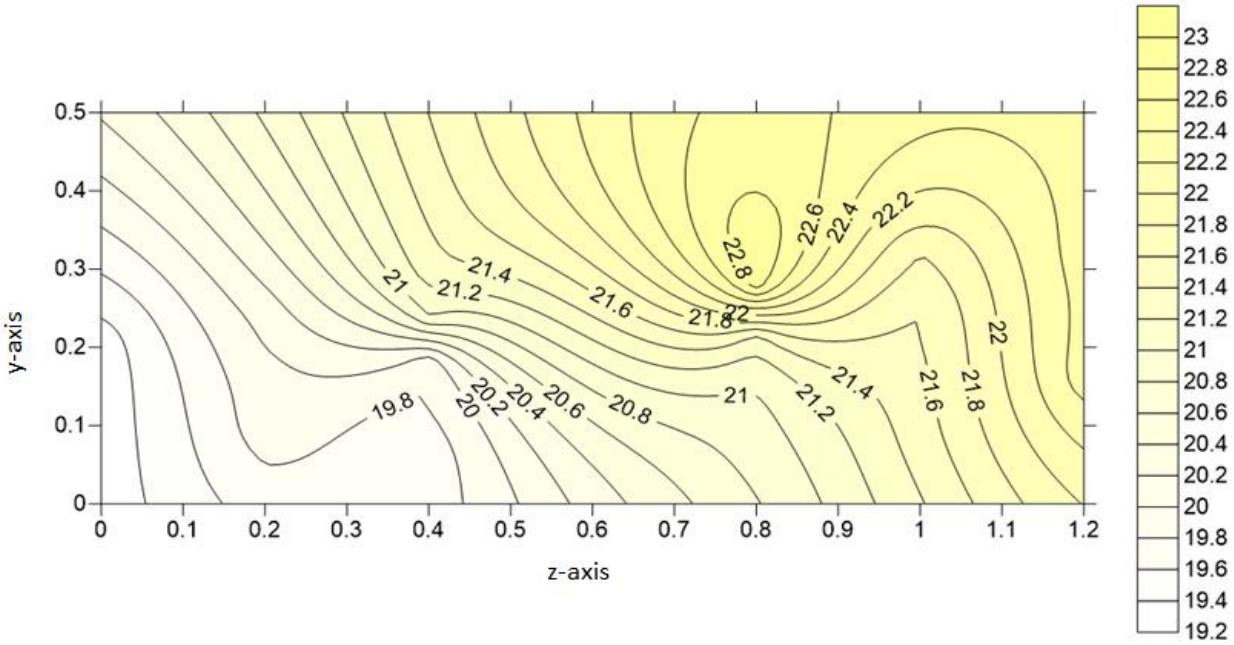

Figure (5-48) theoretical work for isothermal contour of temperature distribution in the test duct through (y-z) plane from left side of rig duct for case three at 1.4m/s.

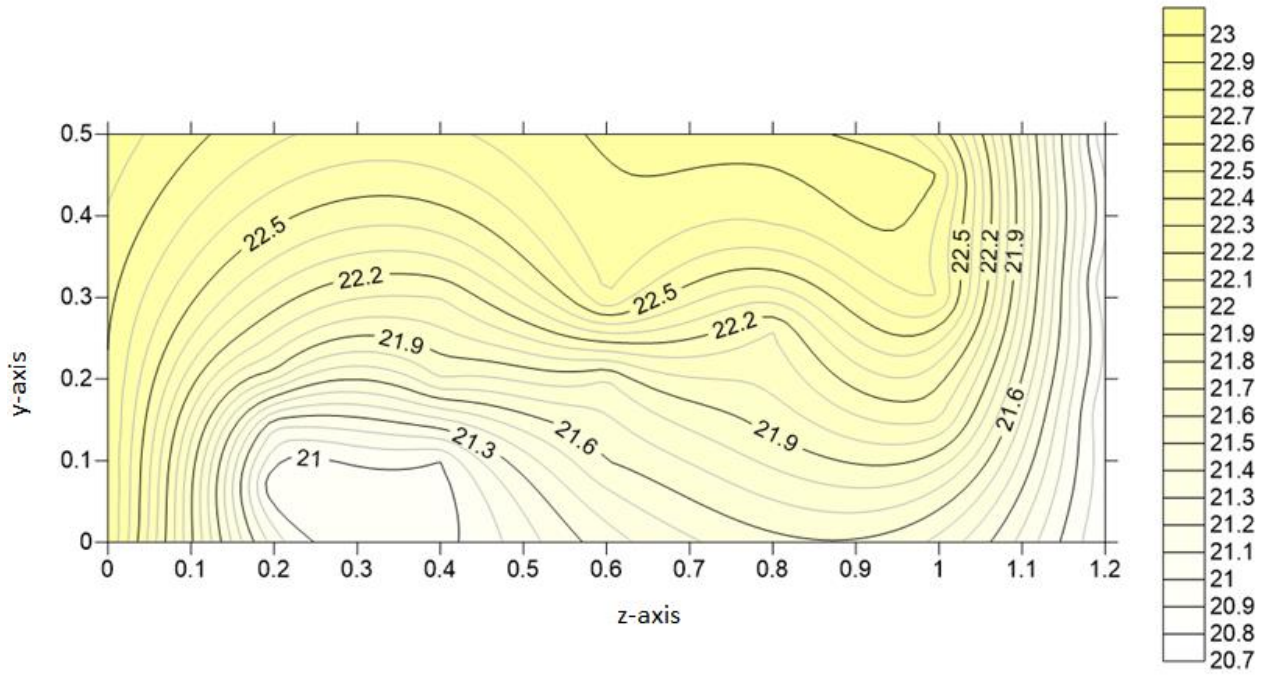

Figure (5-49) experimental work for isothermal contour of temperature distribution in the irregular duct through (y-z) plane from right side of rig duct for case three at 1.4 m/s.

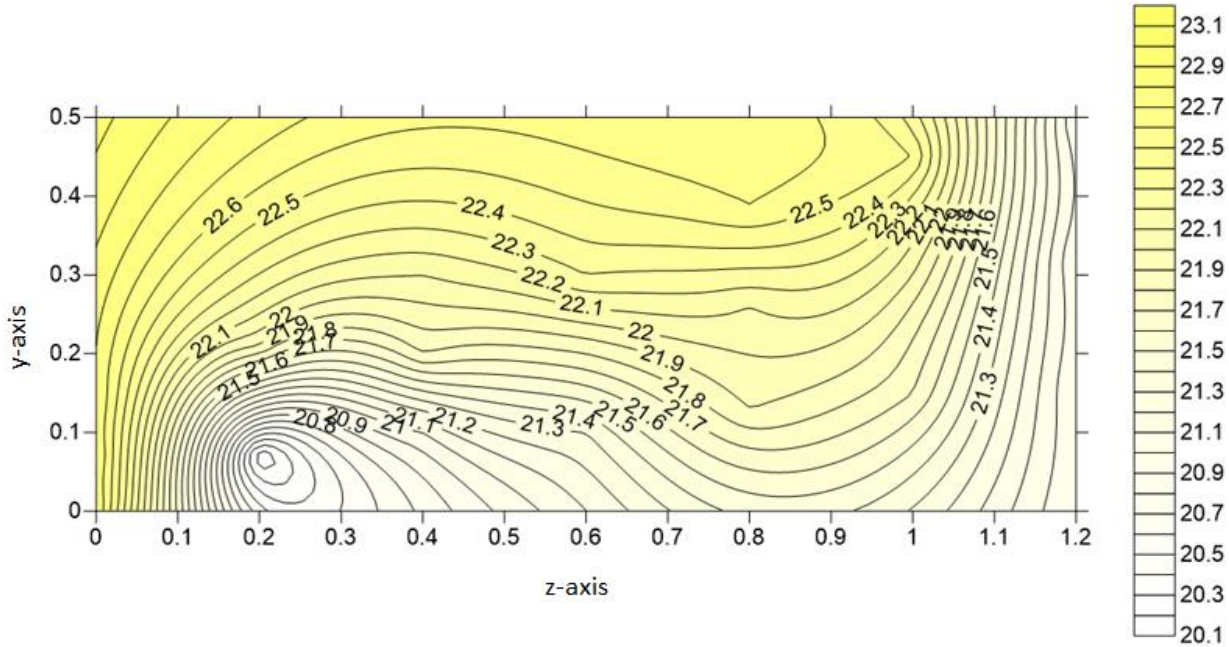

Figure (5-50) theoretical work for isothermal contour of temperature distribution in the test duct through (y-z) plane from right side of rig duct for case three at 1.4 m/s.

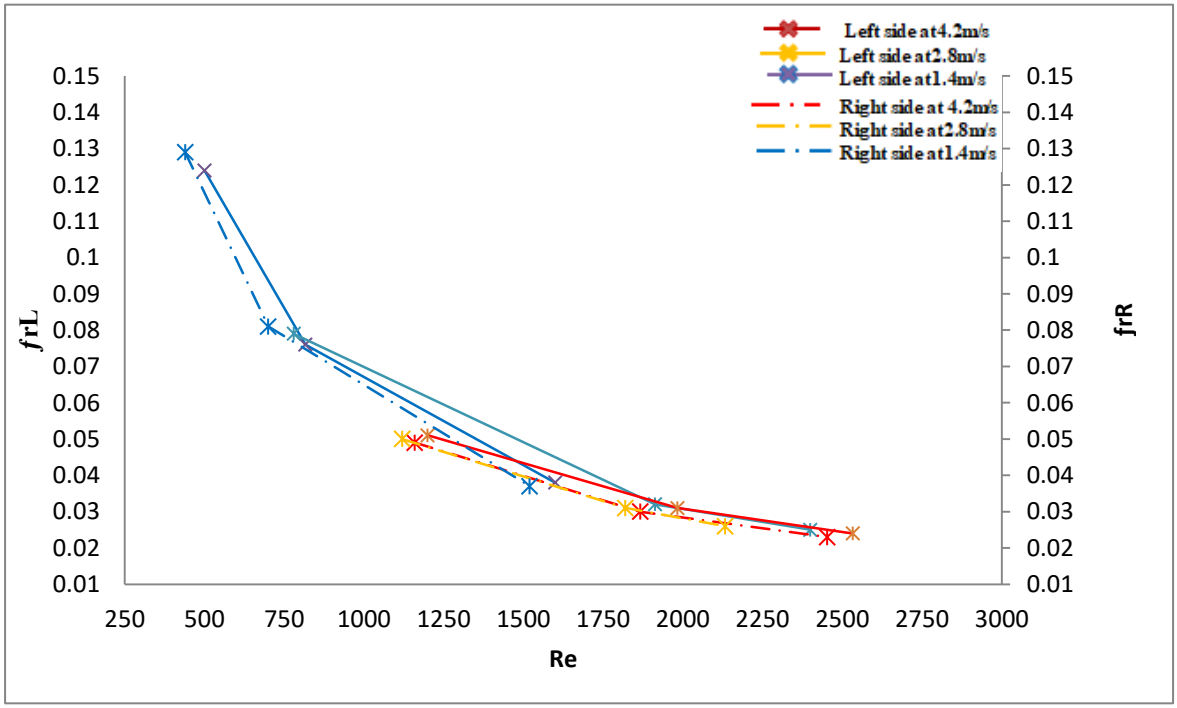

Figure (5-51) variation of friction factor with Reynolds number from left side of test duct for case three.

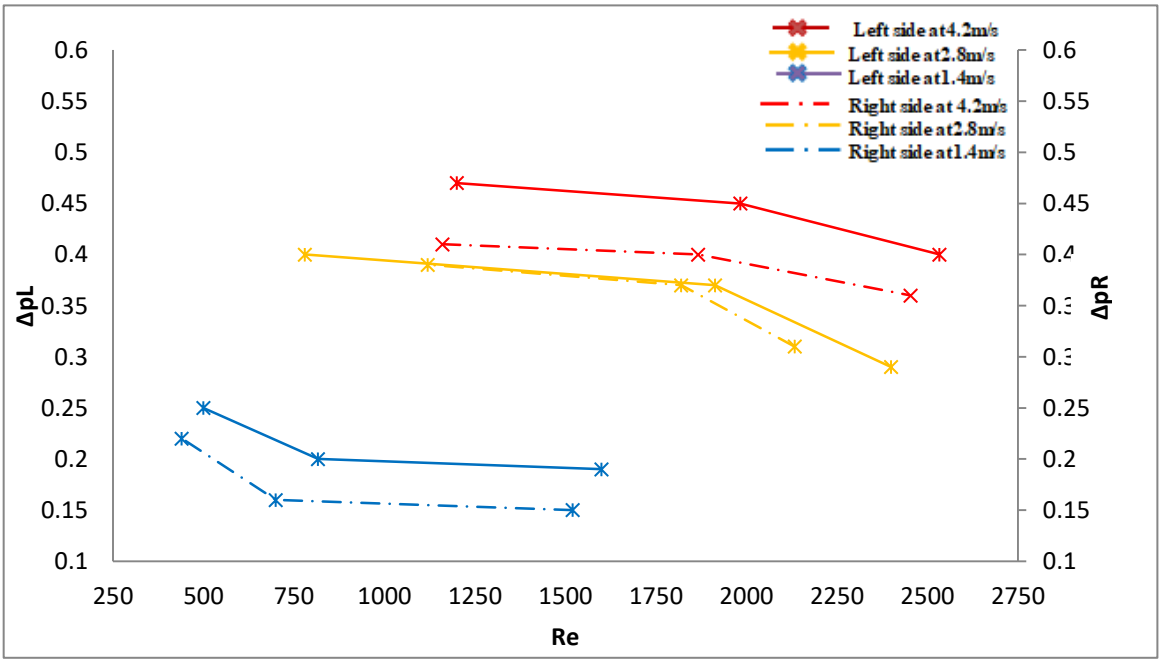

Figure (5-52) variation of pressure drop with Reynolds number from left side and right side of test duct for case three.

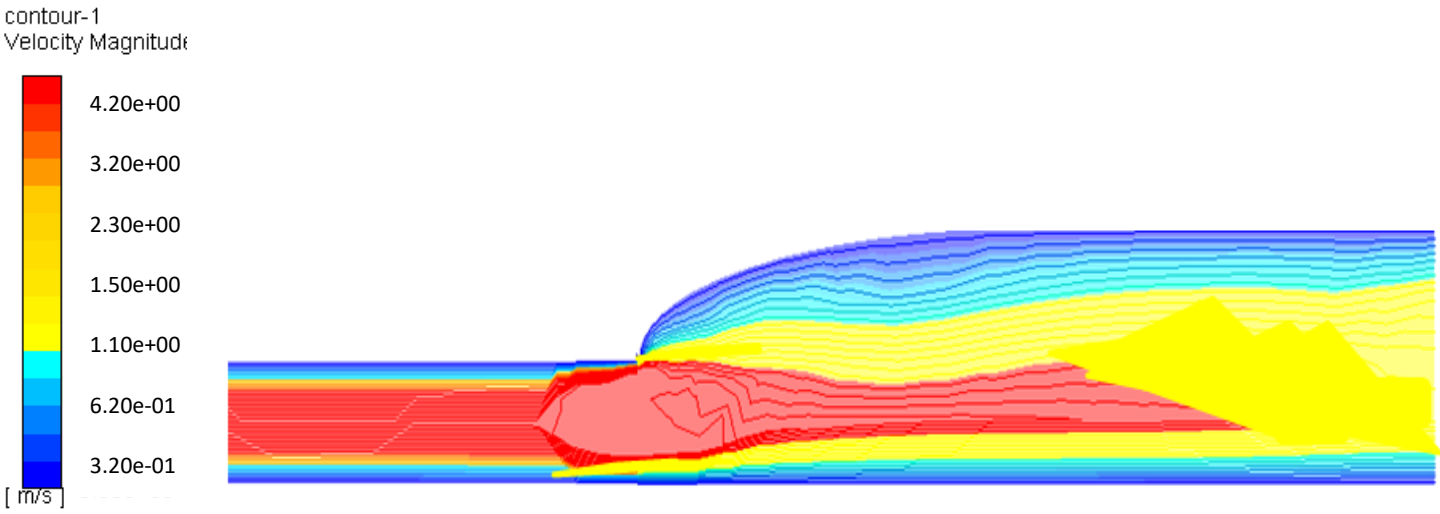

Figure(5-53) map contour of velocity profile in the left-right side through rig duct at inlet velocity 4.2 m/s for case one

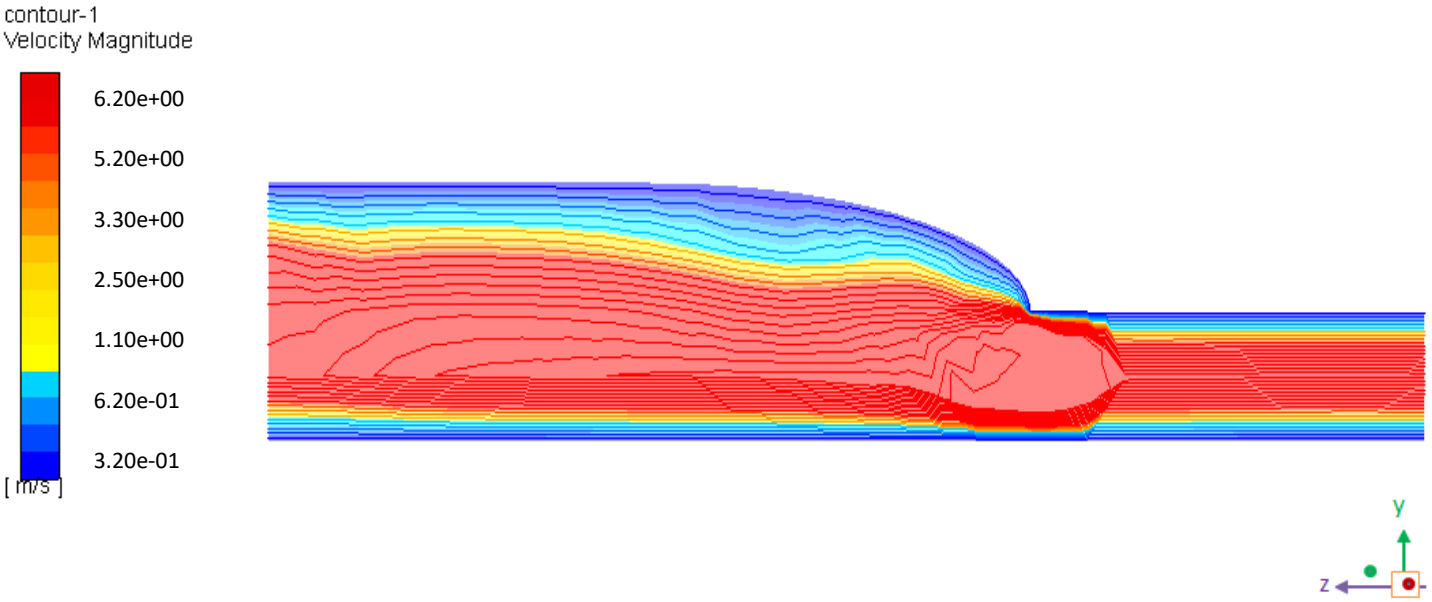

Figure(5-54) map contour of velocity profile in the right-left side through rig duct at inlet velocity 4.2 m/s for case one

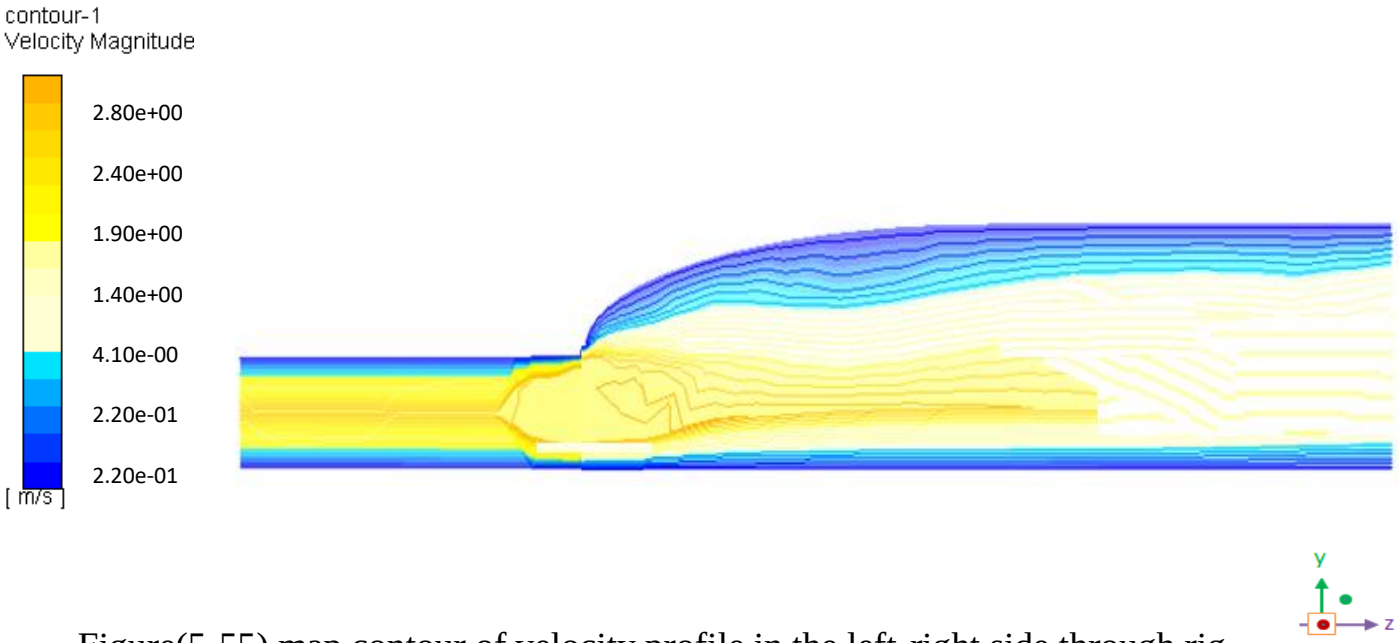

Figure(5-55) map contour of velocity profile in the left-right side through rig duct at inlet velocity 2.8 m/s for case two

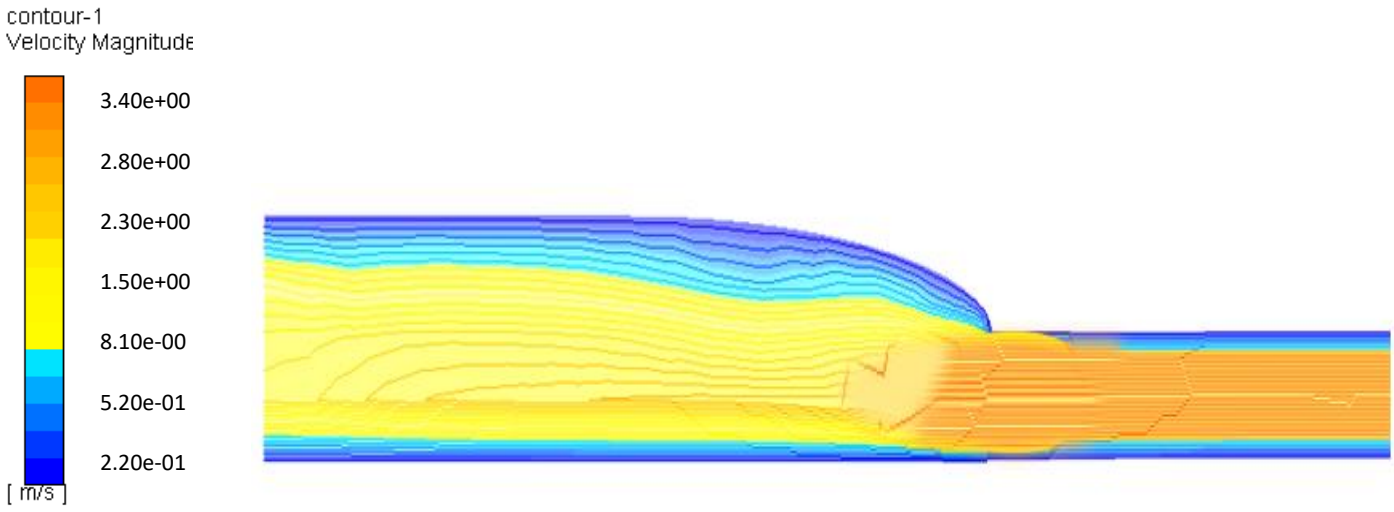

Figure(5-56) map contour of velocity profile in the right-left side through rig duct at inlet velocity 2.8 m/s for case two

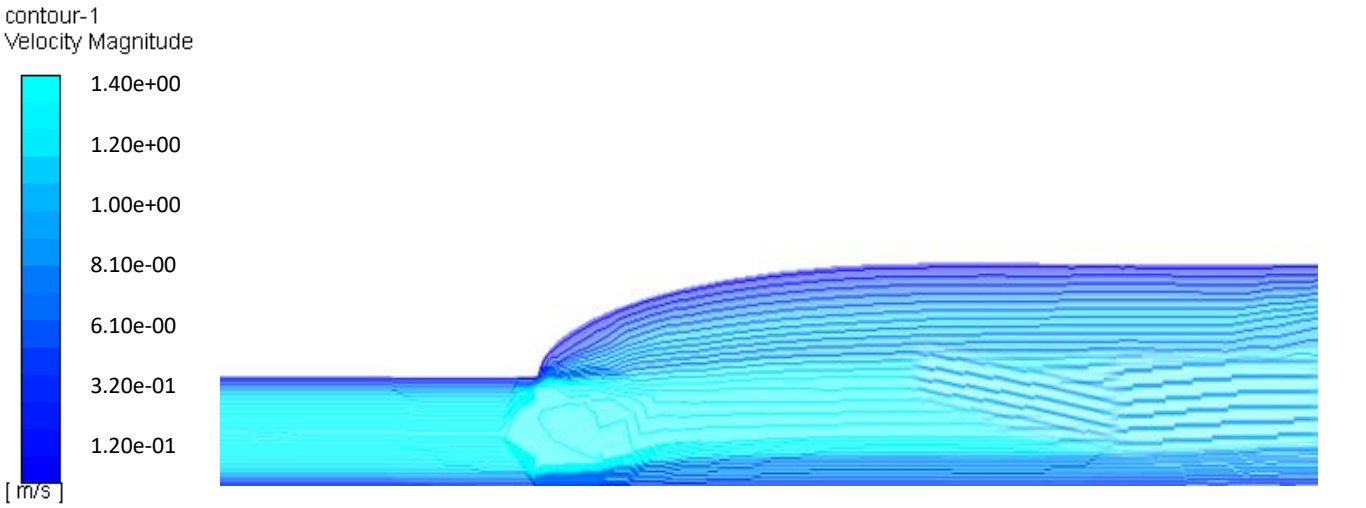

Figure(5-57) map contour of velocity profile in the left-right side through rig duct at inlet velocity 1.4 m/s for case three

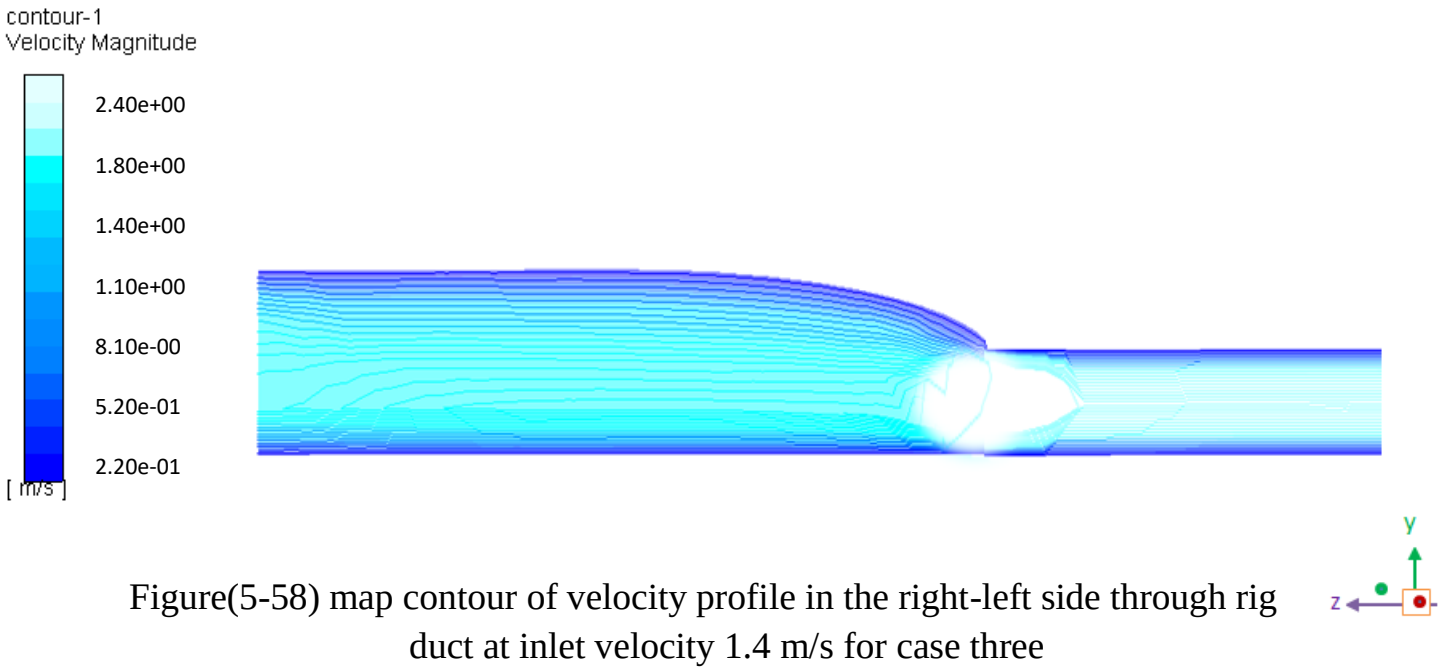

Figure(5-58) map contour of velocity profile in the right-left side through rig duct at inlet velocity 1.4 m/s for case three

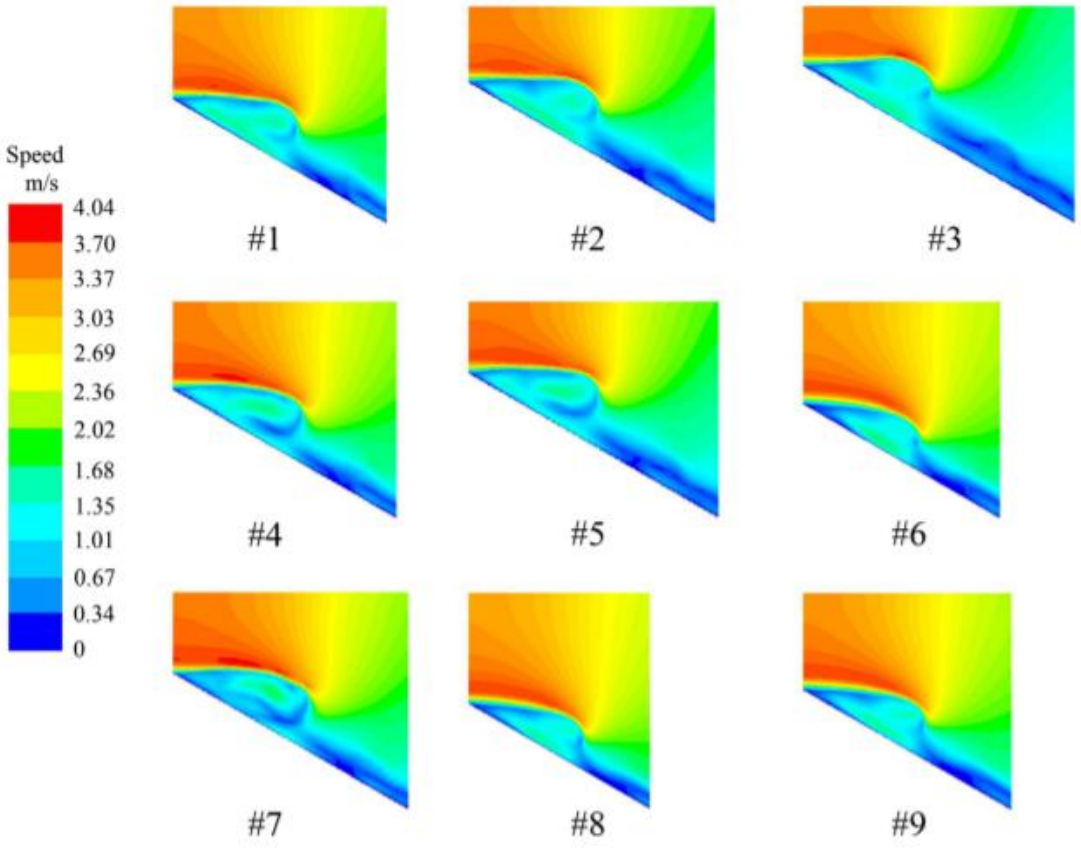

Figure(5-59) map contour of velocity profile Streamline for different samples at Re = 1500,by **Zhang and Chen[8]]**

Chapter Six

Conclusion and Suggestion for Future Work

CONCLUSION

This work presented experimental and theoretical study of the forced convection heat transfer and temperature distribution in an irregular geometric duct. The following conclusions are drawn from this work:

1- During an experimental study for all cases the temperature increases through the y-axis with different values of air velocity supply. It was found the temperature increases a little with increasing the values of air velocity.

2-It was found highest temperature recording in case one is72.2 ^{o}C at inlet velocity 4.2 m/s when the air is heated by heat flux at the top and side wall of irregular duct (test duct). This temperature was measured at value of z-axis 0.8 m, and y-axis 0.39 m.

3- Nusselt number and the heat transfer coefficient were calculated between the air flow and the top wall (curve shape) through the irregular duct in case one only. This is due to the convection heat transfer was happened between the air flow and the curve top wall of test duct. While in other two cases the convection heat transfer was not happen. This is due to the boundary conditions which were assumed for these two cases, and the duct was insulated.

4- In case one, the Nusselt number is directly proportional with Reynolds number. Also, it was showed that the Nusselt number decreases along the length of irregular duct.

5- At the same boundary conditions of three cases, the laminar air flow velocity is measured inside irregular duct (test duct). These values are measured with supplying three values of inlets velocities from the left and right side of rig duct. Also, at the same time, it measured the inlet and outlet velocity for rig duct.

6- At left side of supplying air flow with three values of inlet velocity are 4.2,2.8, and1.4 m/s . It was noted that these inlets velocities decrease inside the irregular duct at the top wall (curve surface). Also, it was recorded decreasing in the values of outlets velocities. This is because the dimensions of exit duct are bigger than the inlet duct.

7- At right side of supplying air flow with the same values of inlets velocities, it was measured also reducing in these values inside the irregular duct especially at the top curve surface. While, it was recorded increasing in outlets velocities at left side. This is because the dimensions of outlet duct of exit duct in this case are smaller than the inlet duct.

8- Through the experimental work for three cases, the Reynolds number is inversely proportional with the values of friction factor, and pressure drop through the irregular duct.

9- In a two-dimensional laminar flow, numerical simulation is performed in a two dimensional and predicted model deals with the temperature distribution inside test irregular duct by solving numerically the finite difference that represents energy equation. These are estimated by mathematical model which is simulated by a computer program in Matlab software.

10- ANSYS - Fluent 19.2. is used to calculate the air flow velocity inside irregular duct . There is no difference in the velocity of air inside the duct for both the experimental and theoretical results.

11-It was found more approximate between the results of experimental and theoretical work. Also, these results are consistent with many authors working in this field.

12- It was concluded that the shape and design duct more affect for the temperature distribution and air flow velocity.

6.2. Suggestions for Future Work

1- Placing rib as an obstacle in order to increase the thermal surface area.

2- Studying the effect of noise inside the duct during air flow.

3- Using of the irregular shape from four directions and the study is in three directions

4- Using multiple shapes on the irregular shape and comparing them with regular shapes

References

References

[1]**Zhang, X., Liu, B., Liu, J., Wang, X., and Zhang, H., "**Experimental and numerical analysis of heat transfer and flow characteristics in parabolic ducts," International Journal of Heat and Mass Transfer, Vol. 147, No. 4, pp. 118-912, 2020.

[2]**Norouzi, M., Kayhani, M. H., Nobari, M. R. H., and Demneh, M. K**., "Convective heat transfer of viscoelastic flow in a curved duct," World Academy of Science, Engineering and Technology, 2009.

[3] **Grondzik, W. T.,** "Air-conditioning system design manual. Elsevier," 2007.

[4]**Farhanieh, B., and Sunden, B.,** "Three-dimensional laminar flow and heat transfer in the entrance region of trapezoidal ducts," International journal for numerical methods in fluids, Vol. 135, pp.537-556, 1991.

[5] **Manglik, R. M., and Ding, J.,** "Laminar flow heat transfer to viscous power law fluids in double-sine ducts," International Journal of Heat and Mass Transfer, Vol. 40, No.6, pp.1379-1390, 1997.

[6] **Campo, A., Morales, J. C., and Larreteguy, A. E.,** "Pressure drop and heat transfer associated with flows moving laminarly in straight ducts of irregular, singly connected cross-sections," Heat and mass transfer, Vol. 32, No.3, pp.193-197, 1997.

[7] **Sadasivam, R., Manglik, R. M., and Jog, M. A.,** "Fully developed forced convection through trapezoidal and hexagonal ducts," International journal of heat and mass transfer, Vol. 42, pp. 4321-4331, 1999.

[8] **Zhang, L. Z., and Chen, Z. Y., "**Convective heat transfer in cross-corrugated triangular ducts under uniform heat flux boundary conditions," International Journal of Heat and Mass Transfer, Vol. 54, No.3, pp.597-605, 2000**.**

[9] **Muzychka, Y. S., and Yovanovich, M. M.,** "Laminar forced convection heat transfer in the combined entry region of non-circular ducts," J. Heat Transfer, Vol.126, No. 1 , pp.54-61, 2004.

[10] **Renksizbulut, M., and Niazmand, H.,** "Laminar flow and heat transfer in the entrance region of trapezoidal channels with constant wall temperature," 2006.

[11] **Chiu, H. C., Jang, J. H., and Yan, W. M., "**Mixed convection heat transfer in horizontal rectangular ducts," International Journal of Heat and Mass Transfer, Vol.50, No. 15, pp. 2874-2882, 2007.

[12] **Kucuk, H., Avci, M. E. T. E., Aydin, O., and Asan, H., "**Analysis of heat and fluid flow in concentric annular square ducts," J. Therm. Sci. Technol., Vol.29, No.1, pp.7-13, 2009.

[13] **Poinsatte, P., Thurman, D., and Hippensteele, S., "**Heat Transfer in a Superelliptic Transition Duct," 2008.

[14] **Ray, S., and Misra, D., "**Laminar fully developed flow through square and equilateral triangular ducts with rounded corners subjected to H1 and H2 boundary conditions," International Journal of Thermal Sciences, Vol.49, No.9, pp.1763-1775, 2008.

[15] **Liu, F., and Wang, L.,** "Analysis on multiplicity and stability of convective heat transfer in tightly curved rectangular ducts," International Journal of Heat and Mass Transfer, Vol.52, pp.5849-5866, 2009.

[16] **Wong, T. T., and Leung, C. W., "**Forced-convection augmentation of laminar flow in a triangular duct with artificially roughened internal surfaces," Experimental heat transfer, Vol.15, No.2, pp.89-106, 2009.

[17] **Norouzi, M., Kayhani, M. H., Nobari, M. R. H., and Demneh, M. K., "** Convective heat transfer of viscoelastic flow in a curved duct," World Academy of Science, Engineering and Technology, Vol.32, pp.327-333, 2009.

[18] **Aharwal, K. R., Gandhi, B. K., and Saini, J. S.,** "An experimental investigation of heat transfer and fluid flow in a rectangular duct with inclined discrete ribs," International Journal of Energy and Environment (IJEE), pp.987-998, 2010.

[19] **Kurnia, J. C., Sasmito, A. P., and Mujumdar, A. S.,** "Laminar convective heat transfer for in-plane spiral coils of noncircular cross sections ducts," A computational fluid dynamics study. Thermal science, pp. 109-118, 2012

[20] **Shahmardan, M. M., Norouzi, M., Kayhani, M. H., and Delouei, A. A.,** "An exact analytical solution for convective heat transfer in rectangular ducts," Journal of Zhejiang University SCIENCE A, Vol.13, No.10, pp.768-781, 2012.

[21] **Khatri, R., and Agarwal, P.,** "Two-dimensional finite element analysis of forced convection flow and heat transfer in a laminar channel flow," 2012.

[22] **Chen, Z., Zhang, L., and Song, H.**, "Investigating the impacts of included angles on flow and heat transfer in cross-corrugated triangular ducts with field synergy principle," Thermal Science, Vol.17, No.3, pp.823-832, 2013.

[23] **Ebaid, M. S., Haddad, O. M., and Batarseh, L. R.,** "Numerical investigation of fully developed laminar flow in irregular annular ducts: Triangular–circular combinations," Energy conversion and management, Vol.85, pp.511-520, 2014.

[24] **Lasode, O. A.,** "Mixed convection heat transfer in rotating vertical elliptic ducts," Journal of the Brazilian Society of Mechanical Sciences and Engineering, Vol.29, No.2, pp.142-151, 2007 .

[25] **Sivakumar, K., Natarajan, E., and Kulasekharan, N.**, "Heat transfer and pressure drop comparison between smooth and different sized rib-roughened rectangular divergent ducts," International Journal of Engineering and Technology (IJET), pp. 263-272, 2014.

[26] **Schrittwieser, M., Marn, A., Farnleitner, E., and Kastner, G.,** "Numerical analysis of heat transfer and flow of stator duct models," IEEE Transactions on industry applications, Vol.50, No.1, pp.226-233, 2013.

[27] **Onur, N., and Arslan, K.,** "Experimental investigation of laminar heat transfer inside trapezoidal duct having different corner angles," Experimental Heat Transfer, pp. 89-105, 2015.

[28] **Tong, J. C. K., Sparrow, E. M., Minkowycz, W. J., and Abraham, J. P.,** "A new archive of heat transfer coefficients from square and chamfered cylinders at angles of attack in cross flow," International Journal of Thermal Sciences, Vol.105, pp.218-223, 2016.

[29] **Bhadouriya, R., Agrawal, A., and Prabhu, S. V.,** "Experimental and numerical study of fluid flow and heat transfer in a twisted square duct," International Journal of Heat and Mass Transfer, Vol.82, 143-158, 2015.

[30] **Ghobadi, M., and Muzychka, Y. S.** A., "review of heat transfer and pressure drop correlations for laminar flow in curved circular ducts," Heat Transfer Engineering, Vol.37, No.10, 815-839, 2016.

[31] **Zhang, X., Wang, Y., Jia, R., and Wan, R.,** "Investigation on heat transfer and flow characteristics of heat exchangers with different trapezoidal ducts," International Journal of Heat and Mass Transfer, Vol.110, pp.863-872, 2017.

[32] **Tokgoz, N., Aksoy, M. M., and Sahin, B.,** "Investigation of flow characteristics and heat transfer enhancement of corrugated duct geometries," Applied Thermal Engineering, Vol.118, pp.518-530, 2017.

[33] **Maithani, R., Silori, A., Rana, J., and Chamoli, S.,** "Numerical analysis of heat transfer and fluid flow of a wavy delta winglets in a rectangular duct," Thermal Science and Engineering Progress, pp. 15-25, 2017.

[34] **Zunaid, M.,** "Numerical study of pressure drop and heat transfer in a straight rectangular and semi cylindrical projections micro channel heat sink," Journal of Thermal Engineering, pp. 1453-1465, 2017.

[35] **Nandana, V., and Janoske, U.,** "Numerical study on the enhancement of heat transfer performance in a rectangular duct with new winglet shapes," Thermal Science and Engineering Progress, pp. 95-103, 2018.

[36] **Zhang, Y., Zhang, X., Li, M., and Liu, Z.,** "Research on heat transfer enhancement and flow characteristic of heat exchange surface in cosine style runner," Heat and mass transfer, Vol.55, No.11,pp. 3117-3131, 2019.

[37] **Zhang, X., Wang, Y., Jia, R., and Wan, R.,** "Investigation on heat transfer and flow characteristics of heat exchangers with different trapezoidal ducts," International Journal of Heat and Mass Transfer, Vol.110, pp.863-872, 2017.

[38] **Zhang, X., Liu, B., Liu, J., Wang, X., and Zhang, H.,** "Experimental and numerical analysis of heat transfer and flow characteristics in parabolic ducts," International Journal of Heat and Mass Transfer, Vol.147, pp.118-912, 2020.

[39] **Rang, H. J., Wong, T. T., and Leung, C. W.,** "Effects of surface roughness on forced convection and friction in triangular ducts," Experimental Heat Transfer An International Journal, pp. 241-253, 1998.

[40] **Ring, K., and Agar, A.,** "The Omega Project. Revision," 1986.

[41] **[]Chen, Z., Zhang, L., and Song, H.,** "Investigating the impacts of included angles on flow and heat transfer in cross-corrugated triangular ducts with field synergy principle," Thermal Science, pp.823-832, 2013.

[42] **Jack P .Holman.,** "Heat Transfer", Book tenth edition, SPIE press publications, 2010.

[43] **Younis, Y. A., and Kifayat, K.,** "Secure cloud computing for critical infrastructure," A survey. Liverpool John Moores University, United Kingdom, Tech, 2013.

[44] **L. W. Wang, K. H. Hou, I. G. Lua, and C. F. Hsu.**, "Flow Patterns of Mixed Convection in a Horizontal Square Channel Flow, Exp," Heat Transf., vol. 9, pp. 257– 265, 1996.

[45] **L. Zhang.,** "Thermally Developing Forced Convection and Heat Transfer in Rectangular Plate-Fin Passages under Uniform Plate Temperature, Numer," Heat Transf. Part A, vol. 52, pp. 549– 564, 2007.

[46]**Bell,S., "**Abeginners guide to uncertaint of Mesurement," National physical laboratory Teddington, Middlesex, U.K, 2001,

[47]**Schaufeli, W. B., Bakker, A. B., and Salanova, M.,** "The measurement of work engagement with a short questionnaire: A cross-national study," Educational and psychological measurement, Vol.66, No.4, pp.701-716, 2006.

[48] **Kim, S. Y., Kang, B. H., and Hyun, J. M.,** "Heat transfer in the thermally developing region of a pulsating channel flow," International journal of heat and mass transfer, Vol.36, No.17, pp.4257-4266, 1993.

Appendices

Appendix(A)

Tables of calculating experimental analysis parameters

Table (A-1) parameters measurement for case one at left side of duct at 4.8 m/s

D_h(m)	Re	Nu	h_x	Δp	fr
0.23	2533.3	**30.03**	**18.54**	**0. 39**	**0.024**
0.35	2053.3	**25.02**	**17.16**	**0. 48**	**0.030**
0.42	1499.9	**18.37**	**14.7**	**0. 54**	**0.042**

Table (A-2) parameters measurement for case one at right side of duct at 4.8 m/s

D_h(m)	Re	Nu	h_x	Δp	fr
0.23	1399.3	**19.83**	**15.87**	**0. 47**	**0.040**
0.35	1866.6	**23.26**	**15.95**	**0. 40**	**0.030**
0.42	2399.9	**27.31**	**16.39**	**0. 34**	**0.023**

Table(A-3) parameters measurement for case one at left side of duct at 2.8 m/s

D_h(m)	Re	Nu	h_x	Δp	fr
0.23	2239.9	**30.31**	**18.19**	**0. 35**	**0.027**
0.35	1423.3	**24.52**	**16.82**	**0. 33**	**0.043**
0.42	1143.3	**18.20**	**14.56**	**0. 31**	**0.054**

Table (A-4) parameters measurement for case one at right side of duct at 2.8 m/s

D_h(m)	Re	Nu	h_x	Δp	*f*r
0.23	999.9	**19.47**	**15.58**	**0. 34**	**0.056**
0.35	1633.3	**23.05**	**15.81**	**0. 33**	**0.032**
0.42	2186.6	**26.83**	**16.10**	**0. 32**	**0.026**

Table (A-5) parameters measurement for case one at left side of duct at 1.4 m/s

D_h(m)	Re	Nu	h_x	Δp	*f*r
0.23	1119.9	**29.9**	**17.94**	**0.16**	**0.055**
0.35	699.9.3	**24.26**	**16.64**	**0.17**	**0.088**
0.42	479.9	**18.01**	**14.41**	**0.18**	**0.130**

Table (A-6) parameters measurement for case one at right side of duct at 1.4 m/s

D_h(m)	Re	Nu	h_x	Δp	*f*r
0.23	439.9	**19.23**	**15.39**	**0.16**	**0.129**
0.35	676.6	**22.88**	**15.69**	**0.15**	**0.084**
0.42	1066.6	**26.51**	**15.91**	**0.14**	**0.053**

Table (A-7) parameters measurement for case two at left side of duct at 4.8 m/s

D_h(m)	**Re**	***f*r**	**Δp**
0.23	2533.3	**0.025**	**0. 37**
0.35	2053.3	**0.035**	**0. 41**
0.42	1459.9	**0.045**	**0. 52**

Table (A-8) parameters measurement for case two at right side of duct at 4.8 m/s

D_h(m)	Re	*f*r	Δp

0.23	1379.9	**0.042**	**0. 46**
0.35	1749.9	**0.034**	**0. 41**
0.42	2399.9	**0.024**	**0. 34**

Table (A-9) parameters measurement for case two at left side of duct at 2.8 m/s

D_h(m)	Re	*f*r	Δp
0.23	2133.3	**0.029**	**0. 34**
0.35	1633.3	**0.038**	**0. 39**
0.42	999.9	**0.062**	**0. 37**

Table (A-10) parameters measurement for case two at right side of duct at 2.8 m/s

D_h(m)	**Re**	***f*r**	**Δp**
0.23	1199.9	**0.047**	**0. 42**
0.35	1773.3	**0.032**	**0. 38**
0.42	2266.6	**0.025**	**0. 33**

Table (A-11) parameters measurement for case two at left side of duct at 1.4 m/s

D_h(m)	Re	*f*r	Δp
0.23	1333.3	**0.046**	**0. 21**
0.35	933.3	**0.066**	**0. 22**
0.42	599.9	**0.103**	**0. 23**

Table (A-12) parameters measurement for case two at right side of duct at 1.4 m/s

D_h(m)	Re	*f*r	Δp
0.23	559.9	**0.101**	**0. 20**

0.35	909.9	**0.062**	**0. 19**
0.42	1279.9	**0.044**	**0. 18**

Table (A-13) parameters measurement for case three at left side of duct at 4.2 m/s

D_h(m)	Re	*f*r	Δp
0.23	2533.3	**0.024**	**0. 40**
0.35	1983.3	**0.031**	**0. 47**
0.42	1199.9	**0.051**	**0. 45**

Table (A-14) parameters measurement for case three at right side of duct at 4.2 m/s

D_h(m)	Re	*f*r	Δp
0.23	1159.9	**0.049**	**0. 41**
0.35	1866.6	**0.030**	**0. 40**
0.42	2453.3	**0.023**	**0. 36**

Table (A-15) parameters measurement for case three at left side of duct at 2.8m/s

D_h(m)	Re	*f*r	Δp
0.23	2399.9	**0.025**	**0.29**
0.35	1913.3	**0.032**	**0.37**
0.42	779.9	**0.079**	**0.45**

Table (A-16) parameters measurement for case three at right side of duct at 2.8 m/s

D_h(m)	Re	*f*r	Δp
0.23	1119.9	**0.050**	**0.40**
0.35	1819.9	**0.031**	**0.39**
0.42	2133.3	**0.026**	**0. 31**

Table (A-17) parameters measurement for case three at left side of duct at 1.4 m/s

D_h(m)	Re	*f*r	Δp
0.23	1599.9	**0.038**	**0. 25**
0.35	816.6	**0.076**	**0. 20**
0.42	499.9	**0. 124**	**0. 19**

Table (A-18) parameters measurement for case three at right side of duct at 1.4 m/s

D_h(m)	Re	*f*r	Δp
0.23	439.9	**0.129**	**0.22**
0.35	699.9	**0.081**	**0.16**
0.42	1519.9	**0.037**	**0.15**

Journal of Mechanical Engineering Research and Developments (JMERD)
(www.jmerd.org.my)

To,

Dhurgham H. Talib
University of Babylon,
College of the Engineering
Department of Mechanical Engineering,
Iraq .

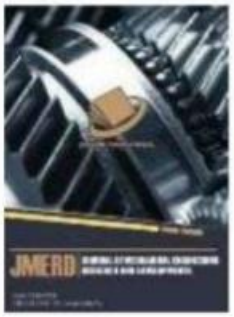

Date: 18/1/2021

Acceptance letter

Dear author,

I am pleased to tell you that your Paper titled " **Heat transfer analysis of air flow through irregular geometric ducts**" by Dhurgham H. Talib , Rafel H. Hameed and Adil A. Alwan has now been accepted for publication in Journal of Mechanical Engineering Research and Developments. Your paper will appear in Vol. …44… No. …3…-2021.

Thank you for submitting your work to this journal.

Editor in Chief

Publisher:The Scientific Press (TSP)
Email: jmerdtsp@gmail.com

Journal of Mechanical Engineering Research and Developments
ISSN: 1024-1752
CODEN: JERDFO
Vol. 44, No. 3, pp. 298-313
Published Year 2021

Heat transfer analysis of air flow through irregular geometric ducts

Dhurgham H. Talib*, Rafel H. Hameed, Adil A. Alwan

University of Babylon / College of the Engineering / Department of Mechanical Engineering

*Corresponding author Email: dhurghamhaider1212@gmail.com

ABSTRACT

In the present work, experimental investigations have been carried out to study the effect of an irregular shape geometry duct on the heat transfer and fluid flow characteristics. During the study, it was measured the temperature distribution, and air velocity through a duct with the different cases study of boundary conditions. The main part of the duct is designed with dimensions 3.65 m length,0.4 m width, 0.5 m height, and 1mm-thickness. Three duct components: length 1.25 m, width 0.4 m and height 0.25 m for the entrance section, length 1.2 m for the test section and length 1.25 m, width 0.4 m and height 0.5 m for the exit section. Ductwork is made of galvanized steel. Galvanized was a standard, most common material used in fabricating ductwork for most comfort air conditioning systems. The specifications for the galvanized steel sheet are ASTM A653, coating G90. The inlet duct section consists of the rectangular duct manufacturing and designed at this length to achieve a zone fully developed, the test duct section consists of an irregular duct, and the exit duct section consists of a square duct used to minimize the exit effects of the test section. Insulation is applied to ductwork to minimize the rate of thermal loss through the metal of the duct. In a two-dimensional laminar flow, numerical simulation is carried out and the projected model deals with the distribution of temperature along the irregular duct test by numerically solving the finite difference method describing the energy equation. ANSYS - 19.2 Fluent. The flow characteristics of airflow through the irregular duct was analyzed.

KEYWORDS

heat transfer analysis, irregular geometric ducts, finite difference method, constant heat flux, temperature distribution

INTRODUCTION

The irregular duct was used to arrange inward flow and heat transfer applications in the field. Due to its workable significance, heat transfer and laminar flow in its irregular duct have received a lot of attention. In applications for heat transfer appointments, such as combustion chambers, gas turbine duct cooling, cooling sections for electronic devices, and interior cooling for engines and nuclear power reactors, channels with an irregular cross-section are typically used, embedded heat exchangers, and fuel cells. These devices must be compressed as long as the heat transfer to the environment is rapid. The application of this kind of duct is becoming more and more common. It is very important to be able to prophesy heat transfer and the pressure drop characteristics of fluid flows in the irregular duct. Numerous studies have been performed on laminar flow in straight and irregular channels presented in the past. Chen et al. investigated heat transfer through irregular channels with cross corrugation and the use of uniform boundary conditions for heat flow was achieved [1]. The Results of the coefficient of friction and a Nusselt number obtained from experiments and simulations exhibit that the flow in the duct has the greatest Nusselt number and friction factor.

K. Sivakumar et al. studied systematic experimental heat transfer and pressure drop comparison between smooth and three different sized square ribbed divergent rectangular ducts [2]. The results obtained from the ribbed ducts were compared with that of the same parameter smooth (without ribs) divergent rectangular duct. The enhanced heat transfer rate for the 3 mm height rib divergent rectangular duct is more than 6, 9 mm rib height rectangular divergent duct, and smooth duct. For pressure drop point of view, 6 and 9 mm rib height is higher than 3 mm and smooth duct respectively. Zhang and Chen studied the fluid flow and heat transfer in a cross-corrugated triangular

الخلاصة

في العمل الحالي تم إجراء البحث العملي لدراسة تأثير مجرى هوائي غير منتظم على خصائص انتقال الحرارة وتدفق السوائل. خلال هذه الدراسة تم قياس توزيع درجة الحرارة وسرعة الهواء من خلال مجرى الهواء مع دراسة حالات مختلفة لظروف الحدود. في الحالة الأولى ، تم استخدام التدفق الحراري كشرط حدي. في الحالة الثانية ، تم استخدام fan coil لتزويد الهواء الساخن. في الحالة الثالثة ، تم استخدام air cooler لتزويد هواء التبريد. في جميع الحالات ، يتم توفير تدفق الهواء إلى القناة بواسطة استخدام منفاخ هواء من الجانب الأيسر والجانب الأيمن من مجرى الهواء. تم قياس توزيع درجة الحرارة لثلاث حالات مع المحور y (العمودي) بقيم مختلفة للمحور z (الافقي) داخل القناة غير المنتظمة (قسم الاختبار).

لوحظ أثناء الدراسة العملية لجميع الحالات أن قياسات درجة الحرارة تزداد عبر المحور y (العمودي) بقيم مختلفة لسرعة الهواء. تمت الإشارة إلى زيادة درجة الحرارة قليلاً مع زيادة قيم سرعة الهواء. تم قياس أعلى درجة حرارة في حالة واحدة هي 72.2 درجة مئوية بسرعة هواء 4.2متر^2/ثانية عندما يتم تسخين الهواء عن طريق التدفق الحراري في الجدار العلوي والجانبي للقناة غير المنتظمة (قناة الاختبار). تم قياس درجة الحرارة هذه بقيمة المحور 0.8 متر للمحورالافقي و 0.39 للمحور العمودي.

في نفس الظروف المحيطية للحالات الثلاث ، تم قياس سرعة تدفق الهواء داخل المجرى الغير منتظم (قناة الاختبار). يتم قياس هذه القيم من خلال توفير ثلاث قيم لسرعات المداخل من الجانب الأيسر والأيمن من مجرى الهواء. أيضًا ، في نفس الوقت ، يتم قياس سرعة مدخل ومخرج قناة مجرى الهواء.

للحالات الثلاثة ، تناسب Reynolds number عكسياً مع قيم عامل الاحتكاك ، وانخفض الضغط داخل القناة غير المنتظمة في العمل التجريبي.

تم إجراء المحاكاة النظرية في نموذج ثنائي الأبعاد يتعامل مع توزيع درجة الحرارة داخل مجرى الاختبار غير المنتظم عن طريق حل الفروق المحدودة التي تمثل معادلة الطاقة عدديًا. يتم تقديرها بواسطة نموذج رياضي تم محاكاته بواسطة عمل برنامج كمبيوتر بواسطة Matlab. تمت محاكاة سرعة تدفق الهواء بواسطة ANSYS - Fluent 19.2 داخل مجرى الهواء غير المنتظم.

جمهورية العراق
وزارة التعليم العالي والبحث العلمي
جامعة بابل / كلية الهندسة
قسم الهندسة الميكانيكية

تحليل أنتقال الحرارة لجريان الهواء عبر القنوات غير المنتظمة هندسياً

رسالة
مقدمة إلى جامعة بابل / كلية الهندسة وهي جزء من متطلبات نيل شهادة الماجستير في الهندسة الميكانيكية (القدرة)

أعدت من قبل
ضرغام حيدر طالب الحسيني
بكالوريوس هندسة ميكانيك
٢٠١٧

بأشراف
أ.د. عادل عباس علوان الموسوي
أ.م.د. رفل حكمت حميد

١٤٤٣هـ ٢٠٢١م